Molecular and Isotopic Characterization of Organic Matter in the St. Lawrence Estuary

Robert James Panetta

A thesis in

The Department of

Chemistry and Biochemistry

Presented in partial fulfillment of the requirements

for the degree of Doctor of Philosophy at

Concordia University

Montreal, Quebec, Canada

July 2009

Your file Votre référence
ISBN: 978-0-494-63437-0
Our file Notre référence
ISBN: 978-0-494-63437-0

Molecular and Isotopic Characterization of Organic Matter in the St. Lawrence Estuary

Robert J. Panetta, Ph.D.

Concordia University, 2009

Sources and processing of carbon in the hypoxic St. Lawrence Estuary are investigated via a coupled bulk (stable carbon isotope and elemental quantitative) and molecular (polycyclic aromatic hydrocarbons and lignin phenols) approach. In order to analyze the stable carbon isotope ratio of dissolved organic carbon ($\delta^{13}C_{DOC}$), a novel method was developed, coupling a total organic carbon (TOC) analyzer to an isotope ratio mass spectrometer allowing the routine analysis of $\delta^{13}C_{DOC}$ in marine waters. Bulk analyses of five pools of carbon (sedimentary, pore-water dissolved organic, water column dissolved inorganic and organic, and particulate organic) distributed through the estuarine transition zone are analyzed to gain further insight into the spatial variability of carbon source(s) and cycling in the system, with particular insight gleaned into the water column. The system identifies with other non-anthropogenically perturbed systems by all indicators, despite its proximity to major industrial centers and one of the historically heaviest polluted watersheds in North America. The extensive elemental and isotopic analyses of five pools of carbon show; (1) a clear spatial shift in trophic state between with Upper estuarine net heterotrophy and primary production resulting in Lower Estuarine net autotrophy; (2) the dissolved and particulate organic pools do share sources, but appear decoupled because physical mixing outpaces transfer; (3) approximately 90 % of primary produced particulate carbon and nitrogen is

consumed prior to sedimentary deposition in the Lower Estuary; (4) stable isotopes indicate the export of riverine dissolved organic carbon is more efficient than estuarine systems from lower latitudes perhaps making similarly located estuaries important sources of terrestrial dissolved organic carbon to the world's oceans; (5) the benthic nepheloid layer may be a site of microbial activity in the hypoxic Lower Estuary; and (6) isotopic fractionation between pore water dissolved organic carbon and sedimentary organic carbon implies compositionally-driven *in situ* sedimentary fractionation. To better understand estuarine processes, directed experiments investigating the role of UV oxidation coupled to microbial respiration and particle dynamics should be conducted in the future. To better understand where and how carbon is consumed in the hypoxic zone the role of benthic layer cyanobacteria should be a primary focus.

Acknowledgements

Firstly, to my family, I know this means a lot and the accomplishment is as much theirs as it is mine. Everyone in the LEGO group, starting with my supervisor, Yves Gélinas who has dealt pretty well with me over these years, and in no particular order; Maggy Mouradian, Marie-Helène Veilleux, Denis Brion, Lisa Barrazzuol, Alexandre Ouellet, Karine Lalonde, and Mina Ibrahim, along with about a dozen or so undergraduate research students for invaluable discussions, help and fun times through this work. Dr. Louis Cuccia is always more than willing to lend a helping hand. Bjorn Sundby, Al Mucci, Denis Gilbert for great support and discussions about hypoxia in the estuary, as well as all other members of the hypoxia research group. Edward Hudson was a great intellectual badminton partner, and Maria Kaltcheva provided great suggestions for aesthetic science. The captains and crews of the *R/V* Coriolis *II* are thanked for help in sample collection. Funded by NSERC – Canada and FQRNT – Québec, and additional financial support came from Concordia University.

"But I don't want to go among mad people," Alice remarked.
"Oh, you can't help that," said the Cat: "we're all mad here. I'm mad. You're mad."
"How do you know I'm mad?" said Alice.
"You must be," said the Cat, "or you wouldn't have come here."

Lewis Carroll, Alice's Adventures in Wonderland

Table of Contents

List of Figures

List of Tables

Chapter 1.

Biogeochemistry of the St. Lawrence Estuary

1.1 Biogeochemistry of Carbon: The Earth as reaction vessel

Throughout planetary history, natural and anthropogenic forces have shaped the chemical composition of the Earth, affecting phenomena such as the oxygenation of the atmosphere (Bekker *et al.* 2004), the permeation of arsenic into water tables (Polizzotto *et al.* 2008), and climate change (Ramanathan and Feng 2008), to name but three examples. Biogeochemistry aims to understand how and why these fluxes occur via the chemical study of natural systems as influenced by the interactive processes of the geo- and biospheres. Because the chemistry of the natural world can be defined by extremely complex pathways and mechanisms, conceptualization to single elemental "cycles" is usually carried out as a simplification. For example, many processes inextricably link the global fluxes of carbon, nitrogen, phosphorous, sulfur and oxygen (e.g., Catling and Claire 2005), however, biogeochemists often work out cycles of individual elements (e.g., "the carbon cycle"), with implicit knowledge that the turnover of each element is interrelated to the others'. Such simplification is common to the study of complex systems whereby interrelated processes are deconvoluted and treated as independent. For example, the catalytic mechanism of phospholipase A in the cellular inflammatory response can be understood without any knowledge of the intracellular signalling cascade that would trigger the enzyme's activation, for example.

In this vein, the carbon cycle is here described (Figure 1-1); primary productivity (on land and in the oceans) fixes CO_2 as biomass, otherwise termed organic matter (or organic carbon when discussing the carbon cycle exclusively).

Organic carbon is then subjected to three possible fates; 1) remineralization via respiration back to CO_2 and flux back to the atmosphere, 2) remineralization followed by carbonate precipitation with Group II metals, notably calcium, or 3)

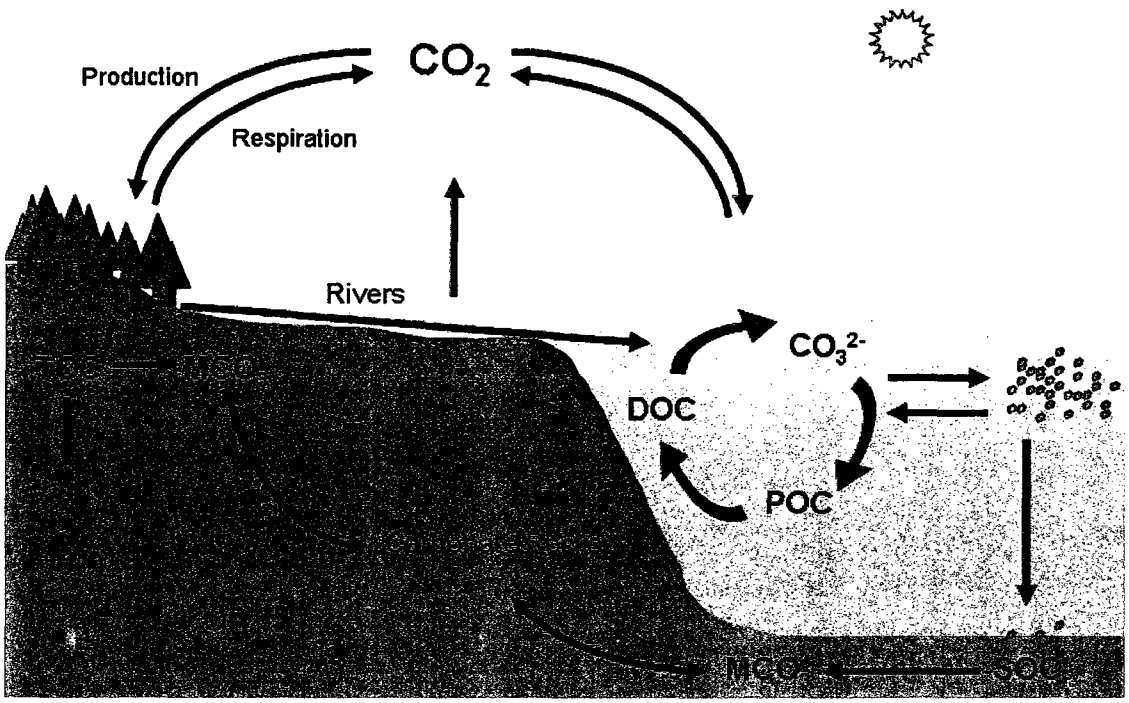

Figure 1-1 Simplified carbon cycling between the atmosphere to the terrestrial and oceanic systems. Photosynthesis by land plants results in the production of terrestrial organic carbon (TOC) which can be (1) remineralized to CO_2 and either flux back to the atmosphere or precipitate with metal ions (M) to form carbonate minerals; or (2) be buried and stored in soils over geological time scales. At the oceans surface dissolved CO_2 is in equilibrium with carbonates which through phyotosynthetic production by phytoplankton forms particulate or dissolved organic carbon (POC and DOC, respectively). POC is remineralized or transported to the sediments supporting benthic respiration and subsequent burial. DOC is remineralized, or escapes degradation and persists over several oceanic cycles forming the largest pool of reactive carbon on Earth. The terrestrial system is connected to the ocean via rivers and estuaries, transporting a significant amount of dissolved carbonates and DOC from land to sea.

deposition and long-term storage in soils (terrestrial carbon cycle) or sediments (oceanic carbon cycle). In biogeochemical terms, a distinction is made between inorganic and organic carbon whereby the former can be defined as carbon –

oxygen molecules in which the carbon atom is fully oxidized (e.g., CO_2, CO_3^{2-}), and the latter as any molecule containing a reduced form of carbon (e.g., $C_6H_{12}O_6$, $CH_3COO^-Na^+$). Thus any use of the term "inorganic carbon" makes no distinction between, say CO_2 and HCO_3^-, whereas "organic carbon" makes no distinction between any class of complex carbon-containing molecules i.e., amino acids, polyethylene glycols and imidazoles are all in the same grouping by this convention.

By extension, the reactivity and other properties of "bulk" DOC (as well as properties of the other bulk pools of carbon referred to throughout the text) are defined by the averaged properties of all organic compounds present in the sample. The redox-based distinction is also relevant in describing the role of organic carbon in planetary chemistry; as an active reducing agent, this matter is directly linked to oxygen via primary production and respiration, triggering such grand-scale events as the "great oxygenation" (Bekker *et al.* 2004) ~2Ga ago and the anthropogenically-driven expansion of oceanic hypoxic zones (Diaz and Rosenberg 1995).

The carbon cycle is compartmentalized according to geospheres, i.e. the terrestrial carbon cycle is often made distinct from the oceanic, which in turn is distinct from the atmospheric. Much like the categorization of elemental cycles, the geospheres are linked with carbon passing from one to another (e.g., Hedges and Oades 1997) but further this partitioning into relevant spheres (i.e., oceanic *vs.* terrestrial *vs.* atmospheric carbon cycles) allows better definition and identification of "elemental highways" in the environment. The atmospheric carbon cycle is the most widely known to the general public due to concerns

relating to greenhouse gas emissions and climate change (IPCC 2007), however very many intricate loops and feedback mechanisms involving terrestrial and oceanic systems are primarily responsible in the regulation atmospheric CO_2 levels (e.g., Goodwin *et al.* 2009). Relevant facets of the terrestrial and oceanic systems will be briefly discussed in order to better appreciate their prime interface, estuaries, which will be introduced in Section 1.2.

Rivers are quantitatively the most significant link between the land and the sea, annually transporting 0.9×10^9 tonnes of carbon to the oceans, enough to account for the annual turnover of the oceanic carbon stock (Maybeck 1983). The carbon being transported exists in three forms: ~60 % is dissolved inorganic carbon (DIC), and the remainder as dissolved organic carbon (DOC) and particulate organic carbon (POC). The distinction between dissolved and particulate is operational; filters of 0.45 μm pore-size are used to remove suspended matter from water samples prior to analyses; any carbon in the filtrate is defined as dissolved, and all retained by the filter as particulate (Strumm and Morgan 1996). This seemingly arbitrary distinction is fortuitous as important differences between DOC and POC chemical composition and reactivity exist in both riverine and marine systems (Hansell and Carlson 2002, Mayorga *et al.* 2005) (particulate inorganic carbon in rivers is a very minor pool and is usually ignored).

In rivers, DOC usually exceeds POC with concentrations of ~300 – 400 and ~150 – 250 μM[a], respectively (methods of analysis are briefly reviewed in Section 1.5), values which are strikingly similar in most systems that are not anthropogenically perturbed (Abril 2002). Although a number of studies have identified *in situ* primary production by phytoplankton as a primary carbon source in some rivers (e.g., McCallister 2006), the most recognizable dominant source of organic carbon in rivers is derived from land plant biomass delivered through soils via run-off. Though a number of anthro- and bio-genic organic classes have been identified and characterized in freshwater systems (e.g., amino acids (Görs *et al.* 2007), carbohydrates (e.g., Hung *et al* 2005), and lipids (e.g., Meyers 2003, McCallister *et al* 2006a and b)) the most characteristic class are polyphenols and tannins originating from vascular plant structural biopolymers, most commonly proxied by lignin phenols (e.g., Opsahl and Benner 1997, Louchouarn *et al* 1999, Benner and Opsahl 2001, Hernes and Benner 2003). Compositional differences between riverine POC and DOC have been noted in a number of studies (Aufedenkampe *et al* 2001, Hernes and Benner 2003, McCallister *et al* 2006a and b), with relevant contrasts in the reactivities of the two pools clearly demonstrated (Mayorga *et al* 2005).

DIC in rivers is very often derived from a combination of remineralized DOC/POC and dissolution of soil carbonate minerals (e.g., Mayorga *et al.* 2005).

---

[a] DOC and POC are expressed in elemental concentration terms. For example, a solution containing a mixture of 1 mM each of benzoic acid ($C_7H_6O_2$), glucose ($C_6H_{12}O_6$) and alanine ($C_3H_7NO_2$) is a 16 mM DOC solution.

Not nearly as chemically diverse as DOC, DIC is the sum of all carbon-oxygen species in equilibrium (Strumm and Morgan 1996):

$$CO_3^{2-}{}_{(aq)} \rightleftarrows HCO_3^{-}{}_{(aq)} \rightleftarrows H_2CO_{3(aq)} \rightleftarrows CO_{2(aq)}$$

There is no generally dominant species in rivers as the equilibria are defined by *in situ* pH and temperature which vary significantly from one system to another. Still, rivers are considerable contributors of CO_2 to the atmosphere but the sources (mineral or respiration of organic carbon) vary from system to system (Moyorga *et al* 2005) and are generally not well constrained (Frankingnoiulle 1999).

Despite an average depth of 4 km, the main source of organic carbon in the oceans is primary production taking place in the top 0.1 km. Phytoplankton growth periods (or "blooms") occur at times and areas where limiting nutrients(s) are in abundance, such as upwelling events transporting iron from deep waters to the surface (Bruland *et al.* 2005)). The phytoplankton biomass (POC and DOC) is mostly consumed in the surface waters by microbial activity (Hedges 1992) to be either remineralized to DIC or cycle through the "microbial loop" (Azam 1998). The portion of POC that escapes remineralization in surface waters either integrates into the DOC pool or sinks through the water column acting as a carbon source in the deep water column and bottom sediments (e.g., Woulds *et al* 2009). Degradation of the POC, whether microbial or abiotic, occurs

during the long descent to the sediments (Wakeham 1997) where it is either respired by fauna in the benthic zone (sediment-water interface) or buried for long-term storage in the deep ocean sediments, forming an additional pool, sedimentary organic carbon (SOC). POC and DOC concentrations during the bloom can be extremely high, but under normal circumstances surficial values across the ocean are typically ~2 and ~80 μM respectively while in the deep waters (exceeding depths of 2 km) DOC shows a gradient from ~50 μM to as low as 30 μM from the North Atlantic, south through the Indian Ocean and back north to the sub-Arctic Pacific (Hansell and Carlsen 1998). Much of the DOC is found to be old (~6000 years, on average), presumably persisting through the mixing of the oceanic basins several times over (Druffel *et al* 1992) and acting as a significant long-term storage pool of carbon that is equivalent in magnitude to the total quantity of carbon dioxide in the atmosphere. Rivers transport significant amounts of DOC and POC from the continents to the oceans, however the exact mechanisms of transport, the microbial and photochemical degradation processes altering bulk and molecular properties remains problematic (Benner 1994).

1.2 Estuaries: where the river meets the sea

In no place is there a clear demarcation between river and ocean. Rather rivers mix with seawater gradually becoming saltier seaward forming a river plume (e.g., the Amazon) or an estuary (e.g. the St. Lawrence), depending on the river flow rate and morphology. Though only estuaries are referred to through the rest of the text, both systems are the same with respect to chemical changes

and reactions. The most significant change that occurs in these zones is increasing ionic strength (I) seaward, going from ≈ 0 to ≈ 0.7mol kg^{-1}, or a salinity (S) of ≈ 0 to ≈ 35 psu.[b] In the estuarine transition zone, the increasing salinity effects a number of physical changes, the most noticeable being turbidity where levels of suspended solids increase significantly, creating maximum turbidity zones in low- to mid-salinity ranges where diagenetic[c] alteration of minerals and organic matter occurs (e.g., d'Angelan 1990). Significant changes in the biological communities also occurs in these zones (e.g. Painchaud *et al* 1995a and b), characterizing estuaries with what ecologists term a high species "richness" at all levels of the food web. The special environmental features of estuaries make them nurseries for many commercially relevant fisheries such as striped bass and blueback herring (Dufour and Ouellet 2007).

In a system experiencing such chemical, physical and biological diversity, it follows that the cycling of carbon will be subject to physichochemical transformations. The turbidity brought about by suspended particles obviously plays a very significant role in quantitatively and compositionally defining the pool of POC. The POC from these zones is transported out of the estuary, towards the ocean and they typically settle (are deposited) in coastal[d] sediments (e.g.,

---

[b] Oceanographic research employs salinity (historically the mass of total salt per unit volume), which is expressed as practical salinity units (psu), derived from the ratio of the conductivity of a water sample against a standard KCl solution (Unesco 1981). Seawater typically has a salinity of ~35 psu.

[c] Diagenesis refers to any changes occurring in sediments, whether they be physical, chemical or biological, incurred on sedimentary materials following their initial deposition. Examples include the reduction of iron oxides in sediments or the formation of oil (petrogenesis) from organic matter over geological time scales.

[d] "Coastal" is a term noted several times through this text and refers to regions of the ocean adjacent the continents, and noticeable inputs from land.

Poynter and Eglinton 1990, Louchouarn *et al* 1999). The amount of terrestrially-borne carbon in surface sediments of coastal zones is found to decrease significantly seaward from the mouth of the river, usually forming a depositional "fan," as such as the Amazon River plume (Schlünz *et al* 1999), to name a few. Despite the amount of DOC exported from rivers to the oceans, very little to no compositional trace of DOC in marine systems is identified as terrestrial in origin, leaving the fate of this pool of carbon unknown (e.g., Benner 2004) and leading to much research into estuarine processing of DOC (e.g., Peterson *et al* 1994, Frankingouille 1995, Benner and Opsahl 2001, Raymond and Bauer 2001, Abril *et al.* 2002, Otero *et al* 2003, Hernes and Benner 2003, Bianchi *et al* 2004, Mayorga 2005, McCallister *et al* 2006a-b, Guo *et al* 2009). DOC too is clearly shown to be affected by turbidity via sorption-desorption reactions at the mineral surfaces of particles (e.g., Aufdenkampe *et al.* 2001), as well changes in the redox conditions of maximum turbidity zone sediments (Abril *et al* 1999). In the water column of estuaries microbial activity (e.g., Benner 1993, McCallister *et al* 2006a and b) and photochemistry (e.g. Hernes and Benner 2003) are thought to be the most significant processes altering riverine DOC. Whether the DOC is fully oxidized in transit or if it is altered in such a manner as to make it indistinguishable from marine DOC is still a topic of debate (Benner 2004), and one that bears relevance on the source of CO_2 outgassed from these systems.

1.3 The Hypoxic St. Lawrence Estuary

The St. Lawrence Estuary of Eastern Canada extends from the St. Lawrence River which drains the Great Lakes watershed into the North Atlantic.

The estuarine system is split into three regions (Figure 1-2); the shallow Upper Estuary extends ~300 km from Québec City to the Saguenay Fjord with surface salinity increasing to 25 psu and is the location of the maximum turbidity zone;

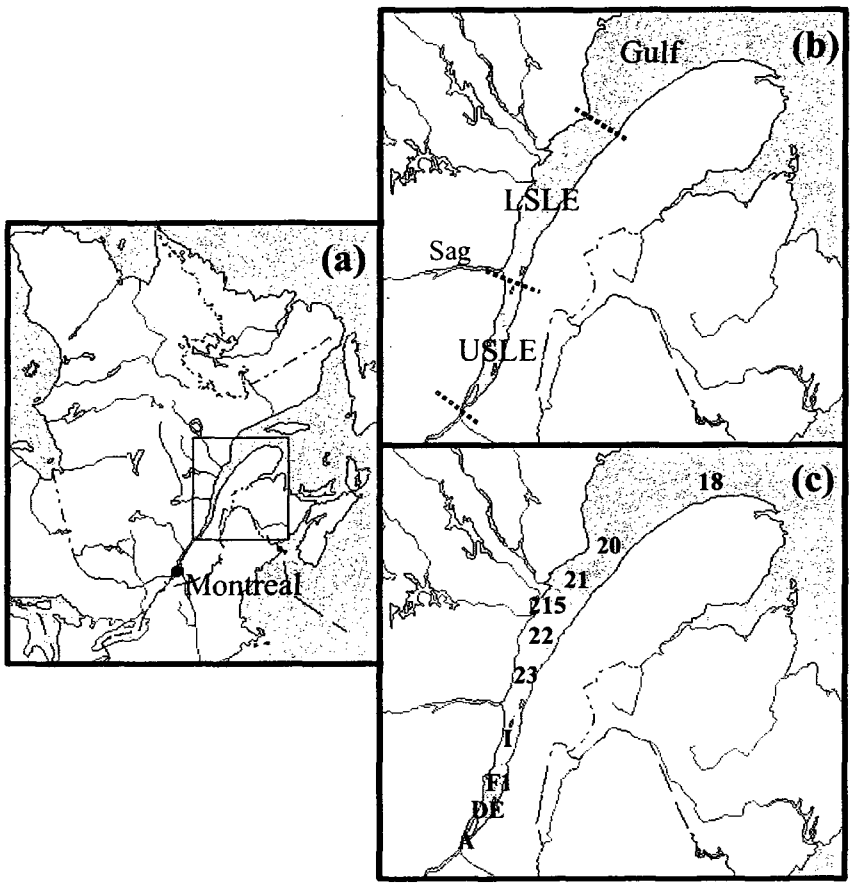

Figure 1-2 The St. Lawrence Estuary (a.) Map of north-eastern North America highlighting the St. Lawrence Estuary; (b) Detail of the sampling area depicting the upper (USLE), lower (LSLE) estuaries and the Gulf. The major tributary the Saguenay Fjord (Sag) is also shown. Dotted red lines demark the boundaries of each region; (c) Main sampling stations visited for the work presented in this thesis, following historical designations as described in Chapter 5.

the Lower Estuary extends another 300 km and characterized by the deep Laurentian Channel, averaging ~320 m depth at its center; and the Gulf that can

be viewed as an enclosed shallow sea. The system is well stratified[e], with the estuarine mixing zone extending from the Upper Estuary into the surface waters of the Lower Estuary. Bottom waters of the Lower Estuary and Gulf are marine in origin, flowing in from the North Atlantic, with a cold intermediate layer isolating the bottom layer from the surface. Extensive sediment and water column characteristics have been published and are discussed in a recent review on the state of knowledge of this ecosystem (Dufour and Ouellet 2007).

Recent anthropogenically-driven eutrophication of populated coastal environments has led to the evolution of numerous hypoxic zones around the world (Nixon 1995, Cloern 2001, Gray *et al.* 2005, Schrope 2006). Defined as dissolved O_2 concentrations below levels necessary to sustain most animal life (<30% saturation, or 62.5 μM), hypoxia can cause significant damage to ecosystems (Diaz and Rosenberg 1995). The evolution of such a state through the 20th century has been described for the Lower St. Lawrence Estuary, with dissolved O_2 in the bottom waters decreasing from 125 μM in the 1930s to an average of 65 μM (range of 51-80 μM) for 1984-2003, covering an estimated 1300 km^2 of seafloor (Gilbert *et al.* 2005). It is suspected that the recent hypoxia has already had a significant negative impact on the Canadian fisheries economy (Benoit *et al.* 2006, Dufour and Ouellet 2007).

One-half to two-thirds of the oxygen depletion is attributed to warming Atlantic water entering the system (Gilbert *et al* 2005) and the remaining

---

[e] Stratification refers to a layered system, in this case bodies of water as a function of depth. Water layers exist because differential densities, for example less dense freshwater floats on denser seawater, or warmer water will tend to float over cold water.

depletion explained by phytoplankton production in surface waters triggering benthic microbial respiration (Benoit *et al* 2006, Thibodeau *et al* 2006). Depleted dissolved O_2 in the St. Lawrence is likely a permanent condition, so understanding how progressive O_2 diminution in the bottom waters will affect the ecosystem as a whole, from elemental geochemical cycles to biological population dynamics, is a subject of great interest (Katsev *et al.* 2007, Dufour and Ouellet 2007).

1.4 Carbon in the St. Lawrence Estuary

Organic inputs to the St. Lawrence Estuary are primarily affected by three anthropogenic activities: industry (aluminium smelting/pulping mills), agriculture and urban runoff. Up until the 1980s, pulp and paper was the most significant activity influencing the carbon cycle in this system, however environmental regulations have significantly diminished its detrimental effects (Louchouarn *et al* 1999). Agriculture is now the main anthropogenic influence on the system, and affects the carbon cycle via eutrophication of surface waters from fertilizer-rich run-off draining fields (Thibodeau *et al* 2006). Though it is accepted that perturbations in the carbon cycle resulting from eutrophication accelerates O_2 diminishment, the magnitude and location of organic matter respiration (water column *vs.* benthos/sediments) are not well understood (Lehmann *et al* 2009).

Detailed studies of the carbon cycle were carried out in the Gulf of St. Lawrence as part of the Canadian Joint Global Ocean Flux Study program (Roy *et al* 2000), but work to understand carbon dynamics to the same extent in the hypoxic zone of the estuary has not been as extensive. Much of the focus has

been on the fate of specific biomarkers (such as lignin (e.g., Louchouarn *et al.* 1999), or lipids (Colombo *et al.* 1997)), or mapping bulk chemical characteristics in particulate matter and surface sediments (e.g., Gearing and Pocklington 1990, Lucotte *et al.* 1991, Colombo *et al.* 1996a and b) collected during the 1980s and early 1990s. Source apportionment in surface sediments has resulted in estimates ranging from 25 – 80 % terrestrial carbon in what is now the hypoxic zone; the large variation was attributed to the high seasonal dynamism of OC inputs before and after the spring phytoplankton bloom in the Lower Estuary (Colombo *et al.* 1996 a and b, 1997, for example). Despite the width of the lower estuary (25 to 45 km from shore to shore), the bulk of knowledge is derived from sampling the center of the channel (east – west directionality) and little attention has been paid to organic matter deposition and diagenesis on either shore which may be considerably different from the main channel due to the presence of several large tributaries along the northern shore.

Work on particulate organic carbon (POC) has delimited three regions in the system (the Upper and Lower Estuaries, and Gulf, Figure 1-2), each comprising a distinct, isolated pool of POC in the water column (Gearing and Pocklington, 1990, Lucotte *et al.* 1991, Dufour and Ouellet 2007). The particles borne in the Upper Estuary are mostly deposited at the head of the Lower Estuary whereas primary production in the Lower Estuary and Gulf is mostly consumed/deposited within their respective zones or very inefficiently exported downstream. Efficient consumption of fresh organic matter in the system certainly contributes to the seasonal variability in source apportionment, as demonstrated

by Colombo *et al.* (1997) who identified dramatic changes in the molecular composition of sinking particles prior to sedimentary deposition. Lucotte *et al* 1991 estimated that ~ 30% of primary production reaches estuarine sediments, a higher estimate than made in the Gulf (Silverberg 2000). Better defined constraints on POC mass balance in the water column of the Lower Estuary are thus needed (Dufour and Ouellet 2007).

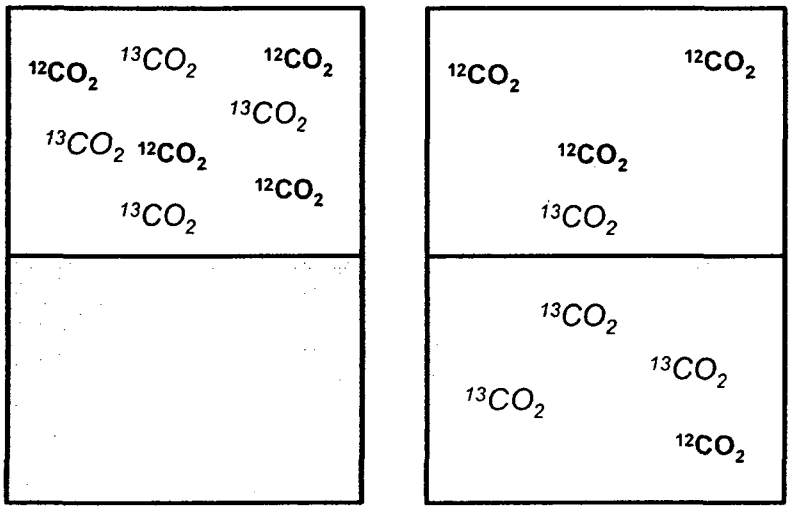

Figure 1-3 Isotopic Fractionation. A sealed container of de-gassed water is allowed to equilibrate with an atmosphere containing known amounts of two isotopologues of CO_2. After equilibration, the heavier isotopologue ($^{13}CO_2$) shows preferential dissolution, resulting in and isotopic enrichment in the water, while the atmosphere becomes isotopically depleted with respect to the heavier isotopologue.

Despite decades of work carried out in the St. Lawrence Estuary, little data exists on dissolved carbon. Seasonal dynamics of DOC have been studied in the river (Hélie and Hillaire-Marcel 2006) and Gulf (Packard *et al.* 2000), however the studied locations are far removed from the estuarine mixing zones where processing and transformations are most significant. In addition to riverine inputs,

sediments are also thought to be important sources of DOC to coastal environments (Burdige *et al* 1999), via DOC fluxes from sediments into the overlying water, where it potentially plays a role in sustaining benthic microbial respiration in the hypoxic zone.

1.5 Measuring the Carbon Cycle: Stable isotope ratios of DOC

A primary staple for understanding geochemical carbon dynamics is natural abundance stable carbon isotope analysis. Stable isotopes are most familiar to anyone working with nuclear magnetic resonance spectroscopy, or those in mass spectrometry, where the main concern is that carbon exists as ~1.1% ^{13}C in nature, for example. However, increasing the precision and accuracy of the estimation, one finds 1.1140% is ^{13}C. Once at this level of precision, many processes including chemical reactions (e.g., enzymatic carboxylation of phosphoenolpyruvate) and physical processes (e.g., dissolution of carbon dioxide in seawater) leads to a slight alterations in the relative abundance of ^{13}C (Figure 1-3). Using this principle of fractionation it is possible to delineate sources, reactivities and trace specific processes in any chemical system (de Groot 2004). Rather than express isotopic composition in terms of absolute amounts, the "delta notation" is employed where the measured ratio of the heavier over the lighter isotope of a sample is compared to the ratio of a known standard:

$$\delta^{n}X = \frac{R_{Sample} - R_{Reference}}{R_{Reference}} \times 1000 \qquad (1)$$

where n is the mass number of the heavier isotope, R_{Sample} is the ratio of the sample and $R_{Reference}$ is the ratio of the measured reference material. Typical values for $\delta^{13}C$ encountered in natural systems include -21 ‰ for marine phytoplankton, -26 ‰ for vascular plant material and -8 ‰ for atmospheric CO_2, for example.

Though particles and sediments have been well studied over spatial and seasonal scales in the St. Lawrence Estuarine system (Gearing and Pocklington 1990), stable carbon isotope values for dissolved organic carbon ($\delta^{13}C_{DOC}$) have only been reported for the river (Hélie and Hillaire-Marcel 2005). The lack of $\delta^{13}C_{DOC}$ coverage is not unique to the St. Lawrence as the methods for measuring $\delta^{13}C_{DOC}$ tend to be long and tedious, requiring highly specialized, expensive equipment, large sample volumes, and a number of steps to remove carbonates and quantitatively convert DOC into CO_2 for eventual off-line analysis by mass spectrometry (Bauer *et al.* 1992, Fry *et al.* 1993). Alternatively, concentrating a sample (by lyophilization or evaporation) to obtain $\delta^{13}C_{DOC}$ by solid-state elemental analysis coupled to an isotope ratio mass spectrometer (EA-IRMS) is a frequently chosen option. This approach works well when the ratio of DOC to inorganic salt is relatively high (Gandhi *et al.* 2004), however the low DOC to salt ratios that characterize estuarine/marine samples introduce a high degree of uncertainty and poor reproducibility in the measurement (St-Jean 2003), limiting this approach to freshwaters. Considering the importance of coastal zones to the general health of the global ocean, the St. Lawrence

included, gaining insight into coastal processing via isotope geochemistry of the carbon cycle is of growing value.

Recent technical advances have, however allowed the routine measurement of $\delta^{13}C_{DOC}$ on small volumes of whole, unprocessed samples (St-Jean 2003, Bouillon *et al* 2006, Lang *et al.* 2007, Osburn and St-Jean 2007 and Panetta *et al* 2008) with large-scale $\delta^{13}C_{DOC}$ data sets of the entire DOC pool now emerging alongside the more accessible POC and DIC stable isotopes to give a more complete understanding of carbon cycling in dynamic systems (Bouillon *et al* 2007 a and b). For high salinity samples, the methods still prove somewhat difficult, especially when DOC is low.

1.6 Constraining Carbon Dynamics in the St. Lawrence Estuary

The aim of this work centers on a better our understanding of carbon dynamics in the St. Lawrence Estuary. Specifically, the two central issues of the organic geochemical paradigm are addressed: source (where is carbon coming from?) and processing (what happens to it in the system?). Stable carbon isotope analyses, and anthropogenic (polycyclic aromatic hydrocarbons) and terrestrial (lignin phenol) markers are employed to gain insight into the carbon cycle in the upper estuary and hypoxic lower estuary. In particular, the role of anthropogenic perturbations needs to be addressed, with a focus on the extent that these perturbations are affecting the hypoxic condition of the Lower Estuary.

Stable isotope analyses of solid samples (POC, SOC) and carbonates (DIC) are routine methods carried out by EA-IRMS. In order to analyse the stable carbon isotope ratio of DOC, a novel method was developed, coupling a total

organic carbon (TOC) analyser to an isotope ratio mass spectrometer. Superior detection limits to other on-line TOC-IRMS systems were obtained allowing the routine $\delta^{13}C_{DOC}$ analysis of marine waters and the more complete isotopic coverage of carbon pools in estuarine systems.

Lignin phenols and polycyclic aromatic hydrocarbons are measured in the system to evaluate anthropogenic vs. natural sources of POC to the system. In addition, a comprehensive quantitative and isotopic assessment of the state of the carbon cycle in the water column and sediments is presented. Bulk analyses of five pools of carbon (sedimentary, pore-water dissolved organic, water column dissolved inorganic and organic, and particulate organic) distributed through the estuarine transition zone are analyzed to gain further insight into the spatial variability of carbon source(s) and cycling in the system, with particular insight gleaned into the water column.

1.7 Arrangement of Thesis

The bulk of this thesis is based on four manuscripts which have been published, or are submitted to refereed journals. Rather than have connection text between chapters, the relationship are described in this subsection. The publications chosen for these chapters do cover a diverse set of fields of study whose associations include the American Chemical Society (*Analytical Chemistry* and *Environmental Science and Technology*), the American Society of Limnology and Oceanography (*Limnology and Oceanography: Methods*), and the American Geophysical Union (*Global Biogeochemical Cycles*), and as such connections between the chapters may not be obvious. They are ordered to follow the

conventional arrangement for scientific reports, i.e. Introduction (current Chapter), Methods (Chapters 2 and 3), Results (Chapters 4 and 5) and a Discussion of the results (Chapter 6). All chapters are formatted in the same manner with Figures and Tables inserted in the text, and numbered according to Chapter (i.e., Figure 2-1 means Figure 1 of Chapter 2). Sections published as "Supporting Information" are appendices placed at the end of the document with an "A" preceding the number (i.e., "Appendix A2" corresponds to the appendix of Chapter 2, and "Figure A2-1" corresponds to Figure 1 of Appendix 2).

Chapter 2 ("Coupling a high-temperature catalytic oxidation total organic carbon analyzer to an isotope ratio mass spectrometer to measure natural-abundance δ^{13}C-DOC in marine and freshwater samples" in *Anal. Chem, 80,* 5232 – 5239) describes the development of a novel technique to measure the stable carbon isotope ratio of dissolved organic carbon in saline samples, and covers method development and validation for application to natural samples. Data expression and interpretation of biomarkers is presented in Chapter 3 ("Expressing biomarker data in stoichiometric terms: shifts in distribution and biogeochemical interpretation" in *Limnol. Oceanogr: Methods, 7,* 269 – 276) which describes the importance of units when quantitatively interpreting geochemically-relevant biomarkers. Chapter 4 ("Polycyclic aromatic hydrocarbons in the St. Lawrence Estuary (QC, Canada): Transport, distribution and patterns as influenced by terrestrial organic matter", submitted to *Environ. Sci. Technol.*) is the first of the results chapters, providing a spatial and historical assessment of direct anthropogenic perturbations in the system via the use of

polycyclic aromatic hydrocarbons and lignin phenol biomarkers and indicates that direct anthropogenic inputs of this class of contaminants are not significant with repect to natural background levels. The second of the results sections, Chapter 5 ("Quantitative and natural abundance stable isotope mapping of five pools of carbon in the St. Lawrence Estuary" to be submitted to *Global Biogeochem. Cycles*) presents a comprehensive assessment of the carbon cycle in the water column and sediments of the St. Lawrence, including the largest data set of $\delta^{13}C_{DOC}$ obtained using the instrumentation described in Chapter 2. In it, the notion of the St. Lawrence as a system unperturbed by direct anthropogenic carbon inputs is further reinforced, and an unprecedented level of detail and understanding of the carbon cycle is reported. Note through Chapter 2 the stable isotope ratio of dissolved organic carbon is published with the symbol δ^{13}C-DOC, while in Chapter 5 it is changed to $\delta^{13}C_{DOC}$. The two manuscripts were prepared at different times and the latter designation is self-consistent with other stable isotope ratio designations.

Specific contributions from other authors need be addressed. In Chapter 2 Mina Ibrahim, currently an M.Sc. in student at Concordia conducted part of the data collection and analysis as part of his CHEM 419 undergraduate research project, specifically part of the β-alanine, and IAEA-CH-6 standard measurements. In Chapter 5, Karine Lalonde, currently a Ph.D. student at Concordia played an integral role in shaping the interpretation of the results described in subsection 5.3.2 and elaborated on in 5.4.3, while Alfonso Mucci and Bjorn Sundby (Earth and Planetary Sciences, McGill University) provided

data described in 5.3.3 and impetus for pushing the interpretation presented in 5.4.2). Lignin phenol analyses were conducted at GEOTOP-UQAM by Sophie Chen.

Chapter 2.

Coupling a high-temperature catalytic oxidation total organic carbon analyzer to an isotope ratio mass spectrometer to measure natural-abundance $\delta^{13}C$-DOC in marine and freshwater samples

Published as

Panetta, R.J., M. Ibrahim, and Y. Gélinas (2008) *Analytical Chemistry*, **80**: 5232 – 5239.

2.1 Introduction

Measurement of the stable isotope composition of carbon ($\delta^{13}C$) has proven a powerful approach for deciphering the sources and cycling of dissolved organic carbon (DOC) in freshwater and marine systems (Druffel *et al.* 1992, Cifuentes and Eldridge 1998, Raymond and Bauer 2001, Bauer *et al.* 2001, Bouillon *et al.* 2007). The methods employed to measure $\delta^{13}C$-DOC in marine samples tend to be long and tedious usually requiring highly specialized, expensive equipment, large sample volumes, and a number of steps to remove carbonates and quantitatively convert DOC into CO_2 (by UV oxidation and/or combustion in an O_2 atmosphere) for eventual off-line analysis by mass spectrometry (Bauer *et al.* 1992, Fry *et al.* 1993). Alternatively, concentrating a sample (by lyophilization or evaporation) to obtain $\delta^{13}C$-DOC by solid-state elemental analysis coupled to an isotope ratio mass spectrometer (EA-IRMS) is a frequently chosen option. This approach works well when the ratio of DOC to inorganic salt is relatively high (Gandhi *et al.* 2004), however the low DOC to salt ratios that characterize estuarine/marine samples introduce a high degree of uncertainty and poor reproducibility in the measurement (St-Jean 2003), limiting this approach to freshwaters. Considering the importance of coastal zones to the general health of the global ocean as well as the significant role they play in the global economy, understanding how coastal phenomena are related to the carbon cycle is of growing importance.

Generally $\delta^{13}C$-DOC is more depleted in freshwater systems (-26 to -30 ‰) and more enriched towards marine sites (-22 to -20 ‰) and the signature in the open ocean is relatively invariant with depth or location (Fry *et al.* 1998).

δ^{13}C-DOC mixing behaviour between the fresh and marine end-members in estuaries and coasts has been modeled (Peterson *et al* 1994) and when unperturbed, most systems can be predicted to a good degree. However when a coastal zone or estuary has been perturbed either due to climate change or land-use changes, the organic carbon dynamics may also be altered in a number of ways that are difficult to detect by current remote sensing techniques or by simple DOC quantitation. Monitoring these alterations allows for a better understanding of carbon biogeochemical cycling and the extent to which the ecosystem as a whole is affected. δ^{13}C-DOC is at the same time one of the most effective and potentially the simplest approach to interpret these processes. Though δ^{13}C-DOC can provide highly informative data towards the understanding of dissolved carbon dynamics, analytical limitations have precluded its routine measurement in estuarine, coastal and marine systems.

The direct coupling of wet oxidation total organic carbon (TOC) analyzers to IRMS instruments (WO-IRMS) has recently been reported (St-Jean 2003, Bouillon *et al.* 2006, Osburn and St-Jean 2007) and greatly simplifies the measurement of δ^{13}C-DOC to a high degree of accuracy and precision, particularly for freshwater samples. In this set-up, a volume of water is injected into a reaction vessel containing a chemical oxidant (e.g., sodium persulfate) and/or exposed to UV light to oxidize DOC to CO_2. The sample flow is then directed through halogen scrubbers and chemical reductants typically used in EA-IRMS instrumentation, and finally to the mass analyzer. However, the large sample volumes required for a typical WO-IRMS analysis of marine DOC (up to

25 mL (Bouillon *et al.* 2006)) preclude its use for volume-limited samples, such as surface sediment marine pore-waters. By modifying a WO-IRMS system to be more amenable to marine samples through adjustments made to the WO system and improving IRMS sensitivity, accurate and reproducible measurement of as little as 2 mL of a coastal marine sample was achieved (Osburn and St-Jean 2007). The authors note however that following as few as 10 sample injections (~2.5 hours of analysis time), halide gases produced from the oxidation conditions as well as salt deposition in the flow lines of this system lead to rapid corrosion of some parts of the reaction vessel, fouling of the halide trap and exhaustion of the reducing agents, in addition to flow restriction in the lines.

In a recent inter-laboratory DOC analysis comparison study, 61 of 68 participants reported results with high-temperature catalytic oxidation (HTC) TOC analyzers, reflecting their use as the overwhelming tool of choice for quantitative DOC analysis (Sharp *et al.* 2002). In these instruments a small volume of sample (50-150 μL) is injected over a catalyst capable of generating oxygen radicals (such as Pt-impregnated alumina (Bauer *et al.* 1993) or silica rods (Qian and Mopper 1996)) at high temperature to quantitatively convert DOC to CO_2, which is then detected by non-dispersive infrared (NDIR) spectrophotometry. One advantage of HTC is the low volumes needed for analysis compared to wet oxidation (0.050 to 0.200 *vs.* 2 to 25 mL per injection), which allow running more replicates from smaller sample volumes. Because of the popularity and convenience of HTC-based analyzers compared to the WO variety, some groups have reported efforts to couple them to IRMS instruments (Kaldy *et al.* 2005,

Lang *et al.* 2007, De Troyer *et al.* 2007*)*. The hyphenated system generally involves trapping, either with sorbents (Kaldy *et al.* 2005) or cryogenically, with liquid N_2, (Lang *et al.* 2007, De Troyer *et al.* 2007) the CO_2 in the stream of carrier gas as it exits the TOC, then directing the flow (on- or off-line) to an EA-IRMS system for $\delta^{13}C$ determination. In an off-line cryogenic trapping system in which trapped sample gases are introduced into the combustion column of an EA-IRMS the accurate determination of the $\delta^{13}C$-DOC of deepwater marine samples (~44 μM C) was made possible but required 2-3 hours of analysis time and up to 20 mL per sample (Lang *et al.* 2007). Applications of on-line HTC-IRMS analysis for $\delta^{13}C$-DOC are generally suited to high-concentration DOC samples such as sediment pore-waters (Kaldy *et al.* 2005) or interstitial soil DOC (De Troyer *et al.* 2007). HTC-IRMS has also been designed to determine the $\delta^{15}N$ of total dissolved nitrogen (TDN) (Huygens *et al* 2007) but again detection limits are poor and are at least a full order of magnitude higher than what is typical of natural systems.

Here we describe an on-line HTC-IRMS system for the simultaneous quantitative and stable isotope measurement of DOC in natural (marine and freshwater) samples using a Shimadzu TOC 5000A instrument, one of the more widely used TOC analyzers (Sharp *et al.* 2002*)*. The overall approach consists of cryogenically trapping gas flowing from the TOC analyzer, then directing the flow to the reduction and gas chromatography columns of an EA-IRMS system, and finally towards the IRMS in a setup similar to one used for the analysis of $\delta^{15}N$-TDN (Huygens *et al. 2007*). In the system described here, comparatively fewer

major modifications to the HTC analyzer are needed and a much cheaper, more available catalyst that allows pure He to be used as a carrier gas is employed. Additionally, cryogenic trapping of combustion gases carry the advantage of focusing CO_2 resulting in sharper IRMS peaks. Superior detection limits to other on-line HTC-based TOC-IRMS systems are obtained owing to the systematic elimination of most sources of background CO_2, and open the door for routine δ^{13}C-DOC analysis of marine waters.

2.2 Experimental

2.2.1 Reagents and Standards.

IAEA-CH-6 certified sucrose standard (International Atomic Energy Agency, -10.45 ± 0.03 ‰ (Coplen *et al.* 2006)), Suwannee River Fulvic Acid standard (SRFA, International Humic Substances Society, -27.6 ± 0.12 ‰) and β-alanine (Sigma-Aldrich, -26.18 ± 0.33 ‰ standardized in-house against several certified materials by EA-IRMS) were used as reference δ^{13}C-DOC compounds. Potassium hydrogen phthalate (KHP) was obtained from Shimadzu and is the conventional quantitative DOC standard. Unless otherwise noted, standard solutions were prepared in ultra pure water (Millipore Simplicity 185 equipped with a Simpak®1 cartridge) over a wide range of concentrations (30-1050 μM C), acidified with 1 drop of TraceSELECT® grade HCl (SigmaAldrich) and prepared regularly. Standard additions of SRFA to marine waters was carried out (see Supporting Information for experimental details). In addition, low-carbon (44-47 μM C) deep Sargasso Sea consensus reference material (DSS-CRM, Lot # 00-12, D. Hansell, U. Miami), routinely used for validation and quality control of TOC

instruments (Hansell and Carlson 2001, http://www.rsmas.miami.edu/groups/biogeochem/CRM.html) was obtained to validate the system for δ^{13}C-DOC in natural waters. Several end-member natural samples were chosen to reflect salinity and DOC concentration extremes expected in the analysis of coastal samples (see Appendix 2 for sample details). Conventionally, marine DOC concentrations are given in terms of μM of elemental C, whereas EA-IRMS measurements are usually expressed in terms of mass, thus to maintain consistency all concentrations and mass concerning DOC or analyte CO_2 are expressed as moles of elemental C.

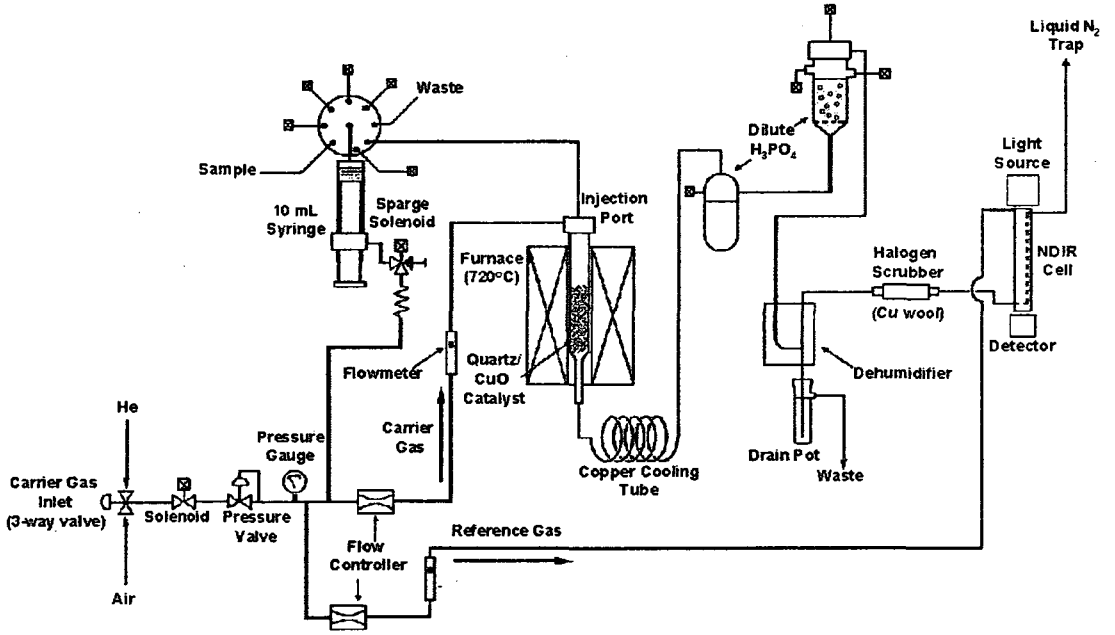

Figure 2-1 Schematic diagram of the modified Shimadzu TOC-V_{CPH} used in this study.

2.2.2 Total Organic Carbon Analyzer.

The Shimadzu TOC-V_{CPH} 5000A Total Organic Carbon Analyzer, with external sparge gas option was used. The original tubing on the instrument consisted of ⅛" o.d. PTFE. Samples are drawn (4-6 mL, acidified to pH ≤ 2 with 6

N HCl), and sparged with carrier gas for 2-5 minutes, to remove dissolved inorganic carbon (DIC) species, i.e., carbonates. After DIC removal, 50-150 μL are injected over 2 mm Pt-impregnated silica spheres (Shimadzu) heated to 720 °C in a 2.8 × 30 cm (12 cm hot zone) quartz tube, where quantitative oxidation of DOC to CO_2 occurs. The combustion gases are directed through a ⅛" o.d. Cu cooling tube, a pure water trap to trap volatile inorganics, the DIC reaction vessel, a dehumidifier, a Cu-wool halogen trap, and a 0.2-μm aerosol filter, before non-dispersive infrared (NDIR) spectrophotometric detection of CO_2. The carrier gas is then stripped of CO_2 by a soda lime scrubber and recycled as CO_2-free reference gas for NDIR.

2.2.3 Total Organic Carbon Analyzer Modifications.

Figure 2-1 shows the schematic of the modified instrument. Firstly, IRMS requires high-purity He to be used as carrier gas, a viable option when the original catalyst (Pt-impregnated silica spheres) is used (Chen *et al* 2002). However this catalyst was found to be a very significant contributor to background CO_2 (see Results section) and was replaced with 2 × 2 mm quartz rods mixed with cupric oxide (Qian and Mopper 1996) (~60:40 mass ratio), thus the catalyst itself is an oxidant in the combustion chamber. The amount of CuO should not exceed this ratio and care should be taken to ensure homogeneity of the catalyst mixture to avoid combustion column cracking when cooled. A three-way valve was installed to allow the user to switch between air and He as carrier gas, depending on whether the instrument is used for TOC (NDIR quantitation only) or TOC-IRMS (NDIR quantitation and δ^{13}C-DOC). The carrier gas is also

switched to air overnight to regenerate the cupric oxide when oxidation efficiency becomes inconsistent (e.g., when the standard deviation for the analysis of quantitative standards exceeds ± 5 %, typically after ~300 natural sample injections). A 1-cm thick layer of cobaltous silver oxide was also added at the bottom of the column as a primary halogen trap.

It has also been recognized that the PTFE tubing used in DOC analyzers is permeable to atmospheric CO_2 (Lang *et al.* 2007), and with the exception of the sampling tube, all were replaced with ⅛" o.d. stainless steel tubing, while retaining the original fittings. Other polymeric tubing materials were considered, such as PEEK or ECTFE, both materials with CO_2 permeabilities significantly lower than PTFE, however permeation with these materials would still occur, as opposed to stainless steel for which gas permeability is zero. In parts where metric sized tubes and fittings are used (such as pressure valves), the original PTFE was used as a sleeve over the end of the ⅛" stainless steel tubing.

Several drops of reagent-grade 85 % phosphoric acid were added to ultra pure water in the water trap to prevent CO_2 dissolution in the system, thus reducing sample carry-over. The only necessary modification to the Pelletier dehumidifying unit was the replacement of the ½" o.d. plastic waste tube with ⅛" o.d. polypropylene tubing to prevent increased flow out of the unit which sometimes occurred when trapping high DOC concentration solutions. Attempts were made at bypassing components of the system that are superfluous when used in the TOC or TOC-IRMS modes (e.g., the DIC reaction vessel), but the result was poor peak shape and varying retention time that adversely affected peak integration of the NDIR signal (data not shown).

Finally, carrier gas exiting the NDIR is redirected away from the CO_2 scrubber and towards a $Mg(ClO_4)_2$ water trap just prior to the cryogenic trapping loop. The external sparge gas option available on the TOC-V_{CPH} is used to provide a flow of CO_2-free gas for the NDIR reference allowing quantitation of TOC.

2.2.4 Cryogenic trapping, chemical reduction and chromatographic separation of TOC gases.

The trapping loop is a 1.5-m long ⅛" o.d. stainless steel tube set in a 10-cm diameter coil. To trap CO_2 exiting the TOC, the coil is immersed in a bath of liquid nitrogen (LN). The pressure from the TOC is insufficient to force gas flow through the gas chromatography column of the EA-IRMS thus a series of valves was set so that the flow from the TOC and the flow towards the EA system do not simultaneously overlap (Figure 2-2), a situation which would cause overpressure in the TOC, and loss of flow to the IRMS resulting in the introduction of ambient air to the ion source of the IRMS. Trapped sample gases produced from combustion (mainly CO_2, and various NO_x) are released by removing the loop from the LN trap. The gas flow is introduced into the reduction column (quartz tube packed with elemental Cu heated to 680°C) of a GV Instruments EuroVector IsoPrime EA-IRMS system under control of MassLynx 4.0 software (Manchester, UK) to chemically reduce the NO_x species present in the sample

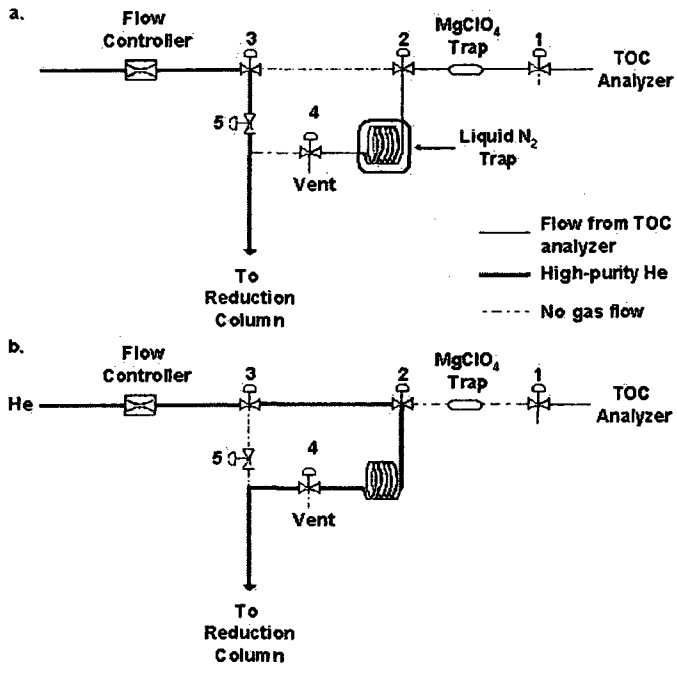

Figure 2-2 Schematic of the trapping loop and valve system. (a) trapping and (b) release configurations. To switch from trapping to release, first valve 2 is switched, followed a few moments later by valve 4 and valve 5, and valve 1 follows to vent the TOC. To return the system to the trapping mode, first valve 5 is switched, followed by valve 4, then valves 1 and 2 simultaneously. This sequence is followed to prevent ambient CO_2 from entering the system, ensure a constant supply of carrier gas to the IRMS and avoid pressure build-up in the TOC.

gas to N_2. Interference from some NO_x species, in particular N_2O (m/z = 44) with the measurement of CO_2 necessitates this step (Rennie *et al.* 1996). A layer of cobaltous silver oxide placed at the beginning of the Cu reduction column acts as a third halogen trap. After passing through a second $Mg(ClO_4)_2$ water trap, gases are separated in the regular GC column (set at 40 °C) of the EA system and transferred to the IRMS.

2.2.5 Isotope ratio mass spectrometer.

The ion source parameters are fine-tuned for carbon regularly and vary within normal limits (see Appendix 2 for details). Research grade CO_2 (Praxair) is used as monitoring gas and set to match the expected intensity of trapped

sample gas, ~1 nA (as major height). Baseline signal of ^{13}C with this instrument is typically $<10^{-4}$ nA resulting in signal to noise ratios of 12 for the lowest sample intensities (Figure A2-1). Because peak intensity of natural samples is low and consequently in a different linear dynamic range than typically used for this instrument, trials were conducted with the trap current set at higher values (up to 400 μA), but the gain in sensitivity is offset by the severe loss of dynamic range (data not shown). Thus to maintain consistency and avoid overlapping linear dynamic ranges, peak heights for natural samples and dissolved standard compounds between 0.2 and 1.5 nA were targeted during routine analyses (Table A2-1, Figure A2-2). Reproducibility of the monitoring gas was typically within ± 0.01 and 0.05 ‰ in a given day.

2.2.6 $\delta^{13}C$-DOC measurement

For $\delta^{13}C$-DOC analysis, the trap setup is initially configured as in 2-2a. The TOC instrument first draws 1 mL of the acidified sample to rinse the syringe, followed by an additional 6 mL of sample which is then sparged of DIC for 6-10 minutes with He (shorter sparge times typically used for NDIR detection proved insufficient for the more sensitive IRMS). Six 150 μL injections are required to reach IRMS detection limits in marine samples (i.e. < 80 μM C), and samples above 200 μM C can be accurately determined with only two traps. For consistency in background correction of $\delta^{13}C$-DOC data it is prudent to keep the number of traps equal for all samples (see Results and Discussion). The sample loop is immersed in LN immediately following the first injection. In some cases (following standard compounds, or the first sample of the day) two 150 μL

samples are injected and not trapped, acting as a system rinse, purging the TOC of carry-over from previous samples. When all injections are complete, the valves are configured as in Figure 2-2b, the sample loop is removed from the LN trap, and the isotope analysis using the IRMS software is launched. Following this sequence resulted in reproducible retention times as detected by the IRMS (265 ± 2 seconds, n = 27 over a two-day span). Immediately following the IRMS run the trap lines are reconfigured as in Figure 2-2a. Analysis time ranges between 38 and 44 minutes for low- to high- concentration DOC samples trapped six times, respectively (10 minutes sparge, 22 to 28 minutes of trapping, 6 minutes for IRMS analysis). When a series of samples is being analyzed time can be saved by sparging the next sample while the first sample is detected by IRMS, so that it takes ~30 minutes per sample, or 16 samples in an 8-hour work day.

2.2.7 Data Analysis.

Calibration and regression analysis is carried out using MATLAB (The Mathworks, Natick, MA, Version 7.0, Release 14). Total least squares was used when two measured quantities were correlated (e.g., $\delta^{13}C$ and NDIR signal area). Data was corrected for TOC background as described in the next section.

2.3 Results and Discussion

A direct coupling of the TOC analyzer to the IRMS inlet with only a halogen trap between the two was first carried out with IAEA-CH-6 and β-alanine dissolved in pure water to investigate the feasibility of hyphenating the two instruments for $\delta^{13}C$-DOC measurements. These experiments resulted in acceptable IRMS peak shape (Figures A2-1(b) and A2-4) and also demonstrated

no discernable isotopic fractionation during combustion in the TOC analyzer (-10.89 ± 1.0 ‰). However, the lower detection limit of

Table 2-1. Analytical performance of the modified TOC analyzer

Characteristic	Before	After modification[b]
Retention Time (minutes)	1.05	1.05
Peak Width (minutes)	1.4	1.4
Precision (%)	1.9	1.6
Accuracy (%)	1.4	0.27
Response Factor(mV·min/mmole C)	1.055	1.082
Stn 23 330m (μM C)[c]	62.8 (± 1.3, n =6)	64.2 (± 0.9, n = 16)

[a]KHP standard solutions (40-800 μM C, n = 43) during routine analyses of marine and estuarine water samples spanning one month, fall 2006 using air as carrier gas. [b]β-alanine, IAEA-CH-6, and KHP standard solutions (30-900 μM C, n = 345), Aug-Nov 2007) with high-purity He as carrier gas. [c]St. Lawrence Estuary, sampled June 2006.

the set-up was only ~1500 μM C for IAEA-CH-6 which is inadequate for most natural waters (typically 40-400 μM C in the water column and up to 1200 μM C in sediment pore-waters). As injection of larger volumes would lead to overpressure and possible cracking of the combustion tube of this TOC system, cryogenic trapping with LN after NDIR detection was set up to increase the amount of analyte CO_2 directed to the IRMS (described above). Hyphenation of the unmodified TOC to the IRMS via the reduction column of the EA system resulted in acceptable accuracy (after blank correction) of L-alanine solutions down to concentrations of 105 μM C with 8 traps (-26.46 ± 0.90 ‰, n = 4). In order to improve both the precision and detection limits to encompass the full range of DOC concentrations found in natural systems, modifications targeting CO_2 permeation through the TOC were carried out.

2.3.1 Performance characteristics of the modified TOC analyzer.

The modifications carried out on the Shimadzu TOC-V_{CPH} improved accuracy and precision without adversely affecting any other performance characteristics (Table 2-1). In addition, the combustion efficiency of the silica rods with cupric oxide using high-purity He as a carrier gas is equivalent to the more expensive Pt-based catalyst, demonstrating the use of an oxygen pulse or He/O_2 carrier gas mixtures for analyses of natural DOC samples is not necessary. Background CO_2 released from the TOC (determined by IRMS) decreased ~2.3-fold following the described modifications. DSS-CRM was measured as 46.5 ± 2.6 μM C (n = 18) with the modified TOC, in agreement with what has been reported for this lot (D. Hansell, U. Miami, pers. comm. 2007). In addition, multiple consecutive injections of a natural and sucrose-spiked freshwater sample collected from the St. Lawrence River near Québec City in June 2006 show no consistent trend in the measured concentration over these consecutive injections indicating that combustion efficiency remains unaffected and carry-over is not significant, as previously demonstrated for a silica rod-based catalyst system (Qian and Mopper 1998).

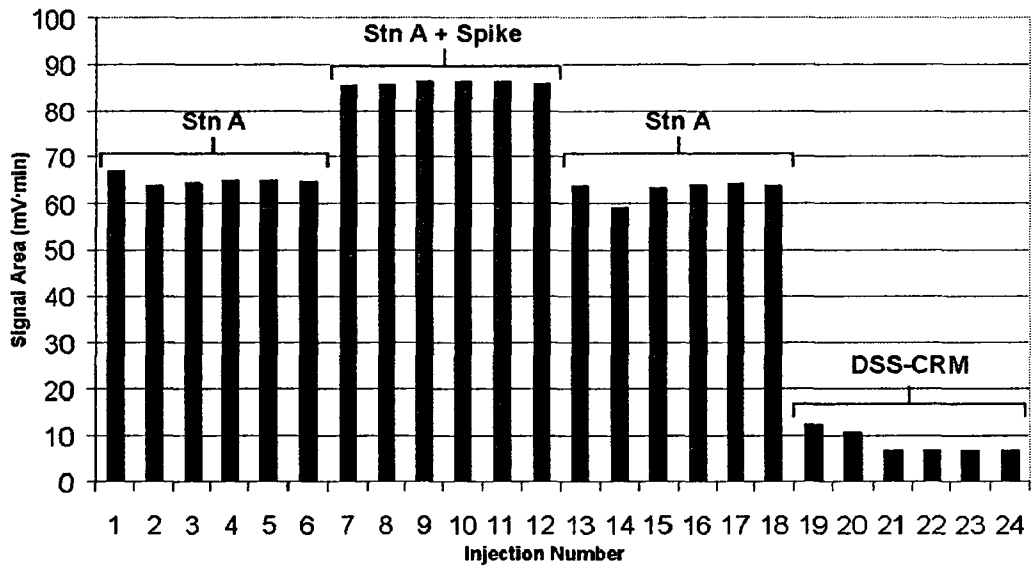

Figure 2-3 Combustion efficiency and carry-over of the catalyst system with He as carrier gas. Six injections of a natural freshwater sample from the St. Lawrence River (denoted Stn A, 424.8 μM) followed by six injections of the same sample spiked with sucrose (578.6 M), six injections of Stn A, followed by six injections of DSS-CRM (45 μM). Only the first two injections of DSS-CRM (# 19 and 20) show evidence of carry-over.

Analysis of DSS-CRM following these freshwater sample injections confirms this result (Figure 2-3). When catalyst regeneration with air was necessary it would usually take two days of ultra pure water blank injections with He carrier gas to purge the system and return the background to acceptable levels for HTC-IRMS analysis of low-DOC marine samples.

2.3.2 δ^{13}C-DOC determination: Background contribution and standard solution measurement.

As was discovered with DOC quantitation over a decade ago, background signal determination largely controls accuracy and precision of isotopic analysis by TOC-IRMS. All TOC systems, regardless of oxidation mode, are characterized by relatively high background CO_2 levels, originating from desorption of CO_2 from surface-active catalyst in the case of HTC analyzers and outgassing/

contamination of reagents in the case of WO analyzers (Peltzer *et al.* 1996) or leaching of carbon from mechanical components (Spyres *et al.* 2000), including CO_2 permeation through plastic and PTFE tubing (Lang *et al.* 2007). Because direct measurement of background is not possible with WO-IRMS systems developed to date, blank signals have been calculated through unsupervised iterative non-linear optimization techniques (Bouillon *et al.* 2006, Osburn and St-Jean 2007) with blank defined as the value resulting in the least variation of the corrected sample δ^{13}C-DOC. This approach results in a highly variable background δ^{13}C (from -12 to -20 ‰ (Bouillon *et al.* 2006)) which seems unlikely since the source of background CO_2 is relatively stable (Peltzer *et al.* 1996, Spyres *et al.* 2000). The calculated variability can be reduced by forcing the precision of the calculated results to match experimental precision, and to repeat the iterative calculation several times to ensure false computational results are rejected. An advantage to this HTC-IRMS system over WO-IRMS is the ability to directly measure the blank signal, allowing experimental validation of background correction procedures, whether they are based on an iterative calculation approach or standard addition experiments.

Calibration with δ^{13}C-DOC standards show that the relative blank contribution to the total signal intensity was strongly correlated to the concentration and not to the absolute mass of CO_2 that is trapped (Figure 2-4). This observation supports previous findings that blank contribution from HTC-based analyzers is constant (Peltzer *et al.* 1996, Spyres *et al.* 2000) and could therefore be determined experimentally.

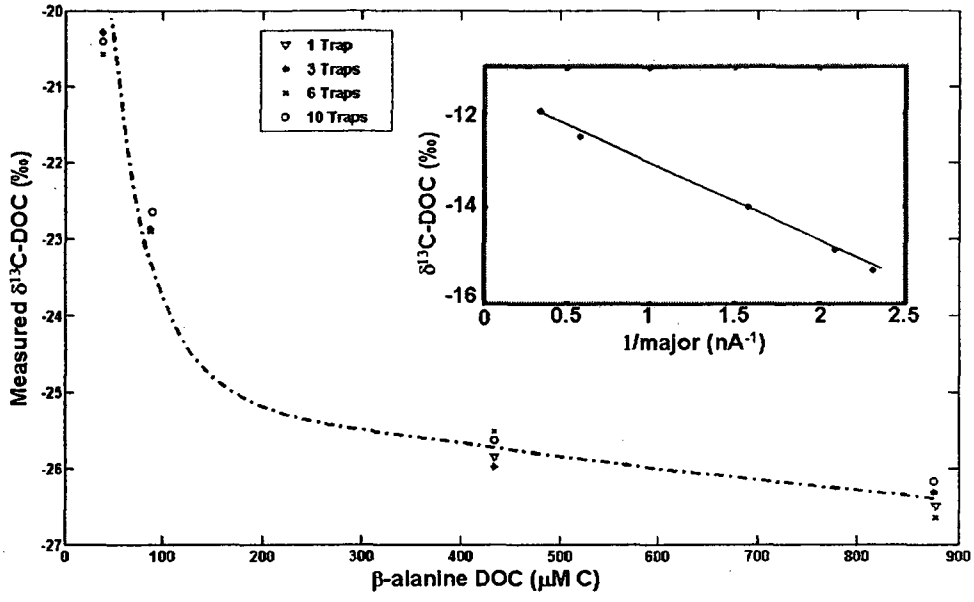

Figure 2-4 Concentration dependence of δ^{13}C-DOC of β-alanine standard solutions. Solutions of 39, 90, 433 and 875 μM C were trapped 3, 6 and 10 times each, with the two higher concentration solutions trapped once. Inset: Plot of IAEA-CH-6 δ^{13}C-DOC and the inverse of the IRMS signal intensity to determine blank contribution. See equation in text for details.

Our results revealed that extrapolation of the blank signal based on isotopic mass balance, as described (Fry *et al.* 1992), from a total-least squares regression analysis of standard solutions is the most appropriate and convenient method to determine blank signal (Equation 1):

$$\delta_m = \frac{(\delta_h - \delta_{bc}) \times \eta_h}{\eta_m} + \delta_{bc} \qquad (1)$$

Plotting the measured δ^{13}C (δ_m) as a function of the inverse of the measured sample intensity (η_m) gives the blank-corrected δ^{13}C (δ_{bc}) as the y-intercept (Inset Figure 2-4). Background δ^{13}C (δ_h) can be calculated from the slope once the intensity of the blank (η_h) is determined, either experimentally or through least squares regression of NDIR and IRMS signal areas. Based on regular, three or four point calibrations with β-alanine and IAEA-CH-6 standard

solutions, the blank in this system was calculated as 0.9-1.2 ± 0.1 nmolC/min and $\delta^{13}C$ drifting between -15.51 to -17.78 ± 0.21 ‰ over a period of 3 months. Generally the more depleted values would follow catalyst regeneration or periods when the TOC is used for NDIR quantitation and over the course of two or three days of regular use return to the more enriched background. These calculated results are validated by time-series traps of the background, which confirmed the magnitude (0.9 ± 0.1 nmolC/min), and isotopic ratio (-15.39 ± 0.32 ‰, n = 5) of the blank. The variation noted above, particularly after catalyst regeneration, highlight the importance of daily measurement of background at the start and end of any run to detect minor drifts in the background. A typical analysis involving 6 traps is, on average, equivalent to ~20 nmoles C of background, or a signal intensity of ~0.11 nA, but has drifted over a span of five months between 0.15 and 0.04 nA. This system is capable of analyzing as little as 9.2 nmoles C for background, and six traps of deep marine samples is typically about 40 nmoles C (Figure A2-1). We attribute the low IRMS detection limits to the fact that we bypass the EA combustion column. After determination of the blank isotopic ratio and signal intensity, the following isotope mass balance equation is applied to a measured sample (Equation 2)

$$\delta_s = \frac{\delta_m \times \eta_m + \delta_h \times \eta_h}{\eta_m - \eta_h} \qquad (2)$$

where δ_s is the stable isotope ratio of the analyte, with other parameters defined above. The procedure was first tested by deriving blank from IAEA-CH-6 calibration and applied to β-alanine standard solutions of 39, 90, 433 and 875 μM

C and is as consistent with respect to accuracy and precision as by EA-IRMS (Table 2-2). Similar precision was obtained for IAEA-CH-6; however the isotope ratio was consistently depleted by ~1 ‰ compared to EA-IRMS analysis. This was attributed to a background contribution from the water used to dissolve the standard. Trapping ultra pure water injections showed the blank signal was consistently depleted compared to the instrumental background. The difference in peak height intensity of the ultra pure water was however not significant enough to differentiate quantitatively from instrumental background. The $\delta^{13}C$ of the contaminant in the ultra pure water was approximated to -29 ‰. Such a value is close to that of β-alanine which may explain why no effect of this contaminant is evident in the more depleted standard. To confirm this hypothesis a St. Lawrence River freshwater sample collected in June 2006 that has been measured for $\delta^{13}C$-DOC by EA-IRMS (Hélie and Hillaire-Marcel 2006) and HTC-IRMS (Table 2-2) was spiked with IAEA-CH-6 (at a 1:4.2 sucrose:natural sample ratio). Following blank-correction and isotope mass balance

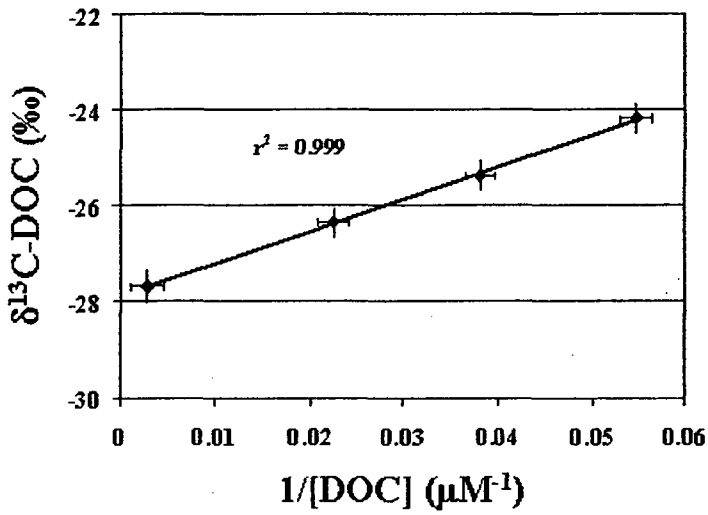

Figure 2-5 Standard addition Experiments. IHSS SRFA standard spiked in deep Lower St. Lawrence Estuary. The intercept of the regression is the $\delta^{13}C$ of the spike compound (Osburn and St-Jean 2007) and is -27.8 ± 0.12 ‰, and r^2 = 0.99 (n = 12).

calculation, the δ^{13}C-DOC of IAEA-CH-6 was comparable to the value obtained using the EA-IRMS. Since the typical δ^{13}C-DOC range of natural samples is -18 to -30 ‰, mixtures of standards (2.2:1 and 6.9:1, β-alanine:IAEA-CH-6) were prepared at 125 and 68 μM C and in both cases match well with the calculated δ^{13}C-DOC (-21.46 *vs.* -21.15 ‰ and -24.22 *vs.* -24.04 ‰, respectively). Following the procedures outlined here results in a correlation coefficient of 0.993 between HTC-IRMS and other methods used to determine δ^{13}C-DOC (from published results or determined by EA-IRMS in our lab, data presented in Table 2-2). It should be noted that blank correction is not necessary for samples with DOC concentrations exceeding 600 μM C (e.g., wastewater, sediment pore-waters, and others).

Table 2-2. Accuracy of δ^{13}C-DOC measurement for standard reference compounds and natural end-members

Sample[a]	Depth (m)	Salinity[b] (psu)	[DOC] (μM)	TOC-IRMS δ^{13}C-DOC[c] (‰ *vs.* PBD)	TOC-IRMS Standard Deviation	TOC-IRMS n	EA-IRMS δ^{13}C-DOC[d] (‰ *vs.*	EA-IRMS Standard Deviation	EA-IRMS n
β-alanine	-	-	45-1050	-26.59	0.29	13	-26.18	0.33	60
IAEA-CH-6[e]	-	-	106.6	-10.63	0.24	3	-10.62	0.19	29
IHSS SRFA	-	-	2188	-27.68	0.09	3	-27.6	0.12	n.a.
DSS-CRM	2600	36.2	46.5	-21.37	0.33	3	-20.9	-	-
St. Lawrence	40	0.1	424.9	-26.76	0.13	6	-26.8	0.2	2
Porewater[f]	2-3 cm	n/a	310.1	-22.84	0.16	3	-	-	-

[a]See text for acronyms and sample details. Further details are found in Appendix 2. [b]Salinity determined *in situ* by conductivity detection. [c]After background correction of data (see text for details). [d]β-alanine and IAEA-CH-6 are obtained from in-house EA-IRMS analysis. DSS-CRM and St. Lawrence are derived from the literature.[3,27] IHSS SRFA is the value reported by the IHSS, however sample number was not available. [e]From standard addition to St. Lawrence freshwater sample. [f]From the marine end of the St. Lawrence Estuary.

2.3.3 Accuracy of δ^{13}C-DOC Measurement.

Because simple soluble organic compounds do not fully represent the structural and functional diversity found in natural DOC, and a consensus reference natural δ^{13}C-DOC sample is not available, accuracy was tested with the IHSS SRFA standard. The δ^{13}C-DOC of the SRFA stock solution was within ± 0.1 ‰ of the value reported by IHSS (Table 2-2). Standard additions to a St. Lawrence Estuary marine end-member sample ([DOC] = 62.8 μM C, S = 34.5 psu) were carried out (Table 2-3, Figures 2-5 and A2-3). In these standard addition experiments the δ^{13}C of the spike can be determined from the *y*-intercept of the linear relationship between the measured δ^{13}C-DOC *vs.* the inverse of signal intensity (Osburn and St-Jean 2007) and this experiment yielded an average δ^{13}C-DOC of the SRFA standard within ± 0.2 ‰ the value given by the IHSS (Figure 2-5). In addition, mass balance calculations for both the natural DOC and SRFA standard agree with values determined experimentally for non-spiked sample and high concentration solutions (Table 2-3). Though our data agrees with the reference isotope data given by IHSS, and IHSS humic substances were used to validate one WO-IRMS system (Osburn and St-Jean 2007), we still feel an unprocessed high concentration DOC freshwater sample is needed to help anchor the analytical validation of δ^{13}C-DOC methods. This is particularly evident in light of the poor precision of the mass-balance-derived δ^{13}C-DOC values compared to the experimental precision typically expected in both systems (Figure 2-5 Osburn and St-Jean 2007 and Table 2-3) and is likely due to solubility problems associated with these materials (Appendix 2).

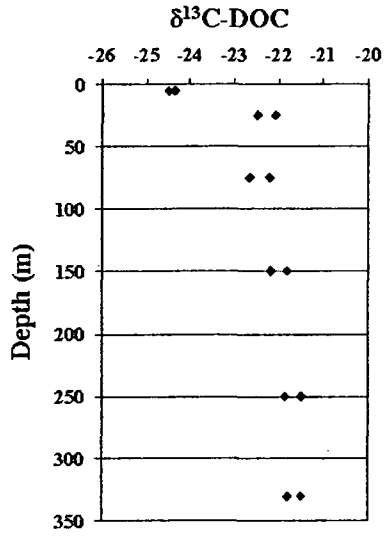

Figure 2-6 δ^{13}C-DOC depth profile for a station in the Lower St. Lawrence Estuary. Samples were measured in duplicate and never exceed more than 0.3 ‰ deviation. See Appendix 2 for sample collection and processing details.

2.3.4 Application to Natural Samples.

The system was used to test extremes of natural samples to include high concentration DOC freshwater (St. Lawrence River), low concentration marine deepwater (DSS-CRM) (Table 2-2), and a stratified estuarine water column profile (Lower St. Lawrence Estuary) (Figure 2-6). After blank correction, the DSS-CRM and St. Lawrence River samples agree with literature data (Druffel *et al.* 1992, Hélie and Hillaire-Marcel 2006, Lang *et al.* 2007). It should be noted that while the δ^{13}C-DOC value for DSS-CRM reported here is similar to what has been reported for off-line HTC-IRMS (-21.7 ± 0.29 ‰, Lang *et al.* 2007), it is slightly more depleted compared to a more classic method (-20.9 ‰, Druffel *et al.* 1992) and significantly different from WO-IRMS (-19.5 ± 0.4 ‰, Bouillon *et al.* 2006), highlighting the need for δ^{13}C-DOC inter-calibration of selected natural samples. The estuarine water column profile shows conservative behaviour of

δ^{13}C-DOC, reflecting a salinity and temperature gradient in the upper 75 m of the water column, with no further variation with depth as well as demonstrating the precision typical of solid-state IRMS measurements (Figure 2-6). It should be noted the full profile was analyzed in one working day (12 sample injections, four standards). Finally, a marine sediment porewater sample was analyzed in triplicate and shows excellent precision for these high-DOC, complex matrix samples (Table 2).

Table 2-3. Measured and calculated values for IHSS SRFA standard addition to a marine end-member[a]

Standard Addition Concentration (μM C)	Measured Concentration (μM C)	Measured δ^{13}C-DOC (‰)	Calculated IHSS SRFA δ^{13}C-DOC	Calculated Deepwater δ^{13}C-DOC
0	62.8 ± 1.8[b]	-22.52 ± 0.11	-	-
54.7	55.4 ± 2.0	-24.20 ± 0.38	-27.04 ± 0.27	-22.93 ± 0.69
109.4	117.5 ± 2.0	-25.38 ± 0.56	-27.70 ± 0.44	-22.28 ± 0.98
218.8	220.7 ± 0.5	-26.35 ± 0.17	-27.98 ± 0.45	-21.77 ± 0.48

[a]Four different solutions were prepared and analyzed at each standard addition level.
[b]The value for the "0" addition is the natural concentration of the sample based on independent calibration, and is subtracted from the total concentration to obtain the measured concentration of the spike.

The on-line HTC-IRMS system described here can withstand a large number (~300) of difficult sample injections (high salinity and/or high DOC) before catalyst regeneration or fouling by salt deposition occurs and is at least as accurate and precise as other methods for δ^{13}C-DOC for a diverse range of sample types. It opens the possibility for large-scale routine δ^{13}C-DOC analysis of the most common natural sample types, and should be of particular use towards a more complete understanding of DOC sources and cycling in complex environments with large DOC concentration gradients such as estuaries, coastal

zones, and interstitial boundaries. If used in concert with the IRMS sensitivity increase reported in Osburn and St-Jean 2007, the sample throughput of HTC-IRMS could potentially increase as much as two-fold. The current lack of certified standard materials can be side-stepped by standard addition of soluble reference standards to isotopically characterized natural samples. However, until the absence of certified reference samples representative of the structural and matrix complexity of natural DOC is properly addressed, assessing the isotopic accuracy of any δ^{13}C-DOC instrumentation will remain problematic. Ideally these references should be unprocessed natural samples and cover DOC freshwater and marine end-members; we suggest using DSS-CRM as the low-DOC high-salinity anchor. Future directions in HTC-IRMS system development should focus on further reducing the background signal of the TOC instrument to lessen the impact of blank correction on natural-abundance stable isotope analyses, which would also aid in reducing total analysis time and material consumption.

Dual isotope analysis, either isotopes of several atoms (e.g., Hélie and Hillaire-Marcel, Peterson *et al.* 1985, McCallister *et al.* 2006, Middelburg and Herman 2007) or multiple isotopes of one element[1] has proven a highly effective method to decipher organic matter sources and cycling in a variety of materials (particulate matter, sediments, plants, etc.) from a number of ecosystems (oceanic, estuarine, lakes) but seldom carried on dissolved species because of difficulties outlined above. As measurement of δ^{15}N-DON has been demonstrated with high concentrations of standard compounds (Huygens *et al.* 2007), the feasibility of dual isotope carbon-nitrogen (δ^{13}C/δ^{15}N) analysis in natural

dissolved organic matter samples should be explored using the HTC-IRMS approach.

Chapter 3.

Expressing biomarker data in stoichiometric terms: shifts in distribution and biogeochemical interpretation

Published as:

Panetta, R.J., and Y. Gélinas (2009) *Limnology and Oceanography: Methods*, 7: 277 – 286.

3.1 Introduction

Compound-specific identification, or biomarker analysis, in organic geochemistry lends an added dimension to the understanding of the carbon cycle in environmental systems, in many cases highlighting subtle yet important details not revealed by bulk analyses alone. For example, the stable carbon isotopic signature of estuarine organic matter is generally proportional to the fraction of terrestrially-derived material, however the analysis of lignin oxidation products can shed light on its degradation state and provide more specificity on the origins of the terrestrial matter (e.g., Louchouarn *et al.* 1999). This higher level of understanding is invariably linked to the quantitative analysis of target biomarkers, and in particular to the calculation of the relative abundance of individual or groups of molecules to the total mass of quantified biomarkers. The analysis of source material (without which biomarker interpretation is extremely limited, as explained in Volkman *et al.* 2008), and its comparison to natural samples has led to the development of a number of effective, simple and robust biomarker-derived proxies that have advanced the understanding of carbon dynamics in environmental systems, including the terrestrial to aquatic ratio (TAR), the alkenone paleothermometer (U^{k}_{37}), and average chain length (ACL), among several others (see Meyers 2003, Eglinton & Eglinton 2008 for two thorough reviews on the topic).

The use of biomarker analysis in organic geochemistry arose from the overlapping interests of petrochemistry, geology and ecology through the link between current biological production of organic matter to its deposition,

diagenesis and ultimate transformations to petroleum products. Alkanes, fatty acids, amino acids, polycyclic aromatic hydrocarbons, lignin, pigments, etc., were identified in a number of studies attempting to address the source of natural organic matter (e.g., Treibs 1936), its transformations in the environment (e.g., Brown 1972), and how it might be converted to petroleum through geological processes (e.g., Breger 1960).

Table 3-1. List of some common proxies and their interpretation.

Proxy	Formula	Interpretation
Terrestrial to Aquatic Ratio[1]	$TAR_{HC} = \frac{C_{27} + C_{29} + C_{31}}{C_{15} + C_{17} + C_{19}}$ $TAR_{FA} = \frac{C_{24} + C_{26} + C_{28}}{C_{12} + C_{14} + C_{16}}$	Used to interpret terrestrial *vs.* aquatic dominance
Alcohol Preservation Index[2]	$API = \frac{C_{24}OH + C_{26}OH + C_{28}OH}{(C_{24}OH + C_{26}OH + C_{28}OH) + (C_{24} + C_{26} + C_{28})}$	Infer TOC diagenesis
Alkenone Paleothermometer[3]	$U^{K'}_{37} = \frac{[C_{37:2}]}{[C_{37:2}] + [C_{37:3}]}$	Surface water temperature
Carbon Preference Index[3]	$CPI_{HC} = \frac{2 \times [\sum Odd\ nC_{23} to\ nC_{31}]}{\sum Even\ nC_{22} to\ nC_{30} + \sum Even\ nC_{24} to\ nC_{32}}$ $CPI_{FA\ or\ OH} = \frac{2 \times [\sum Even\ nC_{22} to\ nC_{30}]}{\sum Odd\ nC_{21} to\ nC_{29} + \sum Odd\ nC_{23} to\ nC_{31}}$	Terrestrial *vs.* aquatic source indicator
Average Chain Length[4]	$TAR_{FA} = \frac{27 \times C_{27} + 29 \times C_{29} + 31 \times C_{31}}{C_{27} + C_{29} + C_{31}}$	Differentiate grasses from leaves Temperature

[1]Bourbonniere and Meyers were the first to formulate the equation as presented. [2]Poynter and Eglinton (1990). [3]Bray and Evans (1961) and Kvenvolden (1966) formulated the hydrocarbon and alkanoic acid/alkanol equations, respectively. [4]Cranwell (1973) first presented the equation.

Historically, the most widely studied group of biomarkers are lipids, broadly defined as any compounds extractable with organic solvents such as dichloromethane or hexane, which comprise hundreds of distinct organic

chemicals. For simplicity, lipids can be liberally separated into three branches; (1) hydrocarbons, (2) alkanoic acids, and (3) sterols. Other biomarkers that are routinely reported in biogeochemical studies include lignin phenols (e.g., Hedges and Parker 1976, Louchouarn *et al.* 1999), pigments (Schubert *et al.* 2005) and amino compounds (e.g., Kaiser and Benner 2008), among others (Killops and Killops 2004)

In the time that has passed since rock extracts were first analyzed by gas chromatography, analytical methodology has become more sophisticated and specialized, particularly over the last decade, but the general approach remains the same: extraction, fractionation, chromatographic separation and quantitation of the compounds of interest. As data analysis has progressed and still evolves, various biomarker proxies identifying the source materials, diagenetic state, and reaction pathways have emerged from the quantitative data and some common ones are summarized in Table 3-1. Biomarker-based proxies are invaluable tools but because they are based on a limited number of compounds they can potentially lead to an oversimplification or generalization of a given system when addressing total organic carbon sources or diagenetic processes. Since a biomarker analysis can result in the identification and quantification of sometimes hundreds of compounds in a single analysis, using all the information obtained (i.e. all biomarkers identified and quantified) would intuitively result in a more powerful interpretation for the system under study (e.g. Oros and Simoneit 2000). However such complex data sets are not easily deciphered, and statistical tools more capable of sifting and sorting data of this nature have recently been put to

use, such as principal components analysis (Zimmerman and Canuel 2001, Yunker *et al.* 2005), clustering analysis (Dittmar *et al.* 2007), and multivariate curve resolution (Salau *et al.* 1997). These methods are all dependent on the precise quantitation of individual compounds and their weighting relative to other compounds within their class. These approaches will likely become more prominent in the search for unique or novel biomarker proxies for additional robust and far-reaching interpretations of environmental processes, as shown by the use of PCA in the development of the amino acid degradation index (Dauwe and Middelberg 1998).

While biomarker data analysis has significantly evolved, an important characteristic remains constant, at least for lipids and lignin: the expression of the concentration of individual compounds in mass yields. This can be attributed to habit borne of day-to-day simplicity; a standard solution containing *n* mg per unit volume is prepared to determine the response factor of the detector used. Even today, the concentration of most commercial analytical standards used in biomarker analysis is given in mg per litres (e.g., ASTM Petroleum standards for gas chromatographic analysis of n-alkanes). Thus biomarker analysts express concentrations of lipid biomarkers including alkanes, alkanoic acids, sterols, n-alcohols, among many others, as either $\mu g\ g^{-1}$ of dry weight or mg g of organic carbon $(OC)^{-1}$; lignin phenols as mg $100mgOC^{-1}$; polycyclic aromatic hydrocarbons (PAH) as part per billion dry weight or mass percent of total PAH, etc. In contrast, amino acids and amino sugars are conventionally expressed as moles, an historical consequence of the fact that these analyses were conducted

by biochemists interested in molar ratios of these biochemicals (e.g., Benson and Hare 1975).

Although it may be more practical in the laboratory to use mass units, one basis of biomarker data interpretation is fuelled by the idea of comparing the total amount of one molecule present in a sample to another, in other words stoichiometric ratios. Stoichiometric expression also allows direct comparability between different classes by introducing molar consistency. The conversion from mass to stoichiometric units is not trivial and results in shifts of the weighted distribution of some biomarker profiles with potential to alter biomarker interpretations, especially those making use of multiple biomarker "fingerprints" that incorporate full suites of compounds (e.g., Oros and Simoneit 2000, Zimmerman and Canuel 2001, Yunker *et al.*. 2005). In this note, theoretical treatments of Gaussian-modeled and randomly generated data sets representing a number of biomarker classes, complemented by recalculated biomarker data from the literature, are used to illustrate the impact of a mass- to a mole-based conversion of biomarker data on their environmental interpretations.

3.2 Analysis

3.2.1 Data sets

Two flavours of modeled data sets comprised of m samples $\times$ n variables (compounds) were generated with routines developed in MATLAB (The Mathworks, Natick, MA, Version 7.0, Release 14). In all cases, there are 50 samples, while the number of compounds varies between biomarker classes (12 for lignin phenols and up to 31 for fatty acids, for example). The first set,

expressed as mass percent, is based on a bimodal Gaussian distribution, designed to mimic a transition from high-molecular weight to low molecular weight dominated envelopes of long-chain lipid biomarkers (n-alkanes, n-alkanols, and n-alkanoic acids) as is found in many natural samples. The second is a random data set representing the long-chain lipid biomarkers as well as the commonly reported sterols, polycyclic aromatic hydrocarbons and lignin oxidation products, expressed as mass percent. The random data are generated as a control to the modeled sets to ensure any differences resulting from changes in units are not due to trends intrinsic to the ordered distribution of Gaussian data. A string of random values was created to represent the summed biomarkers. Each value was then converted in a step-wise fashion from relative mass % to mg gOC^{-1} or mg $100mgOC^{-1}$ for lignin, to μmole $moleOC^{-1}$, and finally to a mole fraction (as %). All data are normalized to the amount of organic carbon to eliminate the influence of mineral dilution, and because biomarkers are typically used to reflect the origin and fate of organic carbon. Direct comparisons are made between absolute (mg gOC^{-1} *vs.* μmol $molOC^{-1}$) and relative (mass percent *vs.* mole fraction) concentrations.

3.2.2 Standardized Data

Since there is no consensus or treatise on how biomarkers should be analyzed using multivariate statistical approaches that exploit factors controlling data structure and variability, we will investigate how data distribution patterns within a sample and how overall data structure can be affected. One of the best approaches to render data sets comparable with respect to distribution and

variability is to autoscale – a procedure commonly used prior to multivariate analyses. Known in Microsoft EXCEL® 2002 as the "STANDARDIZE" function, autoscaling first mean-centers a data point then divides by the standard deviation;

$$Sc = \frac{x - \bar{x}}{\mu}$$

Equation 3-1

where x is the data point in question, $\bar{x}$ is the mean of all data for that sample (e.g., the mean biomarker concentration for 31 fatty acids quantified in a single sample), μ is the standard deviation, and Sc is the unitless scaled value. This procedure eliminates the effects of absolute intensity differences and scales the data so variance is unity and all values occur over the same range (±1.0 units), maintaining data structure, but allowing direct comparisons of data sets through the same lens.

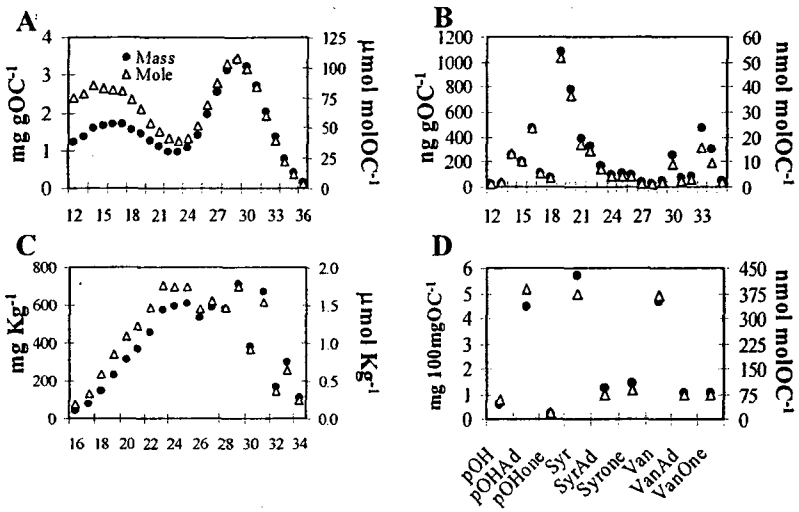

Figure 3-1 Redistribution of relative weighting of biomarker profiles when converting mass-based units to stoichiometric-based units. Numbers below *x*-axis in (*a-c*) denote carbon chain length. (a) Gaussian modeled n-alkane profile of individual biomarkers as mg gOC^{-1} or µmol $molOC^{-1}$; (b) Fatty acid profile, including n-alkanoic and alkenoic acids, reported for St. Lawrence Estuary sediments as ng gOC^{-1} or nmole $moleOC^{-1}$ (Colombo *et al.* 1997) (c) n-alkane homologous series identified in lignite coal smoke particulate matter expressed as mg $Kg(d.w.)^{-1}$ or µmol $Kg(d.w.)^{-1}$ (Oros and Simoneit 2000); (d) Lignin phenols resulting from CuO oxidation of *Pinus Caribeae* expressed as mg $100mgOC^{-1}$ and nmol $molOC^{-1}$ (pOH, Syr and Van are p-hydroxybenzoic, syringyl and vanillyl derivatives, respectively) (Hedges and Parker 1976). In all profiles the relative proportion of low molecular mass components increases, and in the case of (c) and (d) the major compound is changed.

3.2.3 Calculations and Interpretation

A discussion and interpretation of data based solely on relative distributions is conducted for data sets to highlight the effect of the choice of units on the interpretation of biomarker data. Published data that are recalculated and referred to in the text include a coal smoke particulate fingerprinting study (Oros and Simoneit 2000), lipids extracted from Arctic Ocean sediments (Belicka *et al.* 2002), estuarine dissolved organic matter (McCallister *et al.* 2006), estuarine sediments (Colombo *et al.* 1997), and lignin phenols isolated from source materials (Hedges and Parker 1976).

3.3 Results and Discussion

3.3.1 Weighting Redistribution

Figure 3-1a shows a modeled n-alkane profile depicting a typical riverine-influenced system as either mg gOC^{-1} or μmol $molOC^{-1}$. The general bimodal trend exists in both mass and mole-normalized profiles, but it is clear that the abundance of low molecular weight components is elevated in mole-normalized data relative to high molecular weight components, with the ratio of the major peaks of each envelope, C_{17} and C_{27}, increasing from 0.51 to 0.77, or by 51 %. This general trend is true for all biomarkers, regardless of class, however as shown in Figure 3-2, the factor by which the biomarker concentration changes is not constant, thus stoichiometric-based expression may lead to differing interpretation and conclusions compared to mass-based expression. This is especially true for families of biomarkers that cover a wide range of molecular masses (~100-600 amu), such as alkanes, fatty acids, or long-chain alcohols, and potentially other classes that are typically on the low molecular weight end (< 300 amu) of the range, such as lignin phenols.

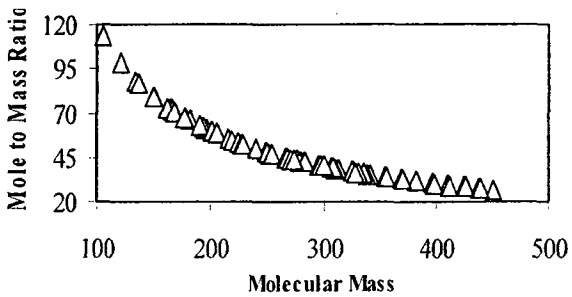

Figure 3-2 The ratio of molar (μmol molOC^{-1}) to mass (mg gOC^{-1}) normalized data. Individual Gaussian and randomly modeled alkyl (n-alkanes, n-alkanoic acids, and n-alkanols) and ring (sterols, polycyclic aromatic hydrocarbons, lignin phenols) biomarkers are calculated. Low molecular weight components are more strongly altered than the higher molecular weight components.

Gaussian-modeled alkanoic acid data in the form of mg gOC^{-1} and μmol molOC^{-1} was autoscaled, and the difference between the two standardized ratios (henceforth "residual") was calculated. If the distribution between data sets remains identical, the residual is equal to zero, but if the weighting has shifted, residuals will be non-zero values. Figure 3-3 shows a plot of the residuals as a function of molecular mass for three modeled samples (A and B are dominated by low mass and high-mass alkanoic acid envelopes, respectively, and M is a mixture of the two), and clearly the scaled values are not identical. Generally, the residuals are positive on the low molecular mass side and decrease with molecular weight, reflecting a shift to higher relative abundances for low mass molecules. The overall trend is for greater deviation between normalizations when the relative abundance of both the high and the low mass compounds are not negligible, further emphasizing how individual data structures can be altered in different manners.

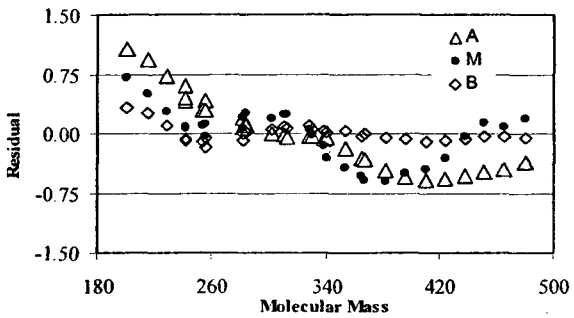

Figure 3-3 Residuals of modeled mass and stoichiometric data. Modeled n-alkanoic acid data expressed as mg gOC^{-1} and to μmol $molOC^{-1}$ is autoscaled. Residual (difference between the scaled mass- and molar-based values) are plotted as a function of molar mass. Shown are three samples (two end-members and a mixture, see text for details).

Biomarkers are often expressed as the percent contribution to the total summed biomarkers, or relative to the major compound in a set, allowing easy comparison between data sets that differ by orders of magnitude in their absolute amounts of target biomarker class. Such relative abundances also lay the foundation for quantitative biomarker interpretation, and an elevation in the relative amount of a compound from one sample to another implies an increasing contribution of the source of that biomarker to the total organic carbon pool of a sample. The expression of biomarkers as a stoichiometric fraction results in the same trends as the absolute concentration, as discussed above.

Figure 3-1(b-d) shows how the overall distribution of biomarkers in real samples is altered when concentrations are mole-normalized. For n-alkanoic acids isolated from the St. Lawrence Estuary (Figure 3-1b), the dominant compound in the series clearly remains the 7-hexadecenoic acid (C_{16}), but the relative abundances of acids greater than 21 carbons in length are significantly reduced relative to the smaller compounds. For example, hexacosanoic acid

(C_{26}) is lowered from 78 to 55 % of the relative abundance of 7-hexadecenoic acid. The n-alkanes of lignite (coal) combustion products (Figure 3-1c) show significant changes in their entire distribution, the most notable being the dominant n-alkane changing from n-C_{29} to n-C_{23}. Interesting differences in the shape of the main envelope is also incurred, where a smooth Gaussian shape is no longer rounded at the apex, but plateaus between the C_{23} and C_{25}. The shift in relative distribution is not limited to alkyl chain-based biomarkers, as the lignin phenol profile of *Pinus Caribeae* wood shows (Figure 3-1d). When expressed as mass (mg $100mgOC^{-1}$), syringaldehyde is dominant over vanillin and p-hydroxybenzoic acid (100:82:79 ratios, respectively), but as moles (μmol $molOC^{-1}$), the ratio is significantly altered, so that all three are almost equally proportioned (100:104:98).

These examples show how the relative distribution may change when biomarkers are expressed as moles and that these differences are not limited to a single class or family of compounds. They also highlight the subtlety by which different samples can be affected, including the "shape" of the data distribution, as well as the abundance order of a biomarker profile.

Extending the average chain length calculation (Table 3-1) to include all alkyl functionality compounds identified (ACL_{TOT}) provides an additional measure of data redistribution upon relative weighting. Again looking at the data found in Oros and Simoneit (2001), the recalculated ACL_{TOT} of some components remain invariant (e.g. n-alkenoic acids of sub-bituminous coal), while for n-alkanoic acids the change varies from a decrease of 0.5 units to as many as 2 full units of chain

length (Table 3-2). In McCallister *et al.* (2006), the majority of estuarine fatty acids identified are < 22 carbons in length, and for 12 samples reported, the average ACL very slightly decreases from 16.8 to 16.6 when switching from mass-based to mole-based concentrations; thus in this case redistribution of abundance does not occur. In another example, the ACL_{TOT} of saturated n-alkanoic acids isolated from nine locations in the Arctic Ocean (Belicka *et al.* 2002) decrease on average 0.8 units, from 20.2 to 19.4, with the largest decrease by 1.1 units. What is clear is that the changes that occur do not affect all samples in a similar manner, and generally, but not as a rule, samples with higher ACL_{TOT} values are affected most strongly.

3.3.2 Biomarker Interpretation

Because the relative abundance of low molecular mass compounds generally increases when expressed in molar fractions, interpretation based on their relative contributions may change as well. Biomarker classes in which the lowest molecular mass is greater than 350 amu such as sterols, hopanoids, and long-chain alkenones are not significantly altered. Though individual relative abundances change significantly, the interpretation of PAHs and lignin phenols are very little affected, but this is because of the manner in which they are treated, with most proxies comparing structural isomers or compounds of relatively close molecular mass (see Louchouarn *et al.* 1999 and Lima *et al.* 2005 for examples of lignin and PAH proxies, respectively). A brief treatment of published lignin data (Hedges and Parker 1976) illustrating changes in the relative distribution of individual phenols, but little change in interpretation of

Table 3-2. Shifts in the ACL_{TOT} of alkyl substituent biomarker classes of four types of coal smoke particulate matter based on either mass (mg kg^{-1}) or moles (nmol kg^{-1}). Data recalculated from Oros and Simoneit 2001.

	Lignite			Brown			Sub-bituminous			Bituminous		
	Mass	Moles	Diff	Mass	Moles	Diff	Mass	Moles	Diff	Mass	Moles	Diff
Alkan-2-ones	26.1	25.0	-1.1	26.0	25.1	-0.9	24.5	23.4	-1.1	21.8	20.8	-0.9
Alkanals	24.2	22.9	-1.3	22.4	21.4	-1.0	-	-	-	-	-	-
Alkanes	26.0	25.3	-0.7	25.9	25.1	-0.8	25.6	25.0	-0.6	23.5	22.8	-0.7
Alkanoic acids	28.5	28.0	-0.5	24.6	23.8	-0.8	22.9	20.9	-2.0	16.5	15.7	-0.8
Alkanols	26.9	26.3	-0.6	25.7	25.5	-0.2	-	-	-	-	-	-
Alkenes	24.1	23.6	-0.5	24.7	24.4	-0.3	20.8	20.7	-0.1	20.3	19.9	-0.5
Alkenoic	17.9	17.5	-0.4	-	-	-	17.5	17.1	-0.4	18.0	18.0	0.0
Alkylbenzenes	26.0	25.1	-0.9	23.6	22.6	-1.0	23.8	23.1	-0.7	21.2	20.4	-0.7

proxies is found in Appendix 3).

The vast majority of biomarker work is derived from lipids, thus consistency in their reporting is of pivotal importance. Using a combination of relative contributions and biomarker proxies, the quantitative analysis of this most widely used class of compounds has been employed to infer source apportionment in recent (e.g, Colombo *et al.* 1997, Yunker *et al.* 2005, McCallister *et al.* 2006) and ancient samples (e.g., Feakins *et al.* 2007), to estimate microbial biomass (Parkes and Taylor 1983), to evaluate diagenetic alterations within settling particles (e.g., Wakeham *et al.* 1997) and subsequent sedimentary processes (e.g., Madureira *et al.* 1995), and for paleoecological reconstruction (e.g., Zimmerman and Canuel 2001, Sluijs *et al.* 2006), among many other environmental and ecosystem conditions and processes examined (see Eglinton and Eglinton 2008 for a recent review). Any changes in the data distribution within this class of compounds could potentially impact the interpretations of a wide swath of biogeochemical processes.

Proxies based on compounds within a narrow mass window, such as U^{k}_{37}, in which molecules differing by 2 amu are compared, or those that make use of the full range of compounds, well distributed over both the numerator and denominator, such as the CPI, (see Table 3-1 for full equations of some lipid biomarker proxies) are the least affected. The proxies that are most altered are those comparing high molecular weight to low molecular weight components, such as the TAR ratios.

The TAR ratio is defined as the quotient of the concentrations of either odd chain length C_{27}-C_{31} over C_{15}-C_{19} n-alkanes (TAR_{HC}) or even chain-length C_{26}-C_{30} over C_{12}-C_{16} n-alkanoic acids (TAR_{FA}) (Bourbonniere and Meyers 1996). Elevated TAR values are generally attributed to terrestrial sources and lower values as aquatic. Because the relative contribution of low molecular weight components (the denominators in TAR equations, Table 3-1) tends to increase when mass-based concentrations are converted to mole-based ones, both stoichiometric TAR ratios give considerably lower values compared to their mass-based TAR counterparts. This is demonstrated with modeled and random data sets where the ratio of molar based TAR ratios are only 56 to 60% that of the mass based ratio, generally trending towards a greater disparity between the differently normalized sets as the TAR decreases. A similar trend is found for Arctic Ocean sedimentary fatty acids (Belicka *et al.* 2002), where the TAR_{FA} decreases by a factor of 0.64 ± 0.01 for nine samples upon conversion to molar units. As long as the TAR value is greater than 0.1, this decrease by a factor of ~0.6 holds true for all literature data tested so far. Though the change in this proxy is relatively constant it highlights an important concept: the abundance of molecules considered of terrestrial origin is stoichiometrically overestimated relative to that of planktonic/microbial compounds when mass-based units are used.

Besides molecular proxies, a very common approach is to report the relative contribution from a sub-class of compounds to a total fraction, such as the relative proportion of phospholipid fatty acids to the total pool of identified

fatty acids. While in some cases this relative proportion remains more or less impartial to mass or mole normalizations, in others important processes can be overlooked with mass-based concentrations. For example, in an estuary with very little terrestrial biomarker influence (McCallister *et al.* 2006), mass-normalized data clearly show that the relative contribution of branched fatty acids in the dissolved phase remains invariant at ~10 % of total fatty acids across a salinity gradient, implying constant bacterial contributions to this pool of organic matter. However, upon conversion of the dataset to moles, a clear spike in the relative contribution of these bacterial markers is found in the marine end-member during the fall sampling season, with about 16% of the total fatty acids pool. This implies increased microbial biomass at this location that was not initially detected in the mass-based data set.

Relative abundance of major alkyl substituent compound classes from the extensive coal smoke fingerprinting study of Oros and Simoneit was recalculated (Table 3-3). In lignite, the most abundant compound class remains the n-alkanoic acids, however their relative abundance decreases from 35.5 to 31.5 %, while n-alkanols, n-alkanes and n-alkenes, originally separated within a range of 3.1 % (15.6 – 18.7 %) become almost equal, separated by only 0.5 % in stoichiometric abundance (17.7 – 18.2 %). In brown coal, the order of most abundant compound classes remains the same, but a noticeable change occurs in the difference between n-alkanoic acids and n-alkenes shrinking from 2.3 to 0.8 %, making them almost equal as the most abundant class. In sub-bituminous coals the relative abundances of alkyl class compounds is not significantly altered. The

Table 3-3. Shifts in the relative proportion (% of total composition) of alkyl substituent biomarker classes of four types of coal smoke particulate matter based on either mass (mg gOC^{-1}) or moles (nmol $molOC^{-1}$). Data recalculated from Oros and Simoneit 2001.

	Lignite			Brown			Sub-bituminous			Bituminous		
	Mass	Moles	Diff	Mass	Moles	Diff	Mass	Moles	Diff	Mass	Moles	Diff
Alkan-2-ones	3.7	3.8	0.1	15.6	15.0	-0.6	5.3	5.2	-0.1	22.1	20.6	-1.5
Alkanals	1.3	1.4	0.2	6.2	7.0	0.8	-	-	-	-	-	-
Alkanes	17.0	17.9	1.0	20.8	20.7	-0.1	60.7	57.8	-2.9	30.3	27.2	-3.2
Alkanoic acids	35.5	31.5	-4.0	25.9	25.1	-0.8	11.3	11.6	0.4	30.1	34.2	4.1
Alkanols	18.7	18.2	-0.5	5.4	5.1	-0.3	-	-	-	-	-	-
Alkenes	15.6	17.7	2.1	23.6	24.3	0.8	9.4	10.9	1.5	11.6	12.0	0.4
Alkenoic	1.2	1.7	0.4	-	-	-	2.4	3.0	0.6	0.7	0.7	0.0
Alkylbenzenes	7.1	7.8	0.6	2.6	2.9	0.3	10.9	11.5	0.6	5.2	5.3	0.1

most interesting and significant change occurs with bituminous coal, where as a function of mass, the relative abundance of n-alkanes and n-alkanoic acids are equal (30.3 *vs.* 30.1 %) but as a function of moles, the n-alkanoic acids are 7.1 % more abundant than the n-alkanes, due to the high abundance of relatively shorter chain components present in the acid fraction, as attested by the ACL_{TOT} (Table 3-1). There is a general trend of increasing relative abundance with decreasing chain length, but again it is neither a constant nor easily modeled change across all samples.

3.4 Conclusions

The underlying goal driving quantitative biomarker analysis is the determination of the quantity of a given compound originating from one source as compared to another, with the aim of deriving information on past or present environmental conditions and/or processes. We argue here that quantitative values should be expressed as moles to best reflect these molecular relationships, because moles, rather than grams, are the currency of molecules. Furthermore, the emergence and development of multivariate statistical analyses of biomarker data sets calls for consistency in the expression of all biomarkers to allow better comparability and transferability between not just different samples, but also different molecules within one sample. The aim of this work was to show that the conversion from mass-based units to mole-based units in biomarker analysis is not a trivial matter, but a calculation with potential to affect the way biomarker data is shaped and interpreted. This is an especially important point as the drive to develop novel molecular proxies through better understanding of the

relationship between biochemistry and environmental conditions has never been stronger (Eglinton and Eglinton 2008).

Chapter 4.

Polycyclic aromatic hydrocarbons in the St. Lawrence Estuary (QC, Canada): Transport, distribution and patterns as influenced by terrestrial organic matter

Submitted to Environmental Science and Technology,

May 26 2009.

4.1 Introduction

Polycyclic aromatic hydrocarbons (PAH) are fully conjugated fused six-membered ring organic compounds that are ubiquitous in the environment, originating from natural sources such as forest fires, microbial and plant biosynthesis, but more importantly from anthropogenic sources as a result of industrial, automotive, and urban activities (McVeety and Hites 1988, Wakeham *et al.* 1980, Silliman *et al.* 2000, and Lima *et al.* 2005). Early studies have clearly demonstrated significantly increased levels of PAH in natural systems since the industrial revolution, a discovery that generated much interest over the last decades as they are highly genotoxic to animals and have been linked to cancer in humans.

One of the more dramatic examples of the genotoxicity of PAH was the discovery of high cancer rates in beluga populations in the St. Lawrence Estuary (Figure 4-1) during the 1980s as reviewed in (Martineau *et al.* 2002). This finding spurred much research in understanding the biological and toxicological effects of organic pollutants in the St. Lawrence ecosystem (Cossa *et al.* 1983, Hellou *et al.* 1995, Lee *et al.* 1999), as well as potential modes of biological partitioning and uptake (Brion and Pelletier 2005, Barthe *et al.* 2008). However direct measurements of native PAH levels in the estuary are few and sparsely distributed (Dufour and Ouellet 2007), leaving an evaluation of primary sources to and distribution in the estuary uncertain.

Detailed investigations of PAH contamination in the St. Lawrence Estuary are limited to the maximum turbidity zone (Coakley *et al.* 1993), a location just offshore an aluminium smelting site in the lower estuary (Lee *et al.* 1999), or a

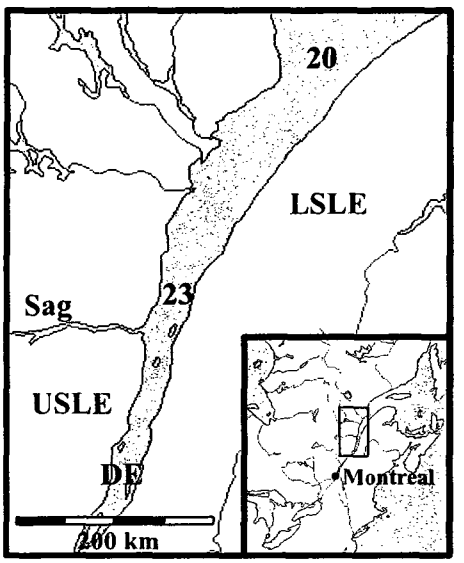

Figure 4-1 PAH Sampling locations in the St. Lawrence Estuary. Maximum turbidity zone (DE), the head (23) and the marine end-member (20) were sampled. Also indicated are the upper and lower estuaries (USLE, LSLE, respectively) and the Saguenay Fjord (SAG). Map generated with The Atlas of Canada Toporama mapping tool, http://atlas.nrcan.gc.ca/site/english/maps/topo/map

heavily contaminated major tributary, the Saguenay (Martel *et al.* 1986, Smith and Levy 1990), and are not usually concerned with the ecosystem as a whole. Some perspective on PAH atmospheric deposition to the lower St. Lawrence Estuary is gained from peatlands along the remote northern coast of the Gulf of St. Lawrence that were made part of a broad survey of the PAH depositional history in Eastern Canada (Dreyer *et al.* 2005a and 2005b). Peatlands, however, account for atmospheric delivery only and not what may be transported to the basin via suspended particulate matter, which at the peak of aluminium smelting in the 1970s was substantial (Smith and Levy 1990). Additionally, fluxes of pollutants into the water column from sediments are currently of concern in the

system as O_2 levels of the already hypoxic bottom waters (Gilbert *et al.* 2005) continue their decline. Knowledge of the sedimentary budget of PAH in these sediments may thus help in predicting the magnitude of such an efflux.

More importantly, PAH profiles in the St. Lawrence have not been analyzed with respect to natural organic matter within the context of organic geochemistry, which has long been recognized as relevant in their distribution and interpretation. Correlations between PAH concentration and total organic carbon content (Schwarzenbach *et al.* 1981) are well documented, as PAH associate strongly with hydrophobic moieties such as aromatic and aliphatic groups (Chefetz and Xing 2009, Keiluweit and Kleber 2009). To better understand distribution and partitioning of PAH, some researchers have coupled their analysis to organic geochemical biomarker proxies to elucidate associations of PAH with particular pools of organic matter, most often n-alkanes (e.g., Wakeham 1996, Yunker and MacDonald 2003, Countway *et al.* 2003, Wu *et al.* 2001) as well as other biomarkers (Prahl and Carpenter 1983, Mitra *et al.* 1999, Simpson *et al.* 2005). Results often show terrestrially-derived markers are correlated with naturally-occurring PAH (such as perylene and retene), while anthropogenic PAH tend to correlate with petrogenic alkanes. In a landmark study comparing PAH distribution to several biomarker classes, Prahl and Carpenter (1983) demonstrated the association of naturally-derived PAH with lignin-rich low-density particles, i.e., wood. Few other studies have used lignin phenols to elucidate PAH distribution, with recent examples (Mitra *et al.* 1999, Simpson *et al.* 2005) finding positive correlation between anthropogenic PAH and

lignin at sites that at one point in time were subject to heavy creosote contamination, a product used in pressure-treating lumber. Otherwise, to the best of our knowledge, the long-range distribution patterns of lignin phenols and PAH have seldom been studied together.

Organic inputs to the St. Lawrence Estuary are primarily affected by three anthropogenic activities: industry (aluminium smelting/pulping mills), agriculture and urban runoff. The significant role of the pulp and paper industry has been thoroughly reviewed via lignin geochemistry in the St. Lawrence Estuary (Louchouarn *et al.* 1999), and as an important factor influencing the organic geochemistry of this system and its tributaries over the last century it can be postulated that the organic-rich effluents may have played an important role in the distribution of PAH, in particular as a conduit for PAH from the heavily contaminated Saguenay Fjord to the estuary. The influence of agriculture on OM dynamics in this system has not been investigated nor the potential influence on downstream PAH deposition from run-off. In this work we present sedimentary PAH levels from three cores collected along an estuarine transect, and relate the distribution to bulk organic geochemical properties and lignin phenol parameters to give an assessment of the current and past state of PAH contamination, as well as the potential modes of transport in the system as affected by organic matter sources.

4.2 Materials and Methods

4.2.1 Sampling Locations, Preparation, and Bulk Analysis

The St. Lawrence Estuary (Figure 4-1) is a stratified system that is separated in two distinct regions (Dufour and Ouellet 2007); the relatively shallow, highly turbid upper estuary extending ~300 km from the mouth of the St. Lawrence River where intense estuarine mixing occurs; the lower estuary extends another ~300 km from the Saguenay Fjord to the Gulf of St. Lawrence, is characterized by the deep (> 300 m) Laurentian Channel, and is very well stratified with estuarine mixing of surface waters isolated from the hypoxic deep marine bottom waters (Gilbert *et al.* 2005). The lower estuary receives inputs primarily from the upper St. Lawrence Estuary as well as the Saguenay Fjord. Three locations along the St. Lawrence Estuary were sampled in June 2007 for this study (Figure 4-1), representing recently deposited fluvial sediments in the shallow (14 m) maximum turbidity zone (Stn DE), the head of the lower estuary (Stn 23) and the marine end-member (Stn 20), both deep water locations (>300 m depth). The top 30-40 cm of the sediments were collected with box-core, sliced and frozen at -80 °C until further treatment. Total nitrogen, organic carbon (OC) and $\delta^{13}C$ were analyzed on a Eurovector IsoPrime EA-IRMS, using sucrose ($\delta^{13}C$ -10.45 ‰, IAEA-CH-6) and β-alanine ($\delta^{13}C$ -26.0 ‰, SigmaAldrich) as certified and in-house standards, respectively. All samples were decarbonated by exposure to HCl fumes for 10 hrs prior to analysis.

4.2.2 Lignin phenol analysis

Lignin phenols were determined by alkaline hydrolysis and CuO oxidation, following the method described in (Louchouarn *et al.* 1999). Briefly, enough

sediment for ~3 mg OC was weighed with CuO, $Fe(NH_4)_2(SO_4)_2 \cdot 6H_2O$, and 8 wt% NaOH solution in an inert atmosphere and taken to 160 °C for 1 hour. Lignin phenols were extracted, derivatized to their trimethylsilyl ethers with BSTFA and quantified by GC-MS using an external calibration mixture. Eight lignin phenols were quantified; (vanillin, acetovanillin, vanillic acid, syringaldehyde, acetosyringone, syringic acid, *p*-coumaric acid, and ferulic acid) to calculate total dry-mass based (Σ_8, mg g d.w.$^{-1}$) and organic carbon-normalized (λ_8, mg 100 mgOC^{-1}) lignin phenol yields.

4.2.3 Polycyclic aromatic hydrocarbon analysis

Wet sediments corresponding to 200 – 1000 mg OC were spiked with deuterated absolute recovery standards and extracted with dichloromethane/methanol (2:1) until the extract was colorless. The crude extracts were concentrated to ~1 mL and silica gel chromatography run to isolate three polarity-defined fractions for lipid biomarker analysis (Panetta and Gélinas, in prep). The fraction containing PAH was eluted with a 10 % (v/v) toluene/hexane mixture, dried under N_2, and stored at -80 °C until time of analysis. Identification and quantitation was accomplished by single ion monitoring on a Varian Saturn 2200 GC-MS equipped with a HP-5 column (60 m, 0.25 mm i.d., 0.25 μm, J&W Scientific), using an external calibration with TCL Polynuclear Aromatic Hydrocarbons standard mixture (Supelco). Compound identification of PAH not present in the standard mix was done using their mass spectrum and by comparison to peak order in published chromatograms using the same stationary phase (Wu *et al.* 2001). Fifteen PAH were identified and

quantified (abbreviation and molar mass); Acenaphthalene (Ace, 152), Fluorene (Flu, 166), Anthracene (Ant, 178), Phenanthrene (Phe, 178), Fluoranthene (Flt, 202), Pyrene (Pyr, 202), Benzo[a]anthracene (BaA, 228), Chrysene (Chr, 228), Benzo[b]fluoranthene (BbF, 252), Benzo[k]fluoranthene (BkF, 252), Benzo[e]pyrene (BeP, 252), Benzo(a)pyrene (BaP, 252), Perylene (Per, 252), Dibenz(ah)anthracene (DahA, 278), and Benzo(ghi)perylene (BghiP, 276).

4.2.4 Statistical Analyses

For simplicity and comparability to previous studies, all compounds are expressed in conventional terms (e.g., ng g^{-1}). However for correlation analyses and principal components analysis (PCA), all compounds were converted to molality units (e.g., pmol g^{-1}) to reflect stoichiometric relationships (Panetta and Gélinas 2009). Pearson correlations and PCA were carried out using the WinSTAT® package for Microsoft Excel® (Version 2007.1). For PCA several robust normalizations have been used in PAH source apportionment modeling (e.g., Yunker and MacDonald 2003 and ref. therein), however in this work only associations between compounds was desired thus molal data are only autoscaled (mean-centered then scaled to standard deviation).

4.3 Results and Discussion

4.3.1 Bulk Organic Geochemistry

Complete data tables for all parameters (bulk, lignin, and PAH) can be found in Appendix 4. Sediments across the St. Lawrence Estuary are silty with an average porosity of 0.83 ± 0.04 (range 0.76 – 0.88), varying little with depth or location. Bulk organic geochemical characteristics follow expected trends based

on two end-member estuarine conservative mixing (Table A4-1). Stn DE, in the maximum turbidity zone, is clearly a terrestrially influenced location ($\delta^{13}C$ -25.5 ± 0.3 ‰); Stn 20 is relatively stable in the measured bulk parameters down core, showing a more marine isotopic signature ($\delta^{13}C$ -23.4 ± 0.4 ‰); Stn 23 falls between these two locations ($\delta^{13}C$ -24.2 ± 0.5 ‰), with 26 % OC loss and a 1 ‰ depletion in $\delta^{13}C$ from surface to ~40-cm sediment depth, both highly suggestive of diagenetic alteration (Gälman *et al.* 2009).

4.3.2 Lignin Phenols

The sedimentary lignin phenol geochemistry as well as the importance of pulp and paper mill effluents has been treated in this system and unless noted otherwise, all previous lignin values referred to in the text are published in (Louchouarn *et al.* 1999). In brief (Table A4-1), excellent correlation between Σ_8 and OC content ($r^2 = 0.94$, $p < 0.001$), as well as good correlation between Σ_8 (and λ_8) and $\delta^{13}C$ through the whole system ($r^2 = 0.84$, $p < 0.001$) attests to the importance of terrestrial inputs to the estuary and agrees with the interpretation of a conservative depositional regime (Dufour and Ouellet 2007 and ref. therein). Surface sediment λ_8 follows estuarine mixing, decreasing seaward. In the maximum turbidity zone (Stn DE), λ_8 is comparable to a previous measurement (4.33 in 1985 *vs.* 4.76 mg 100 $mgOC^{-1}$ here). Results obtained for Stn 20 are also consistent with nearby surface sediments reported previously. Lignin quantity and parameters measured in sediment layers 2 – 5 cm at Stn 20 reflect the pulp and paper inputs of the early half of the 20^{th} century, indicating the

relatively long-distance transport of particles through the water column from these industrial effluents.

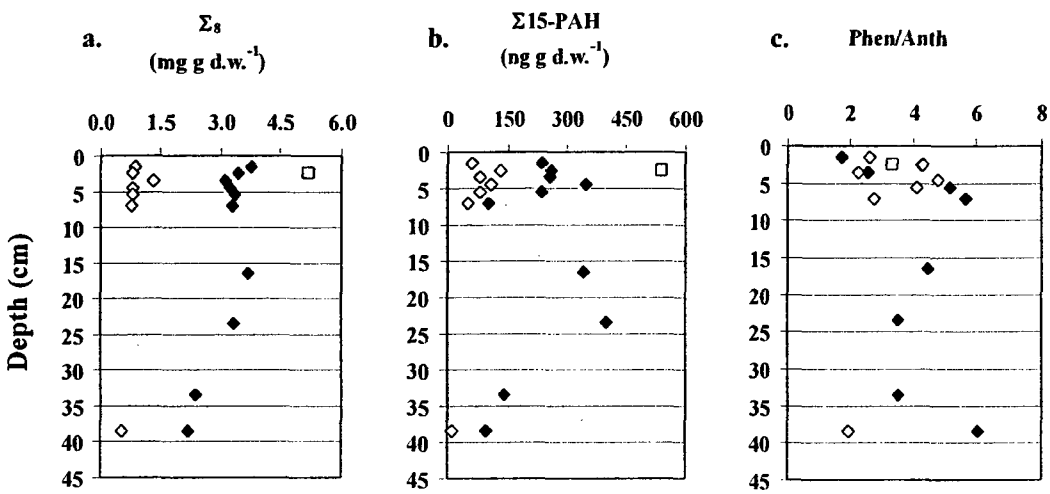

Figure 4-2 Sediment depth profiles of; (a) total lignin phenols; (b) total PAH; and (c) Phen/Anth diagnostic ratio. Stn DE (□), 23(♦), and 20 (◊).

Stn 23 is also in good agreement with previous studies, both quantitatively and qualitatively, including a maximum corresponding to the peak of pulping effluents into the Saguenay (Figure 4-2a). However, the increase in Σ_8 in the upper 4 – 5 cm at Stn 23 reported here is a phenomenon not seen in previous studies in the estuary and may be due to new or increased inputs from unidentified sources at this depth (e.g., increased runoff transported by tributaries), or degradation of lignin in the upper layers of the sediment. A follow-up to the detailed studies of Louchouarn *et al.* (1999) to understand the current state of lignin geochemistry in the system may therefore be warranted.

4.3.3 Polycyclic Aromatic Hydrocarbons – Trends

Concentrations of total PAH (Table A4-3) detected in this study (Σ15 – PAH) are in agreement with previous measurements of surficial sediments made in the system (Brion and Pelletier 2005), falling within the range of pristine to lightly perturbed systems removed from direct deposition from point sources (e.g., Yunker and MacDonald 2003, Wade *et al.* 2008). The lowest values are recorded at Stn 20, averaging 85.9 ± 29.6 ng g d.w.$^{-1}$ in surface (0-6 cm) and decrease to pre-industrial levels in the deepest layer (e.g., Wakeham 1996). Stn 23 is generally higher in PAH concentration averaging 244 ± 105 ng g d.w.$^{-1}$ through the whole core. The distinctive feature in the Σ15 – PAH profile at Stn 23 (Figure 4-2b) is a maximum at 21 – 26 cm, followed by relative stabilization in recent sediments. Stn DE, in the maximum turbidity zone, agrees with measurements published in tidal flats near this location (Coakley *et al.* 1993) and displays the highest Σ15 – PAH, but is lower than what may be expected considering (*i*) its proximity to an urban area (Québec City), and (*ii*) that it is a repository for particles originating from the industrialized Great Lakes watersheds (Stark *et al.* 2003). Normalization to organic carbon content results in the same trends and relative quantities (not shown).

PAH mass accumulation rates (MAR) are calculated from sedimentation rates published for the Lower Estuary (Smith and Schafer 1999), which are considered to have remained unchanged through the depositional period sampled here. MAR calculated at Stn 20 (55 – 118 ng cm^{-2} yr^{-1}) is on the same order as that measured in nearby peat bogs (Dreyer *et al.* 2005a and 2005b),

while at Stn 23 they range from ~200 – 600 ng cm^{-2} yr^{-1}. These rates remain well below values typically measured in other contaminated coastal zones, in particular the Saguenay Fjord which at one point had a MAR close to 1000-fold higher (Smith and Levy 1990). Because atmospheric deposition has not been measured at these precise locations, it is difficult to discern what proportion of PAH are the result of non-atmospheric deposition.

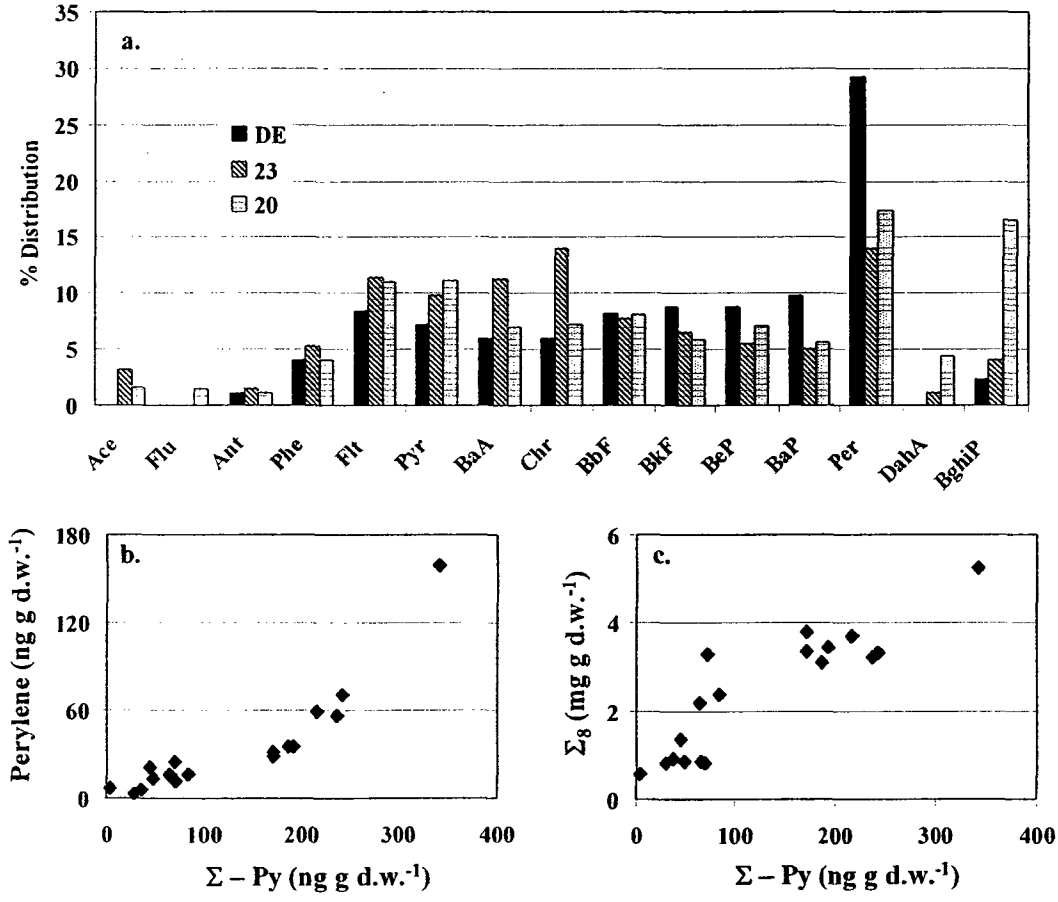

Figure 4-3(a) PAH profiles and relationship with non-anthropogenic paramters Relative mass percent distribution of 15 PAH identified in surface sediments; Relationship between ΣPy with; (b) Per, and (c) Σ_8 for all samples analyzed.

As a function of organic carbon, two trends exist in the system – a negative trend between Σ15 – PAH and OC for layers 1 – 26 cm of Stn 23 (r^2 = 0.84, $p < 0.001$), and a positive trend for all other samples (r^2 = 0.89, $p < 0.01$). A positive correlation has been recorded in many other systems, and sorption of PAH to organic matter has been postulated as a dominant factor in PAH transport and distribution patterns (Countway *et al.* 2003, Mitra *et al.* 1999). However, to the best of our knowledge, a negative trend between PAH and OC has not been reported in any other studies. Bulk properties (total carbon and $\delta^{13}C$) indicate diagenesis of organic matter in this core and a negative correlation likely reflects faster degradation of bulk organic matter than PAH. No correlation between total solvent extractable carbon and Σ15 – PAH is discernable (r^2 = 0.07, $p = 0.4$), a reflection of the independence of PAH delivery to the primary sources of lipids at these locations.

With some exceptions, the relative proportions of individual surface PAH across the transect varies little (Figure 4-3); BaA and Chr are more elevated at Stn 23; Per is by far the most dominant PAH at Stn DE; and BghiP is proportionately elevated at Stn 20. Otherwise, proportions of all other PAH are relatively constant and remain below 20 %, a situation typical of environments remote from primary PAH sources (Wade *et al.* 2008). Per is the most abundant in the entire system, constituting 17.3% of all PAH measured, similar to a lightly contaminated Chilean River system (Barra *et al.* 2008). In bogs studied along the north shore of the lower estuary, Phe was the most dominant compound, usually exceeding 30 % of total PAH (Dreyer *et al.* 2005a and 2005b), and though

present in most samples, neither Phe nor its isomer Ant ever exceed a 14 % proportion in the sediments studied.

Stn 20 is dominated by Per and BghiP at all depths, with Pyr and Flt also relatively important contributors (~10 % each) in the upper 6 cm. PAH above 200 amu all follow a similar trend, reaching a maximum at 3 – 4 cm, and generally correlate with $\Sigma 15 - PAH$. More variability, as well as an increased preponderance of other PAH is found at Stn 23, where Per is dominant at the surface, shifting to Chr in sub-surface (1 – 4 cm), and back to Per at 23.5 cm. With the exception of DahA and BghiP, compounds above 200 amu are important throughout the core and drive $\Sigma 15 - PAH$ ($r^2 = 0.99$, $p < 0.0001$). At Stn DE, PAH between mass 202 – 252 (except Per) average a proportion of ~8 % each. Overall, the PAH distribution in these sediments contrast sharply with those reported for nearby peat bogs (Dreyer *et al.* 2005a and 2005b), where Per was absent, and low-mass, more volatile compounds dominate profiles. The contrast between the bogs receiving direct atmospheric inputs and the sediments lying 300 m below the water surface is a testament to the importance of physical association and sorption/desorption chemistry of PAH in the water column prior to sedimentary deposition (e.g., Countway *et al.* 2003, Mitra *et al.* 1999).

4.3.4 PAH Sources and Delivery

PAH source apportionment in the absence of samples fully representative of a potential source is often accomplished by comparison to published PAH profiles for various carbonaceous materials (e.g. petroleum exhaust), in which specific PAH may dominate, and often isomer ratios are applied as "fingerprints."

However, due to the complexity of incomplete combustion processes (Lima *et al.* 2005), the significant role played by organic matter in the distribution of PAH (Countway *et al.* 2003, Mitra *et al.* 1999), as well as difficulty in deconvoluting multiple sources (Yunker and MacDonald 2003), caution must be applied with this approach. Many elegant models have been presented to deconvolute PAH sources in complex systems (e.g., Yunker and MacDonald 2003), but to obtain good results such models require a large number of samples, preferably from a diverse set of depositional settings and source regimes to better constrain particular sources. Due to these limitations and the lack of clear source profiles, we here use published ratios and certain diagnostic PAH to discern either pyrolytic, petrogenic or natural origins for PAH.

Comparison of the PAH distribution pattern and isomer ratios to those reported for surficial sediments collected downstream an aluminium smelter on the northern shore near Stn 20 (Lee *et al.* 1999) indeed demonstrates that PAH delivered to these sites become diluted and well mixed prior to deposition and point to multiple sources. Slight variability of several isomer ratios with depth occurs (illustrated with Phe/Anth in Figure 4-2c), however the changes are not on a large enough scale to conclude which source changes (if any) may have caused the discrepancy. Isomer ratios at Stn DE as well as all depths in both stations in the lower estuary (with the exception of the deepest layer at Stn 20) indicate a combination of engine exhaust and coal burning as anthropogenic PAH sources (Yunker and MacDonald 2003, ref. therein). The relatively constant levels of BghiP, particularly at Stn 20 points to engine exhaust, suggesting long-

range atmospheric deposition, a conclusion also reached by Dreyer *et al.* (2005a and 2005b). The similarity of BghiP in all samples also indicates the atmospheric delivery of petrogenic particulate matter is approximately the same throughout the estuary. However, BghiP is not correlated to other combustion-derived PAH in the sediments, and the lack of low-mass, volatile PAH typically associated with petrogenic sources suggests that direct atmospheric deposition may not be the primary delivery mechanism for all compounds to the sediments; direct inputs into the water column by industrial practices (pulp and paper and aluminium smelting) and agricultural run-off is thus the likely delivery mechanism for anthropogenic and natural PAH to the system, respectively.

Per is naturally occurring and dominates PAH profiles in relatively pristine areas, likely through microbial production under anoxic conditions in soils (Gocht *et al.* 2007) as well as lake and marine/coastal sediments (Silliman *et al.* 2000), as its abundance usually increases with sediment depth. However we do not find a consistent trend of increasing Per with depth, thus *in situ* production by the anoxic microbial community likely is not the only source of this PAH to the system. One group hypothesized the microbial community supporting Per production does not effectively compete with other microbes for nutrients (Silliman *et al.* 2000), and previous studies of microbial abundance in the water column of the maximum turbidity zone report relatively low amounts of bacterial biomass when compared to other temperate estuarine systems (Painchaud *et al.* 1995), perhaps making this a good setting for bacterial Per biosynthesis. The fact that this compound not only persists, but dominates most profiles, even in oxic

surface sediments at all three locations can also suggest a source other than *in situ* production, possibly soil from run-off. Typically, Per is found decoupled from anthropogenic PAH (Silliman *et al* 2000, Countway *et al.* 2003, Gocht *et al.* 2007), however we report good correlation between Per and the pyrogenic-derived PAH (mass 202 – 252, excluding Per, $\Sigma - Py$) (r^2 = 0.88, $p < 0.001$, Figure 4-3b), a correlation that remains strong even when the extreme (Stn DE) and pre-industrial (Stn 20, 36 – 41 cm) values are removed (r^2 = 0.92, $p < 0.001$). The association may be due to similar terrestrial sources or mixing in the water column/maximum turbidity zone prior to deposition.

4.3.5 Lignin Phenols and PAH Transport to the Lower St. Lawrence Estuary

A good correlation between Σ_8 and $\Sigma 15$ – PAH ($r = 0.79$, $p < 0.01$) was found through the whole system. To shed light on the role played by organic matter geochemistry in PAH distribution, Pearson correlation analysis between general diagnostic PAH parameters and relevant organic geochemical variables are presented in Table 4-1. Because Stn DE presents an extreme value and was found to drive many regression variables it was excluded from the analysis, as was the deepest layer from Stn 20 since it is a pre-industrial end-member and leads to the opposite skewing of regression.

Table 4-1. Pearson coefficients for diagnostic PAH with several organic geochemical and lignin phenol measurements[a]

Parameter	OC (mmol g^{-1})	$\delta^{13}C$ (‰)	ExC[b] (mmol g^{-1})	Σ_8 (μmol g^{-1})
Σ15–PAH	0.76*	-0.38	-0.15	0.79*
ΣPy	0.83*	-0.34	-0.12	0.83*
Per	0.64*	-0.47	-0.22	0.67*
BghiP	-0.39	0.46	0.79*	-0.44

[a]Stn DE and Stn 20 (36 – 41 cm) were excluded. Correlation of quantitative values is calculated from molal units. [b]Solvent-extractable carbon.

Σ_8 and Per are significantly correlated (Table 4-1), agreeing with previous studies of estuarine and coastal sediments linking this PAH to terrestrial sources (e.g., Countway *et al.* 2003, Prahl and Carpenter 1983), and providing further evidence of an allochthonous source for Per in the St. Lawrence estuary. Further support for a possible terrestrial origin of Per is inferred from the dominance of this PAH at Stn DE, which is downstream from tributaries draining the agricultural center of the province of Québec. Since Per and $\Sigma - Py$ co-vary, a good relationship between Σ_8 and these PAH naturally follows ($r^2 = 0.83$, $p < 0.0001$, Figure 4-3c). However, the first study to compare lignin phenols and PAH distribution patterns revealed a correlation with only Per (Prahl and Carpenter 1983). When lignin and ΣPAH have been found to co-vary, the reason is attributed to heavy creosote contamination (Mitra *et al.* 1999, Simpson *et al.* 2005), however due to its highly hydrophobic nature this pollutant is not usually transported far from its source (significantly less than 1 km in Mitra *et al.* 1999 and Simpson *et al.* 2005). Considering the two lower estuary stations are far

removed from likely creosote source points, coupled to the magnitude of PAH contamination from aluminium smelters in the region, creosote is not likely the driving force behind the association.

To further understand the association between lignin phenols and the pyrogenic PAH, principal components analysis (PCA) was carried out, now excluding only the deepest layer at Stn 20. PCA is often employed in qualitative PAH source apportionment (e.g., Yunker and MacDonald 2003), but it has also been applied to confirm characteristic groupings of PAH (e.g., Countway *et al.* 2003). A PCA of all compounds confirmed the correlation tests by grouping Per in the same quadrant as Σ – Py while distinguishing several other associations as well, especially within the Σ – Py (Figure 4-4). The cross-plot of the first two principal components clusters isomers together. The shared variability of isomers can be due to common sources (e.g., petroleum exhaust as a source of BghiP) or could be just as likely rooted in physicochemical reactivities (e.g., octanol-water partitioning, solubility constant, volatility, etc.) which play an important role in dictating the distribution of PAH at sites so removed from point sources.

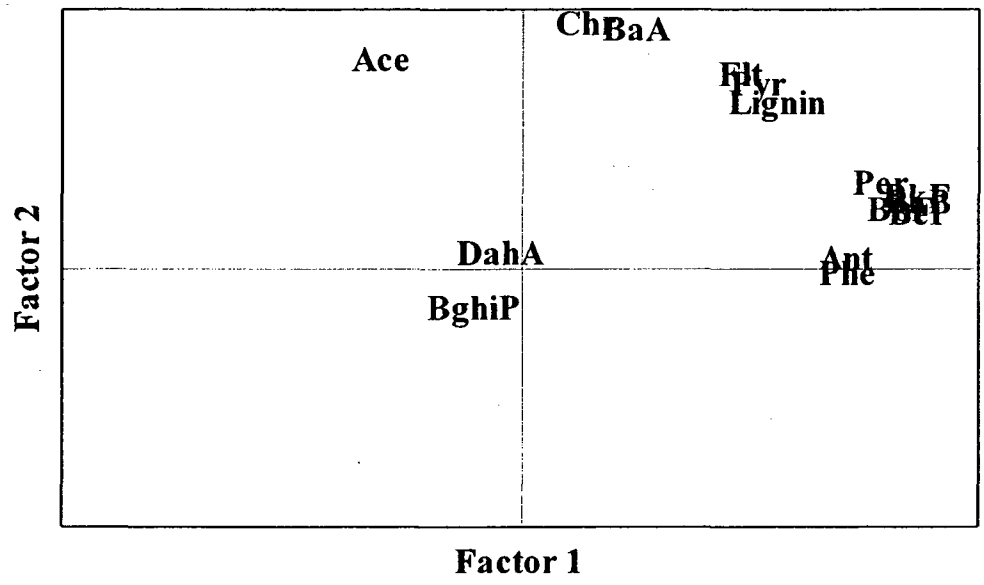

Figure 4-4 Crossplot of the factor scores for the first two components of the PCA analysis. Refer to text for symbols.

A telling grouping is that of Σ_8 with mass 202 (Flt, Pyr), and not 252 (i.e., Per). This result comes as a surprise because, as discussed above, Per is usually associated with terrestrial biomarkers in coastal and estuarine systems and is thus expected to cluster with lignin. That it is not indicates pulping mills are not a source of Per and direct input from run-off of agricultural soils or *in situ* production in the maximum turbidity zone are more likely sources. The association of Per with other mass 252 PAH (BbF, BkF, BeP, BaP, and Per) could be explained by a physicochemical steady-state being attained in the maximum turbidity zone resulting in a secondary common source causing variability in downstream sediment cores to converge. Another possibility is run-off from soils contaminated with these particular PAH, however North American agricultural practices are not an important source of anthropogenic PAH to the

environment. Still, the potential downstream influence of agricultural run-off on PAH distribution is a study that may be warranted.

The separation of BaA and Chr (mass 228), common to aluminium smelting activities and other industries, from other anthropogenic PAH and either Per or Σ_8, suggests a source of relatively nearby contamination such that physicochemical mixing does not take place over a long enough time scale to exert its influence and allow a full mixing as occurs in the maximum turbidity zone, while also explaining the slightly elevated levels of these isomers at Stn 23. An atmospheric source from smelting is also likely. Finally, the association of Flt and Pyr (mass 202) with Σ_8 suggests the production of these PAH at pulping mills, as they have not been reported to be of especially elevated levels due to smelting activity (Lee *et al.* 1999, Martel *et al.* 1986, Smith and Levy 1990). Passive sorption of other PAH to pulp mill effluent in the water column still cannot be discounted especially considering the good relationship between Σ_8 and $\Sigma - Py$. However, in the case of Flt and Pyr, passive sorption of PAH of mass below 228 amu to terrestrial particulate matter was shown to occur at very low levels in at least one estuarine system (Countway *et al.* 2003), thus contamination from pulping is the likeliest explanation for the strong association between these two PAH and Σ_8 in the lower estuary sediments.

Sedimentary PAH are below levels considered toxic to marine life in the St. Lawrence Estuary, attesting to the relatively low particle loads from the St. Lawrence River as well as the effectiveness of the heavily contaminated

Saguenay Fjord at trapping particulate matter due to a sill at its mouth (Louchouarn *et al.* 1999). Three main sources appear to dominate the lower estuary: low-level atmospheric deposition from long distances reflecting mostly petroleum burning, direct inputs from industrial activities (mainly metal smelting and pulp and paper), and possibly run-off from agricultural soils mixing with urban/industrial inputs from the Great Lakes watersheds in the maximum turbidity zone, with water-borne deposition being more important than atmospheric. Physicochemical partitioning appears to play a highly significant role in determining the patterns of PAH distribution in the sediments of this system, with low mass, high-volatility PAH for the most part below detection limits. The results do not directly implicate sorption of PAH from smelters to solid pulping effluents (i.e., lignin) as a process occurring in this system, but indicate some PAH putatively linked to the pulping process associate with the organic, lignin-rich effluents. Whether this affects the relative magnitude that pulping mills and aluminium smelters each contribute to the loads in the lower estuary is uncertain, and warrants further investigation into the role of pulp mill solid waste in the distribution of PAH. Despite the industry in the region, the dominance of Per in all samples might indicate agricultural run-off as an important source of natural PAH to the system. The clear association of Per with Σ – Py certainly warrants further investigation into the role played by run-off from agricultural lands, not just as conduit for export, but in the distribution and reactivity of organic pollutants, such as PAH following transport into rivers and estuaries, as well as the potentially

larger significance on organic geochemical processes in estuarine systems as a whole.

Chapter 5

Quantitative and stable isotope mapping of five pools of carbon in the St. Lawrence Estuary

To be submitted to *Global Biogeochemical Cycles*.

5.1 Introduction

The bottom waters of the lower St. Lawrence Estuary of Eastern Canada (Figure 1-2) are perennially hypoxic with one-half to two-thirds of the oxygen depletion attributed to warming Labrador Sea water entering from the Cabot Straight (Gilbert *et al* 2005) and the remaining depletion explained by surface water eutrophication spurring water column and benthic microbial respiration (Benoit *et al* 2006, Thibodeau *et al* 2006). Depleted dissolved O_2 in the St. Lawrence is likely a permanent condition, so understanding how progressive O_2 diminution in the bottom waters will affect the ecosystem as a whole, from elemental geochemical cycles to biological population dynamics, is of pivotal importance to appropriately model and predict the process (Katsev *et al.* 2007, Dufour and Ouellet 2007).

Though it is accepted that perturbations in the carbon cycle resulting from eutrophication accelerates O_2 consumption, the magnitude and location of organic matter respiration (water column *vs.* benthos/sediments) are not well understood in this system. Detailed studies of the carbon cycle spanning six sampling seasons in the sediments and water column of the Gulf of St. Lawrence and adjacent shelf were carried out as part of the Canadian Joint Global Ocean Flux Study program (Roy *et al* 2000), but work to understand carbon dynamics to the same extent in the hypoxic zone of the estuary has not been as extensive. Much of the focus has been on the fate of specific biomarkers (such as lignin (e.g., Louchouarn *et al.* 1999), or lipids (Colombo *et al.* 1997)), or mapping bulk chemical characteristics in particulate matter and surface sediments (e.g.,

Gearing and Pocklington 1990, Lucotte *et al.* 1991, Colombo *et al.* 1996a and b) collected during the 1980s and early 1990s. Source apportionment in surface sediments has resulted in estimates ranging from 25 – 80 % terrestrial carbon in what is now the hypoxic zone; the large variation is attributed to a high seasonal dynamism of sediment OC inputs before and after the spring phytoplankton bloom in the Lower Estuary (Colombo *et al.* 1996 a and b, 1997, for example). Despite seasonal variations in source apportionment calculations, it is clear that the relative proportion of terrestrial organic matter decreases exponentially seaward (Dufour and Ouellet 2007) as is usually the case for coastal sediments downstream major rivers. Despite the width of the lower estuary (25 to 45 km from shore to shore), the bulk of knowledge is derived from sampling the center of the channel (east – west directionality) and little attention has been paid to organic matter deposition and diagenesis on either shore, which may be considerably different from the main channel due to the presence of several large tributaries along the northern shore.

Previous work on particulate organic carbon (POC) has delimited three regions in the system (the Upper and Lower Estuaries, and Gulf, Figure 1-2) each comprising a distinct, isolated pool of POC in the water column (Gearing and Pocklington, 1990, Lucotte *et al.* 1991, Dufour and Ouellet 2007). The particles borne in the Upper Estuary are mostly deposited at the head of the Lower Estuary whereas those derived from primary production in the Lower Estuary and Gulf are mostly consumed/deposited within their respective zones or very inefficiently exported downstream. Efficient consumption of fresh organic

matter in the system certainly contributes to the seasonal variability in source apportionment, as demonstrated by Colombo *et al.* (1997) who identified dramatic changes in the molecular composition of sinking particles prior to sedimentary deposition. Lucotte *et al* 1991 estimated that ~ 30% of primary production reaches estuarine sediments, a less efficient mineralization than has been estimated more recently in the Gulf (Silverberg 2000). Better defined constraints on POC mass balance in the water column of the Lower Estuary are therefore needed if we are to properly link oxygen consumption to carbon dynamics (Dufour and Ouellet 2007).

Rivers are quantitatively significant contributors to the pool of dissolved organic carbon (DOC) to the world's oceans (Maybeck 1983), however very little to no compositional trace of DOC in marine systems is identified as such using current analytical techniques, leaving the fate of this pool of carbon unknown (Benner 2004). Estuaries and coastal zones are the conduits and reactors of riverine DOC into the ocean and as a consequence much effort is currently put into understanding dissolved carbon cycling in these ecosystems (Peterson *et al* 1994, Frankingouille 1995, Benner and Opsahl 2001, Raymond and Bauer 2001, Abril *et al.* 2002, Otero *et al* 2003, Hernes and Benner 2003, Bianchi *et al* 2004, Mayorga 2005, McCallister *et al* 2006a-b, Guo *et al* 2009). Estuarine zones are also well recognized as ecosystems that transition from net CO_2 source to net sink (Frankingouille 1995, Mayorga 2005, Chen and Borges 2009), thus understanding the processes affecting this dynamic pool of DOC would better constrain the calculation and prediction of regional carbon budgets. Despite

decades of work carried out in the St. Lawrence Estuary, little data exists on dissolved organic carbon. Seasonal dynamics of DOC have been studied in the river (Hélie and Hillaire-Marcel 2006) and Gulf (Packard *et al.* 2000) however the studied locations are far removed from the estuarine mixing zones where processing and transformations are most significant. In addition to riverine inputs, sediments are also thought to be important sources of DOC to coastal environments (Holcombe and/or Burdige), via DOC fluxes from sediments into the overlying water, where it potentially plays a role in sustaining benthic microbial respiration in benthic zones. The dearth of knowledge between the river and the edge of the Gulf leaves the fate of one of the most dynamic pools of carbon in the St. Lawrence Estuary an open question.

A primary staple for understanding geochemical carbon dynamics is natural abundance stable carbon isotope analysis. Though particles and sediments have been well studied over spatial and seasonal scales in the St. Lawrence Estuarine system (Gearing and Pocklington 1990), stable carbon isotope values for dissolved organic carbon ($\delta^{13}C_{DOC}$) have only been reported for the river (Hélie and Hillaire-Marcel 2005). The lack of $\delta^{13}C_{DOC}$ coverage is not unique to the St. Lawrence as analytical limitations have made this measurement very tedious in high-salt, low-DOC systems. Only a few studies have focused on the characterization of $\delta^{13}C_{DOC}$ in estuarine environments, and very rarely on bulk DOC since samples are often pre-treated and/or pre-concentrated using methods that often result in the fractionation of the DOC pool (e.g., Peterson *et al* 1994, Raymond and Bauer 2001, Otero *et al* 2003, Bianchi *et al* 2004, and Guo *et al*

2009). Recent technical advances have however allowed the routine measurement of $\delta^{13}C_{DOC}$ on small volumes of whole, unprocessed samples (St-Jean 2003, Bouillon *et al* 2006, Lang *et al.* 2007, Osburn and St-Jean 2007 and Panetta *et al* 2008) with large-scale $\delta^{13}C_{DOC}$ data sets of the entire DOC pool now emerging alongside the more accessible POC and DIC stable isotopes to give a more complete understanding of carbon cycling in dynamic systems (Bouillon *et al* 2007a and b).

Here, a comprehensive quantitative and isotopic assessment of the state of the carbon cycle in the water column and sediments of the St. Lawrence Estuarine system collected over two sampling seasons is presented. Five pools of carbon (sedimentary, pore-water dissolved organic, water column dissolved inorganic and organic, and particulate organic) distributed through the estuarine transition zone are analyzed to gain further insight into the spatial variability of carbon source(s) and cycling in the system.

5.2 Materials and Methods

5.2.1 Location

The St. Lawrence Estuary of Eastern Canada extends from the St. Lawrence River which drains the Great Lakes watershed, to the North Atlantic. The estuarine system is split into three regions (Figure 1-2); (*i*) the Upper Estuary extends ~300 km from Québec City to the Saguenay Fjord with surface salinity increasing to 25 psu, depths ranging from 15 to 190 m, and comprises the maximum turbidity zone; (*ii*) the hypoxic Lower Estuary extends an additional ~300 km and the dominant feature is the Laurentian Channel, averaging ~320 m

depth at its center; and (*iii*) the Gulf which is essentially an enclosed shallow sea. The system is well stratified, with the estuarine mixing zone extending from the Upper Estuary into the surface waters of the Lower Estuary. Bottom waters of the Lower Estuary and Gulf are marine in origin, flowing in from the Labrador Sea and North Atlantic, with a cold intermediate layer isolating the bottom layer from the surface. This cold layer originates from ice that spent the winter at the surface, spending months exposed to UV radiation where extensive organic matter degradation takes, and has melted in the spring sinking to just above the bottom water layer. The Extensive sediment and water column characteristics have been published and are discussed in a recent review on the state of knowledge of this ecosystem (Dufour and Ouellet 2007).

5.2.2 Sampling

Samples were collected over three cruises in June and August 2006, as well as May 2007 (sampling sites are detailed in Figure 1-2 and Table 5-1) on board the *R/V Coriolis II*. In 2006, only the main channel was sampled, while the 2007 campaign included stations from the main channel as well as locations just north and south of the main channel stations. Complete CTD data from these cruises are freely available from the website of Fisheries and Oceans Canada St. Lawrence Observatory (http://www.osl.gc.ca). Water was collected in 12-L Niskin bottles mounted on a rosette with CTD and immediately vacuum filtered over combusted (500 °C, 4 hrs), pre-weighed GF/F filters (nominal pore-size 0.7 μm). Filters capturing particulate matter (PM) were stored at -80 °C until time of analysis. Filtered water was transferred to pre-combusted 30-mL amber bottles

Table 5-1. Sampling station coordinates and physico-chemical characteristics at the time of sampling, May 2007.

Stn[a]	Latitude (°N)	Longitude (°W)	Depth (m)	Surface Salinity[b]	Bottom O_2[c]
DE	47°10.81	70°37.20	14	4.9	290
F1	47°24.37	70°16.80	47	12.3	293
I	47°45.48	69°54.02	140	21.0	293
K	48°06.17	69°25.77	90	27.0	232
23N	48°41.64	68°46.18	345	26.8	63
23	48°42.04	68°39.18	330	23.9	60
23S	48°38.89	68°35.87	310	24.0	59
22N	48°58.84	68°09.45	295	24.6	63
22	48°56.04	68°05.44	305	22.7	61
215N	49°10.28	67°54.79	165	25.2	116
21N	49°17.81	67°20.63	305	25.5	98
21	49°05.71	67°16.73	310	25.3	101
20N	49°37.18	66°27.69	281	31.5	103
20	49°25.43	66°19.62	316	31.8	97
20S	49°20.12	66°15.11	235	31.2	90

[a]Station identification follows historical designations. Lettered stations are in the Upper Estuary, progressing from the mouth of the St. Lawrence River seaward, and numbered stations are in the Lower Estuary, decreasing from the head of the estuary seaward. [b]Expressed as practical salinity units; [c]Expressed as μM, measured by Winkler titration on board.

with no head-space and immediately acidified to pH < 2 with 100 μL 6 N HCl, capped with PTFE-lined screw caps and stored at 4 °C until time of analysis. In June 2006, ultrafiltration to isolate the high molecular weight DOC (>1000 Da) (UDOC) was conducted with Prep/Scale Spiral Wound TFF-6 (MilliPore®) ultrafiltration modules from large volumes (12-120 L) along the salinity gradient from the mouth of the St. Lawrence River to the open Gulf. Ultrafiltration concentrates and isolates the operationally-defined high molecular weight fraction of DOC based on hydrodynamic volume whereby molecules (or aggregates of molecules) with a volume corresponding to a nominal mass > 1000 Da are retained by the membrane filters, and those with smaller volumes pass

through. Sediments were collected by box-corer and the top 30 cm sub-sampled by push-cores with PVC tubing and sliced. Sediments were transferred to 50-mL tubes, centrifuged at 3000 × *g* and the supernatant filtered over GF/F by syringe filtration into combusted 30-mL amber bottles and treated and stored as were the water column samples. The remaining sediment was stored at -80 °C until further on-shore processing.

5.2.3 Elemental and Isotopic Analyses

Sediments and PM-bearing filters were lyophilized. Dry filters were weighed to determine total particulate mass, sub-sampled with a hole-puncher and placed in Ag capsules to obtain 20-30 mg of PM. Dry sediments were homogenized with a mortar and pestle and weighed (20-30 mg) directly into Ag capsules. Both PM and sediments were de-carbonated by exposure to HCl fumes in a sealed container for 10-12 hrs, and then placed in an oven at 55 °C for ~1 hour to remove traces of acid. Elemental (C, N) and stable isotopic composition ($\delta^{13}C$, $\delta^{15}N$) were determined on a GV Instruments (now Elementar) EuroVector IsoPrime EA-IRMS. Isotope data was calibrated with and corrected for daily instrumental drift with certified sucrose (IAEA-CH-6, $\delta^{13}C$ = -10.47 ‰), ammonium sulphate (IAEA-N-1, $\delta^{15}N$ = +0.47 ‰) and in-house β-alanine (SigmaAldrich, $\delta^{13}C$ = -26.0 ‰; $\delta^{15}N$ = -2.3 ‰) standards. Elemental composition is reported in terms of mmol g^{-1} for sedimentary nitrogen (TN) and organic carbon (SOC) and as both molarity (μmol L^{-1}) and μmol g^{-1} for PM organic carbon (POC). Isotopes are reported using the V-PDB convention against reference gas of known isotope composition. Quantitative and isotope precision are ± 3.2 %

(relative) and ± 0.2 ‰, respectively. C/N and N/C ratios are used for interpretation of N and C, respectively (Perdue 2006). C/N is expressed as a mole fraction, and to maintain a similar scale N/C is expressed as a mole percent. Dissolved inorganic carbon (DIC) and $\delta^{13}C_{DIC}$ was determined as described elsewhere (Helie and Hillaire-Marcel 2006).

Quantitative and isotopic dissolved organic carbon (DOC) composition was measured simultaneously in water column, ultrafiltrate and pore-water samples using High-Temperature Catalytic oxidation coupled to an IRMS (HTC-IRMS) (Panetta *et al.* 2008), with minor modifications. Briefly, 4-10 mL of a sample is drawn into the syringe injector of a modified Shimadzu TOC-5000 TOC Analyzer (stainless steel tubing, in-house designed and built injector head and combustion tube), sparged of dissolved inorganic carbon with He gas. A volume of 150 μL of the sparged sample is then injected over CuO/quartz catalyst, and the CO_2 generated upon combustion is quantified by the NDIR detector of the TOC analyzer, cryogenically trapped and injected into the reduction column of the EuroVector IsoPrime. For water column samples, six injections were trapped while ultrafiltrate and pore-waters needed only two or three injections per sample. The IRMS gives quantitative data as well and is used in concert with the NDIR results for DOC quantification. The above $\delta^{13}C$ standards as well as Suwannee River Fulvic Acid (IHSS, #1S101F) and Deep Sargasso Sea Reference Water (D. Hansell, U. Miami Lot # 00-12) were used for quality control. Quantitative and isotope precision are ± 1.6 % (relative) and ± 0.3 ‰, respectively.

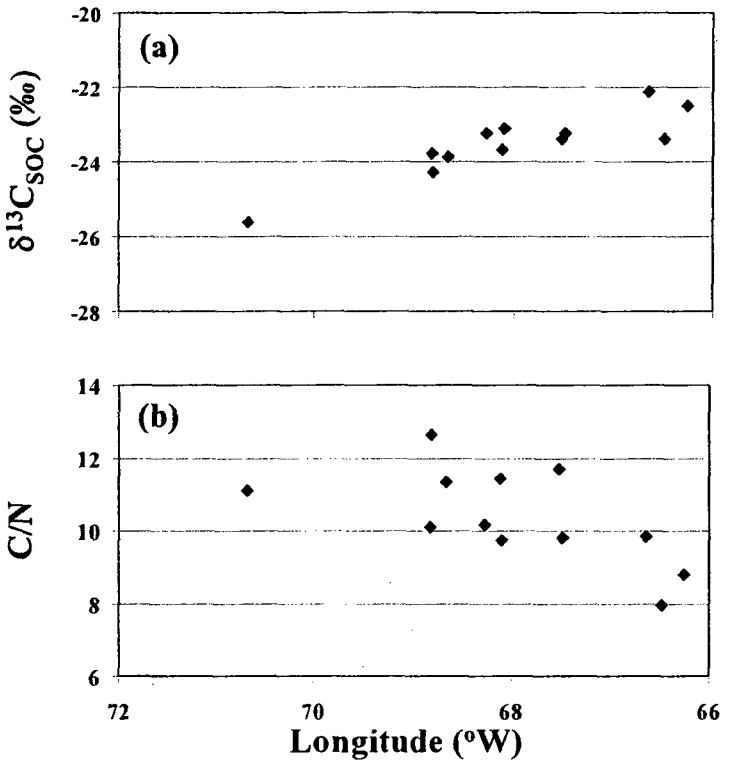

Figure 5-1 Spatial variability of organic matter in the St. Lawrence Estuary. Distribution of (a) stable carbon isotopes and (b) elemental ratios in surface sediments.

5.2.4 Lignin phenols

Lignin phenols were measured in ultrafiltrates by alkaline hydrolysis and CuO oxidation as described elsewhere (Louchouarn *et al.* 1999). Briefly, lyophilized and homogenized samples were weighed (~3 mg OC) with CuO, $Fe(NH_4)_2(SO_4)_2 \cdot 6H_2O$, and 8 wt% NaOH solution in an inert atmosphere and taken to 160 °C for 1 hour. Glucose was added to samples which contained less than 3 mg OC to reach the desired carbon content. Lignin phenols were extracted, derivatized to their trimethylsilyl ethers with BSTFA and quantified by GC-MS using an external calibration mixture. Six lignin phenols are quantified;

(vanillin, acetovanillin, vanillic acid, syringaldehyde, acetosyringone, and syringic acid). Volume (Σ_6, $\mu g\ L^{-1}$) and organic carbon-normalized (λ_6, $\mu g\ mgOC^{-1}$), lignin phenol yields are reported.

5.3 Distribution of carbon in the St. Lawrence Estuary

5.3.1 Sedimentary organic matter

Elemental and isotopic values measured in sediments in 2006 and 2007 agree with what has been reported previously (Gearing and Pocklington 1990, Lucotte *et al* 1991, Colombo *et al.* 1996b, Louchouarn *et al.* 1999), showing a

Table 5-2. Organic geochemical parameters measured in surface (0 – 6 cm) sediments.[a]

Station	Porosity	SOC (mmol g^{-1})	$\delta^{13}C_{SOC}$ (‰)	$\delta^{15}N$ (‰)	N/C (mole %)
DE	0.79	1.3	-25.6	5.3	9.0
23N	0.77 (0.04)	0.9 (0.1)	-24.3 (0.2)	1.3 (0.5)	7.9 (0.3)
23	0.86 (0.02)	1.3 (0.0)	-23.9 (0.1)	2.3 (1.0)	8.8 (0.3)
23S	0.85 (0.02)	1.1 (0.2)	-23.8 (0.3)	5.9 (1.5)	9.9 (0.9)
22N	0.73 (0.04)	0.8 (0.1)	-23.2 (0.1)	5.6 (1.2)	9.8 (0.5)
22	0.85 (0.03)	1.1 (0.1)	-23.1 (0.4)	5.9 (0.8)	10.3 (0.8)
21N	0.57 (0.03)	0.4 (0.1)	-23.4 (0.1)	0.6 (1.4)	8.6 (0.3)
21	0.86 (0.02)	1.3 (0.0)	-23.2 (0.1)	5.8 (0.2)	10.2 (0.1)
215	0.76 (0.04)	1.0 (0.1)	-23.7 (0.1)	4.8 (0.2)	8.7 (0.2)
20N	0.83 (0.02)	1.2 (0.1)	-22.1 (0.2)	3.6 (0.3)	10.2 (0.2)
20	0.86 (0.02)	0.8 (0.2)	-23.4 (0.4)	4.8 (0.4)	12.6 (2.6)
20S	0.71 (0.06)	0.5 (0.0)	-22.5 (0.2)	6.9 (0.5)	11.4 (0.4)

[a]At least 4 depths at each station except DE which was homogenized. Standard deviations in brackets are between-sample variability ($n \geq 5$).

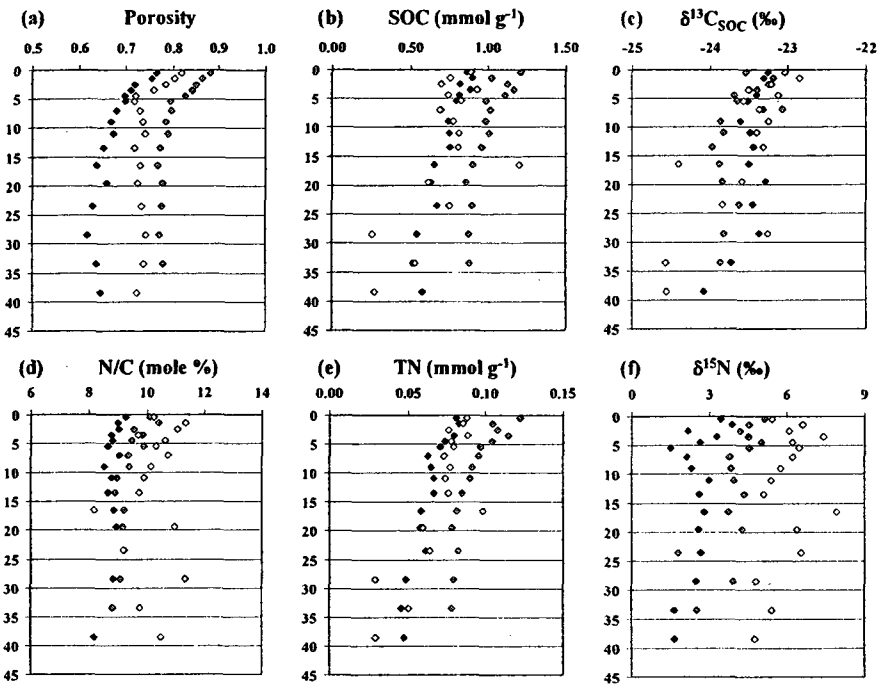

Figure 5-2 Sedimentary profiles of organic geochemical parameters in the St. Lawrence Estuary. Spatial regions are averaged the lower estuary (black, North shore; grey, Main channel; and white, South shore) of (a) porosity; (b) sedimentary organic carbon; (c) stable carbon isotopes; (d) elemental ratio; (e) total nitrogen; and (f) stable nitrogen isotopes. In all cases, y-axis is sediment depth in cm.

conservative estuarine deposition pattern, as exemplified by the spatial distribution of elemental ratio and stable isotope composition (Figure 5-2, Table 5-2). No inter-annual variation was found in Main Channel sediments thus in the proceeding section only the 2007 campaign is detailed. To determine whether North shore riverine inputs are influencing the system, and to simplify the data interpretation, samples are grouped according to region (North (5 cores), Main (4 cores) and South (2 cores)) and average values shown (Figure 5-2). Porosity is typical of silty sediments averaging 0.74 ± 0.10 (all cores, all sediment depths) and decrease from the sediment-water interface down. The main channel is generally more porous than either shore (Figure 5-2a) reflecting hydrodynamic

forcing on deposition as less dense particles forming more porous deposits are prone to accumulate in the deeper parts of the estuary. SOC and TN are clearly higher in the main channel than along either shores (Figure 5-2b,e, Table 5-2), agreeing with the hydrodynamic control of particle settling as organic-rich particles tend to be lower density. Elemental (N/C) and isotope ($\delta^{13}C_{SOC}$, $\delta^{15}N_{TN}$) data show that the North shore of the LSLE receives input from tributaries such as the Saguenay River, the south is more marine in nature and the main channel is intermediate between the two. Differences are to some extent confirmed with cross-plots of elemental and isotopic variables but clearly they are not significant (Figure 5-3). The great overlap between regions still exists, reflecting the importance of water column processing and mixing prior to deposition.

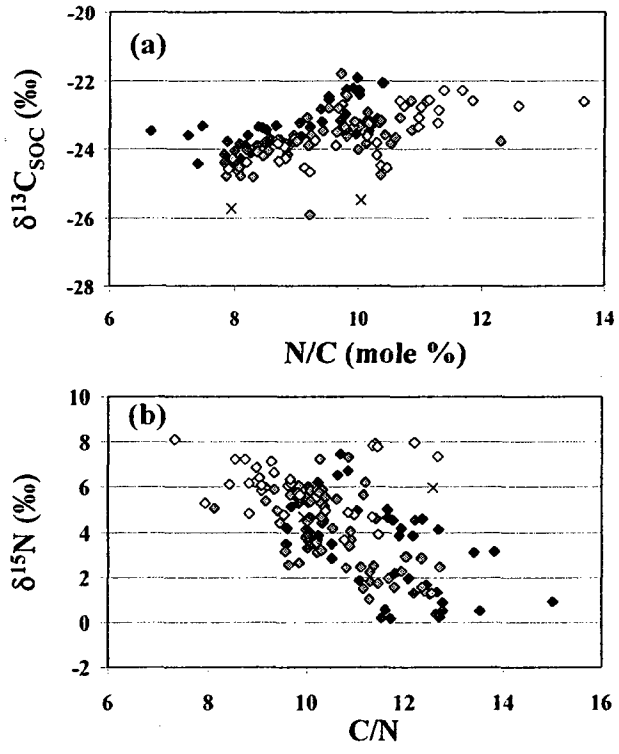

Figure 5-3 Elemental and isotopic cross plots of sedimentary organic matter. Sedimentary cross plots of (a) carbon and (b) nitrogen elemental and stable isotope variables (× = Stn DE, all other symbols as in Figure 5-2).

SOC and TN sediment profiles both decrease with depth in all three regions, similarly to previous profiles from the Estuary and Gulf (Louchouarn *et al* 1999 and Mucci *et al.* 2000); North and Main channel profiles appear to be diagenetically stable below 15 cm, while the South shore samples are too variable to say with certainty. Decreases in N/C in the upper 10 cm indicate SOC and TN are not subjected to the same rate of change, demonstrating the preferential mineralization of nitrogen-rich organic matter in the top few centimetres of the sediments. Despite the surficial North shore N/C values being on average 1 full unit lower compared to the Main channel, both settle at the same ratio at a depth of 10 cm. Downcore profiles of $\delta^{13}C_{SOC}$ show a depletion

from the surface to 10 – 15 cm (Figure 5-2c), which is typical of organic matter sedimentary diagenesis (Gälman *et al* 2009). Again, differences between the shores and main channel exist, depleting by ~0.2 ‰ and 0.5‰ from surface to 10 cm, respectively. These small but distinct differences between the Main channel and shores (Figures 5-2 and 5-3) indicate compositional differences in the organic matter being delivered, with more labile organic-rich particles transported to the south and center of the trough. Diagenetic processing appears mechanistically similar for all regions, as evidenced by the downcore elemental ratio profiles, suggesting that the labile molecules being degraded in sediments have the same reactivity throughout the system. From the intermediary geochemical values of the main channel, it is also clear that particles from runoff entering from the North shore are mixed with primary production prior to deposition so that a planar gradient describes the system better than a simple linear depositional environment.

5.3.2 Sediment porewater dissolved organic carbon

Porewater DOC (pwDOC) profiles in five lower estuary cores (Figure 5-4a) agree with measurements made in the St. Lawrence Gulf (Mucci *et al* 2000) and are typical of marine sediments (e.g., Holcombe *et al* 2001), with lowest concentrations at the surface, sub-surface maxima (~3-7 and ~15 cm at Stns 23

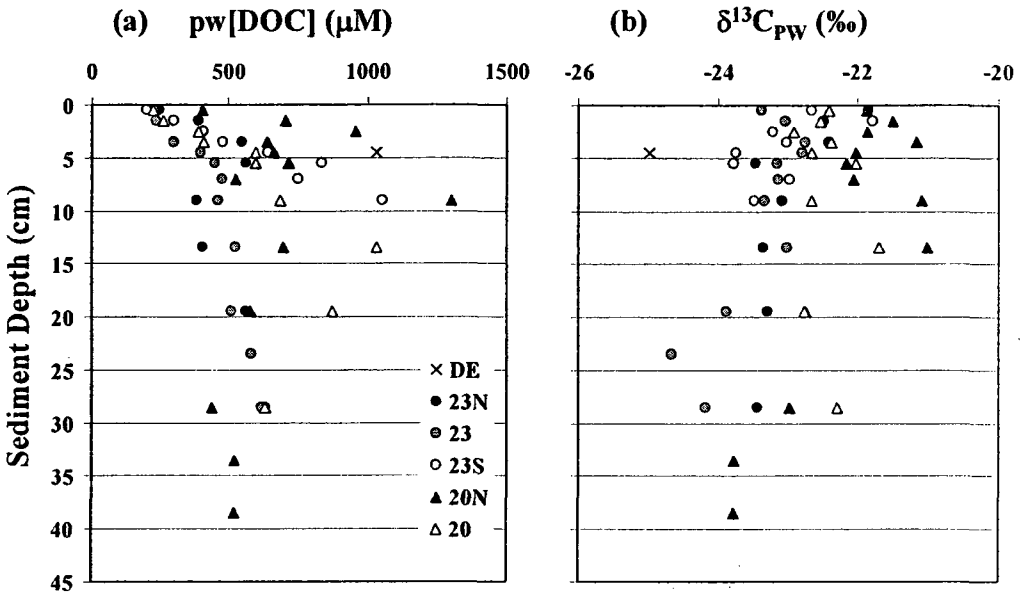

Figure 5-4 Pore-water DOC profiles. Down-core quantitative (a) and stable carbon isotope (b) sediment depth profiles in 5 sediment cores from May 2007.

and 20, respectively), and down-core stabilization. Highest concentrations are found in the sediments of the maximum turbidity zone (MTZ, Stn DE, 1029 μM), which are nearly quadruple the average lower estuary surface concentration and of the same magnitude than another MTZ of a temperature estuary (Miller 1999). With the exception of Stn 20N, concentration profiles between stations are relatively invariant in the upper 5cm of Lower Estuary cores, increasing from 224 ± 19 to 547 ± 132 μM from the sediment-water interface, suggesting a mechanism that maintains pwDOC concentrations at a similar level in the uppermost layers of all sediment cores. The elevated concentration as well as the increased variability found at Stn 20N may be due to biological activity at this site. The reason for the difference in depth of the maximum pwDOC between Stn 23 and 20 is still uncertain and warrants a direct comparison to the inorganic redox geochemistry in these sediments.

$\delta^{13}C_{PW}$ follows the same spatial trend as $\delta^{13}C_{SOC}$ with Stn DE ~2 ‰ lower than the Stn 23 series, which in turn is ~1 ‰ more depleted than Stn 20, suggesting that pwDOC is derived from sediment OC. Unlike the quantitative profiles, downcore $\delta^{13}C_{PW}$ show no smooth, consistent trends (Figure 5-4b). However, a depletion of ~ 2 ‰ from surface to the deepest layers is still evident in these sites indicating compositional changes with depth. If the down-core isotopic changes were due to mixing and dilution with DOC from the overlying marine waters, over 40 % of pwDOC would originate from bottom waters down to a depth of 5 cm, based on isotope mixing calculations from experimentally-determined end-members. More plausibly, pwDOC fractionation ensuing from the selective microbial consumption and associations with inorganic sedimentary components (Arnason and Keil, 2000) are likely driving this down-core isotopic shift.

5.3.3 Dissolved inorganic carbon

DIC (comprising dissolved carbonates and CO_2) is the largest pool of carbon in the water column (Table 5-3) accounting for ~60 – 80 % of the total. The riverine end-member measured here is in agreement with previous isotopic and quantitative measurements made in the St. Lawrence River (Hélie and Hillaire-Marcel 2006). DIC is quantitatively and isotopically conservative in the Upper estuary (Figure 5-5a,b), despite inter-annual variability in temperature and salinity (as illustrated for surface waters at Stn 23 in Figure 5-6c). Deviations from conservative mixing are apparent in $\delta^{13}C_{DIC}$ of some surface samples collected in the Lower Estuary during 2007 (Figure 5-5b) where isotopic

enrichment coincides with quantitative depletion as a result of primary production.

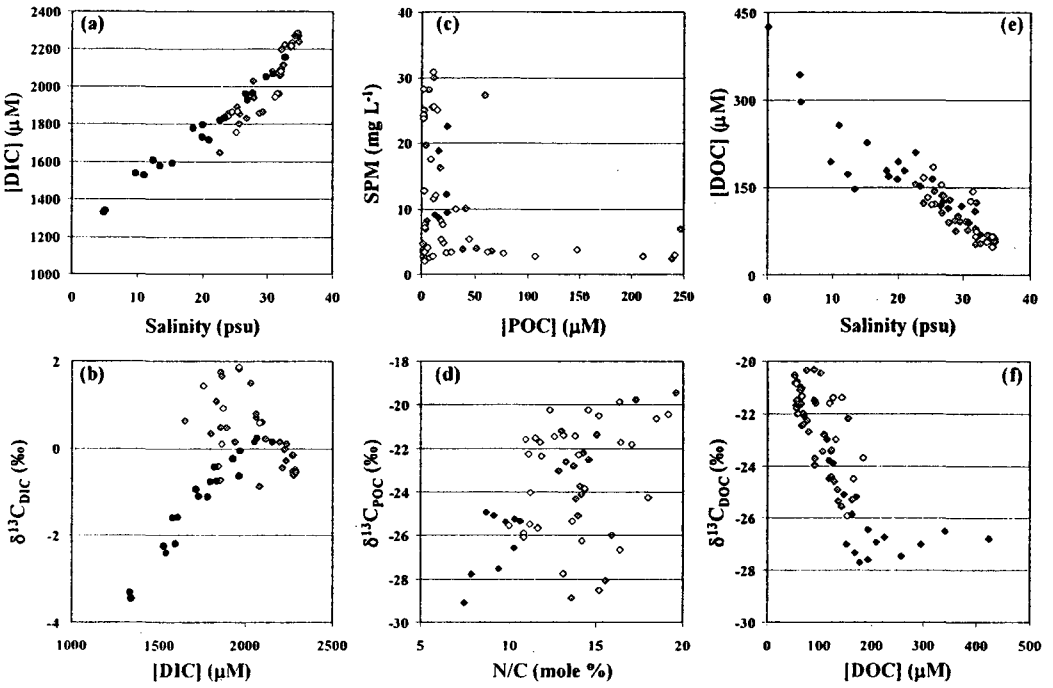

Figure 5-5 Water column quantitative and stable isotope measurements. Quantitative and stable isotopic values of DIC (a,b), POC (c,d), and DOC (e,f) from all sampling season in the water column of the St. Lawrence Estuary (black, Upper Estuary; grey, Lower Estuary Main channel; white, Lower Estuary Shores.

5.3.4 Water column particulate organic matter

Suspended particulate matter (SPM) peaking in the MTZ is on par with similar estuaries (e.g., Abril *et al* 2002) and in agreement with previous studies in the St. Lawrence (Lucotte *et al* 1991, Dufour and Ouellet 2007). In the Lower Estuary, SPM is usually highest at the surface (9.1 ± 3.1 mg L^{-1}) and decreases rapidly within the top 10 m to an average of 3.4 ± 0.8 mg L^{-1}. Stations 23, 23S, 20 and 20N present exceptions to this trend, with highest PM levels occurring between 75 and 300 m depths. These high SPM levels generally coincide with low [POC] (Figure 5-5c) suggestive that these are highly degraded particles,

Table 5-3. Surface water measurements, May 2007.[a]

Station	Salinity (psu)	[SPM] (mg L^{-1})	[DIC] (μmol L^{-1})	$\delta^{13}C_{DIC}$ (‰)	[DOC] (μmol L^{-1})	$\delta^{13}C_{DOC}$ (‰)	[POC] (μmol L^{-1})	$\delta^{13}C_{POC}$ (‰)	N/C_{POC} (mol %)	$\Delta^{13}C_{Water}$[b] (‰)	[DOC] : [POC]
DE	4.9	347.6	1329	-3.31	342	-26.5	82	-25.8	8.5	-0.7	4.2
F1	12.3	77.0	1607	-1.57	172	-25.2	62	-25.1	9.1	-0.1	2.8
I	21.0	18.8	1714	-0.94	178	-27.7	16	-29.1	7.4	1.4	11.4
K	27.0	12.2	1929	-0.23	126	-23.9	23	-25.4	9.8	1.5	5.5
23N	26.8	6.9	n.d[c]	n.d	154	-25.9	4	-25.9	10.8	0.0	39.5
23	23.9	7.0	1857	-0.73	123	-24.4	248	-25.3	n.d.	0.9	0.5
23S	24.0	7.2	1843	-0.41	166	-24.5	4	-25.3	16.4	0.8	46.6
22N	24.6	8.2	1865	0.11	132	-23.0	18	-24.3	18.0	1.3	7.5
22	22.7	10.1	1649	0.63	155	-22.2	41	-19.8	17.3	-2.4	3.8
215N	25.2	12.0	1756	1.44	120	-21.6	434	-20.3	12.3	-1.3	0.3
21N	25.5	11.8	1870	0.92	184	-23.7	11	-20.6	18.8	-3.1	16.4
21	25.3	8.1	1890	0.47	163	-25.3	5	-19.4	19.6	-5.9	30.7
20N	31.5	4.8	1963	1.87	143	-21.4	20	-20.5	15.2	-0.9	7.0
20	31.8	16.3	1962	1.82	109	-22.8	17	-21.2	13.0	-1.6	6.4
20S	31.2	7.6	1944	n.d	126	-21.4	3	-21.7	16.4	0.3	40.7

[a]Analytical SD of individual samples are as described in materials and methods; [b]$\Delta^{13}C_{Water} = \delta^{13}C_{DOC} - \delta^{13}C_{POC}$; [c]not determined;

perhaps trapped in the cold intermediate layer where extensive degradation of organic matter ensues.

POC concentrations show some general spatial trends, albeit with no consistent distribution pattern with water column depth (not shown). Elemental and stable isotope data for most samples follow a conservative trend from $\delta^{13}C$ – depleted, low-N terrestrial matter towards $\delta^{13}C$ – enriched, high-N matter from marine phytoplankton production (Figure 5-5d, $r^2 = 0.53$, $p < 0.0001$). The Upper Estuary is distinct from the Lower, and within the Lower Estuary set the North shore separates from the Main channel and South shore. Samples from the upper estuary are compositionally stable ($\delta^{13}C_{POC}$ = -25.8 ± 1.0 ‰, N/C = 9.4 ± 1.0 mol %, n = 8), consistent with previous $\delta^{13}C_{POC}$ measurements made in the system (Lucotte 1991, Hélie and Hillaire-Marcel 2006). Station I is an exception showing extreme terrestrial values in surface and deep layers ($\delta^{13}C_{POC}$ = -29.1 and -27.8 ‰, N/C = 7.4 and 7.8 mol %), which may be due to inputs of organic matter from nearby tidal flats mixing with particles from the (MTZ).

A distinct grouping of 10 POC samples that do not follow a conservative mixing trend reveals a collection of elevated N/C and depleted $\delta^{13}C_{POC}$ values to be either in the deep waters or at the cold intermediate layer of the Lower estuary. Highly depleted $\delta^{13}C_{POC}$ values have also been measured in the nepheloid layer at the edge of the continental slope in the Mid Atlantic Bight (Druffel *et al.* 1992, Bauer *et al* 2003) and were attributed to either highly degraded terrestrial matter or an abundance of cyanobacteria; the elevated N/C

values measured in samples from the benthic nepheloid layer of the Lower Estuary argue strongly for a high abundance of cyanobacteria.

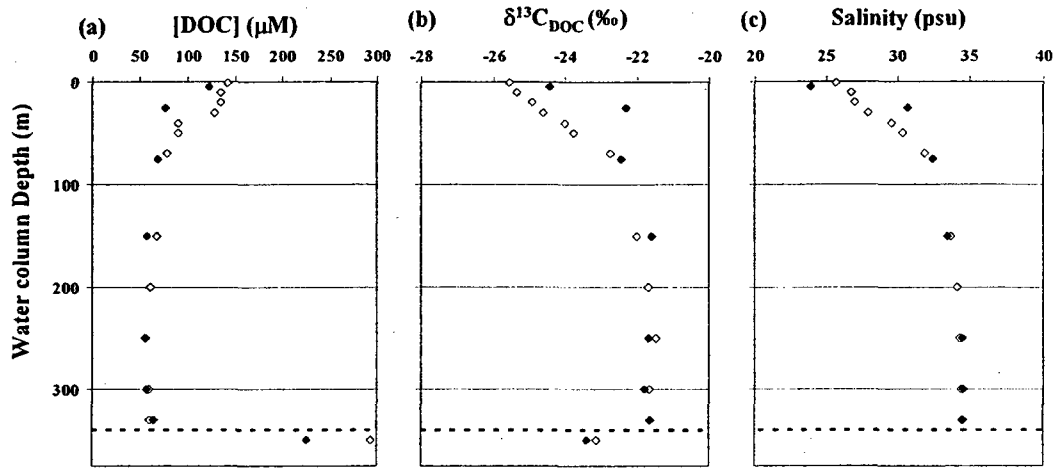

Figure 5-6 Quantitative and isotopic dissolved organic carbon profiles in the hypoxic zone. (a) Quantitative and (b) isotopic dissolved organic carbon profiles in the water column and sediment surface pore-water of Station 23 from June 2006 (white) and May 2007 (black), sediment-water interface is denoted by the dotted line; (c) salinity profiles from CTD casts of the two samplings (solid line, June 2006, dotted line, May 2007).

5.3.5 Water column dissolved organic carbon

For the most part the concentration and isotopic composition of DOC shows conservative mixing behaviour through the whole system (Figure 5-5e,f, Table 5-3). A previous quantitative and isotopic assessment of the St. Lawrence riverine end-member is in good agreement with measurements reported here over both sampling seasons (Hélie and Hillaire-Marcel 2006) indicating little temporal variation in the composition of riverine DOC transported to the estuary. At depths shallower than 40 m, the Upper estuary displays a window of $\delta^{13}C_{DOC}$ (-26.9 ± 0.4 ‰, n = 13, range of 1.3 ‰) that remains relatively narrow even as salinity reaches 23 psu and DOC concentrations decrease nearly 3-fold from the riverine end-member, indicating that dilution with the marine DOC pool is

minimal, and that any additional inputs to the system (e.g., *in situ* production, run-off, etc.) are isotopically similar to removed DOC. Possible sites of DOC removal in the upper estuary are found around and just after the MTZ, where sorption to SPM and photo-oxidation would be important players to different extents, depending on turbidity. Near-shore tidal flats are implicated as an additional source of DOC to the system, as shown by the slight $\delta^{13}C_{DOC}$ depletion at Station I over both sampling years (Table 5-3, Figure 5-5e and f).

The Lower Estuary, on the other hand, presents a more heterogeneous scenario in the surface mixed layer, where phytoplankton production is evident as elevated DOC concentrations coincide with enriched $\delta^{13}C_{DOC}$ at high salinity and the outflow from northern tributaries range from $\delta^{13}C_{DOC}$ = -19.1 to -25.9 ‰. Departures from conservative mixing are mostly attributed to primary production in spring. Physical forcing is certainly important in driving surface water DOC concentration and composition, as evidenced by the seasonal variability of depth profiles at Stn 23 (Figure 5-6). At depths greater than 50 m, DOC is quantitatively and isotopically more stable across the system at 60 ± 6 μM and -21.0 ± 0.7 ‰ respectively (n = 18, six stations, samples ranging 60 – 316 m in depth), agreeing with a previous quantitative assessment of DOC in the deep waters of the Gulf of St. Lawrence (Packard *et al.* 2000). The relatively depleted value at Stn 21 (-25.3 ‰) may indicate run-off from the spring freshet This is the first data set measuring $\delta^{13}C_{DOC}$ in the deep waters of the St. Lawrence system, and the results clearly indicate its marine origin (Druffel *et al*, 1992, Bauer *et al.* 2003)

5.3.6 Ultrafiltered dissolved organic carbon and lignin phenols

High molecular weight DOC (> 1 kDa) isolated by ultrafiltration (UDOC) during the June 2006 sampling campaign follows the same quantitative conservative trends as bulk DOC (Table 5-4). The proportion of UDOC to the total pool of DOC is negatively correlated to salinity (r^2 = 0.97, $p < 0.001$), decreasing from 62 to 22 % across the entire surface transect and 15 % in a deep-water marine end-member (Stn 23 330m). Two stations located at and immediately downstream from the MTZ (Stn DE and F1) appear to have less UDOC than expected from conservative mixing, indicating flocculation and sorption to particles, or photo-oxidation as removal mechanisms for high molecular weight DOC at these sites. UDOC is isotopically much less variable than bulk DOC at the surface of the Upper estuary (-25.4 ± 0.1 ‰, four stations), and enriching by ~2 ‰ seaward to the Gulf. Similar cross-estuarine $\delta^{13}C_U$ enrichment trends have been identified in other transition zones, such as the Mississippi River plume (Guo *et al* 2009) and York River estuary (McCallister *et al* 2006a and b), however in these studies the surface marine end-member carries a marine isotope signature (i.e., -21 ‰) while in this study only the deep Stn 23 UDOC sample is fully marine (Table 5-4). Fractionation with respect to bulk DOC is evident for all estuarine surface samples, with $\delta^{13}C_U$ becoming more depleted relative to bulk DOC seaward, which is not usually the case for other systems (Benner 2002, Bianchi *et al* GCA 2004, McCallister *et al* 2006a) indicating less phytoplankton-derived UDOM is extracted from the Lower St. Lawrence Estuary than has been reported in other systems.

Table 5-4. June 2006 ultrafiltered DOC elemental, isotopic and lignin phenol parameters.

			Bulk		Ultrafiltrate						
Stn	Depth (m)	Salinity (psu)	[DOC] (μmol L^{-1})	$\delta^{13}C_{DOC}$ (‰)	[UDOC] (μmol L^{-1})	$\delta^{13}C_U$ (‰)	$\Delta^{13}C^a$ (‰)	Σ_6 (μg L^{-1})	λ_6 (μg mgC^{-1})	$(Ac/Ad)_V$	S/V
A	46	0.1	425	-26.8	265	-25.5	1.3	16.99	5.3	0.95	0.38
DE	14	6.0	296	-27.0	137	-25.3	1.7	7.64	4.7	0.97	0.28
E	3	8.4	324	-26.4	153	-25.3	1.2	5.44	3.0	1.00	0.07
F1	3	13.4	147	-25.1	54	-25.5	-0.4	3.11	4.8	1.02	0.36
I	3	18.3	178	-27.7	62	-24.9	2.8	2.12	2.9	1.14	0.19
23	5	25.7	143	-25.6	32	-23.9	1.7	1.75	4.5	1.56	0.38
18	5	29.0	93	-21.6	20	-23.2	-1.6	0.60	2.4	1.24	0.32
23	330	34.5	61	-21.6	9	-21.7	-0.1	0.16	1.6	0.74	0.003

[a] $\Delta^{13}C = \delta^{13}C_{DOC} - \delta^{13}C_U$;

Lignin phenols analyzed in UDOC (Table 5-4) identify clear similarities to the Mississippi River plume (Benner and Opsahl 2001, Hernes and Benner 2003). The initial 66 % decrease of Σ_6 from the freshwater inlet to the MTZ suggests flocculation and sorption to particles as an important process in the removal of water column lignin. UDOC lignin compositionally differs from the Mississippi River plume in that vanillyl phenols are much more predominant and can be interpreted either as low angiosperm inputs, and/or evidence for older, more photo-oxidized lignin (Opsahl and Benner 1998; Hernes *et al.* 2007) flowing in from the St. Lawrence River. The acid-to-aldehyde ratio of vanillyl phenols, $(Ad/Al)_V$, is often used to infer degradative state of lignin (Opsahl and Benner, 1997); the more acidic functionalities relating to more oxidation and therefore more extensive degradation. However, recent work has shown that the use of such diagnostic markers in the water column can be misleading due to physical processes such as sortion to mineral surfaces (Hernes *et al* 2007). Across the estuarine transect the $(Ad/Al)_V$ ratio increases, particularly after the MTZ and as these are surface samples photo-oxidation is a probable cause, but can easily be a physical chemistry phenomenon. A spike in $(Ad/Al)_V$ at Stn 23 could be due to inputs from the Saguenay Fjord which is heavy in pulp and paper industries whose solid effluents are characterized by higher $(Ad/Al)_V$ than natural sources (Louchouarn 1999). Lignin parameters measured in the deep Stn 23 are unique compared to the rest of the estuary, reflecting the main source of water to this location, the North Atlantic Ocean (Opsahl and Benner 1997); it is clearly a low end-member in the system, but still significantly higher than the deep

Atlantic, indicating fluxes of dissolved lignin phenols from sediments and/or descending particles.

Except at two locations, Σ_6 is excellently correlated to UDOC concentration ($r^2 = 0.99$, $p < 0.001$). Stn I, which as noted above may be receiving inputs from nearby tidal flats, is characterized by somewhat lower lignin yields than expected and Stn E, in the MTZ, has a much lower Σ_6 than expected from its UDOC concentration. Unlike Stn I, there exists no quantitative or isotopic evidence to suggest deviations from conservative behaviour at this location, thus the increased UDOC concentration (with respect to Σ_6) is likely from inputs within the MTZ from sediment resuspension that parallels lignin sorption and flocculation. Though S:V ratios are low through all samples measured, these two stations are marked by a sharp decrease in the amount of syringyl phenols, indicative of sources distinct from the main river or preferential removal of this marker from the water column such as sorption to particles.

5.4 Sources and processing of carbon in the St. Lawrence Estuary

5.4.1 Apparent conservative estuarine mixing

The water column of the St. Lawrence Estuary falls within the range of unperturbed conservative systems (Maybeck 1982, Abril *et al* 2002 and references therein); Total organic carbon (TOC = DOC + POC) contributes ~40% to the total carbon pool in the water column in the upper estuary; TOC concentration in the riverine end-member (577 μM) corresponds to a natural soil end-member value; mixing layer POC concentrations are inversely correlated

with SPM concentrations; pCO_2 is supersaturated through the length of the upper estuary; and neither DIC nor DOC concentration deviates enough from conservative mixing to imply significant anthropogenic perturbations contrary to the heavily populated Scheldte estuary in Northern Europe (Abril *et al* 2002), for example. Sediments demonstrate a clear depositional pattern in agreement with previous assessments (Dufour and Ouellet 2007 and ref. therein), with the added confirmation that inputs from the northern tributaries compositionally influence sediments from the Lower estuary.

Few recent reports exist of both $\delta^{13}C_{DOC}$ and $\delta^{13}C_{POC}$ measurements in estuaries, leaving a scant data set to which the St. Lawrence can be compared (Raymond and Bauer 2001). Two of the more recent studies demonstrate decoupling between DOC and POC sources and cycling in the Amazon (Mayorga *et al* 2005) and an African mangrove-dominated estuary (Bouillon *et al* 2007a and b). Despite being a temperate conservative estuarine system in the Northern Hemisphere, the St. Lawrence is similar to these two tropical systems with no obvious general trends linking the two pools, but with common sources that can be discerned (Figure 5-7a). Several of the surface mixed layer samples from the Lower Estuary show isotopic enrichments in both pools which coupled to quantitative measurements agree with primary productivity, whereas carbon isotopes are depleted in both pools in the maximum turbidity zone. The extreme values of both pools in several samples (< -27 ‰, at Stn I) also indicate a source of depleted DOC and POC putatively assigned to tidal flats. However, bizarre patterns such as the hyperbolic relationship for the Upper estuary as a whole

(Figure 5-7a) preclude any clear general trend and suggests that the two pools are governed by independent processes. By taking the difference between the two pools ($\delta^{13}C_{POC}$ subtracted from $\delta^{13}C_{DOC}$), a clear trend of fractionation between the phases with respect to POC composition (atomic N/C ratio) is noted with POC progressively getting more enriched with respect to DOC seaward (Figure 5-7a, inset). The results demonstrate that water column mixing outpaces

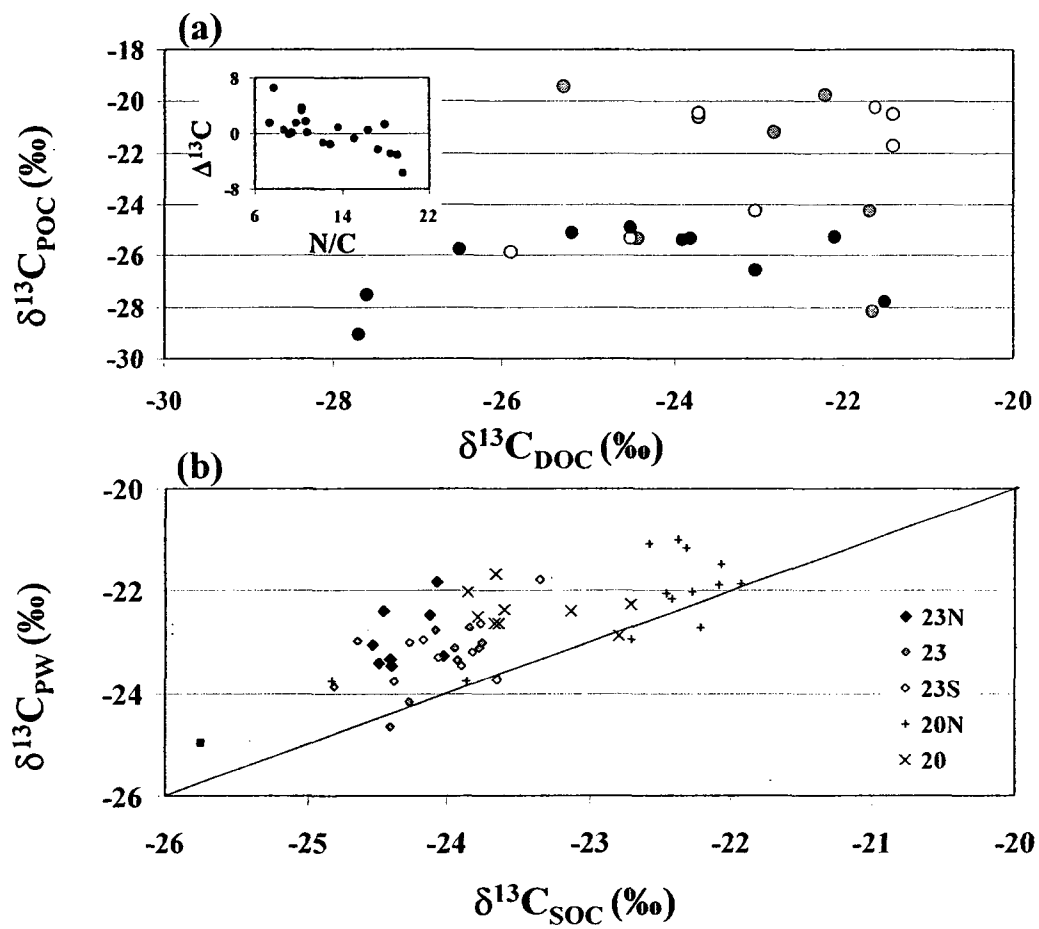

Figure 5-7 Dissolved and solid phase organic carbon stable isotopes in the St. Lawrence Estuary. (a) surface water column (symbols as Figure 5-6) and (b) sediments. The 1:1 line is depicted for sediments only. Inset (a); $\delta^{13}C_{DOC} - \delta^{13}C_{DOC}$ as a function of elemental ratio through the entire system.

the rate of POC turnover in the upper estuary, while in the lower estuary, influx and persistence of riverine DOC may mask DOC derived from primary production in surface waters. Though it appears the two are decoupled it is possible that the intense chemical-physical transitions in the estuary are masking exchange between the two pools and perhaps a more experimental approach (e.g., pulse-chase[6] of isotopically labelled organic carbon (Woulds *et al* 2009)) may be needed to shed light on these processes as they occur *in situ*.

Though UDOC is derived from 8 samples and bulk DOC on 74 samples, the comparison between the two highlights several important points; (*i*) turnover of primary produced carbon from the spring bloom appears to be rapid; (*ii*) isotopic variability in DOC appears driven primarily by low molecular weight (<1000 Da) compounds not isolated using ultrafiltration; and (*iii*) UDOC transported out of the Upper Estuary is seemingly well preserved and efficiently transported out of this system, making the St. Lawrence unique in this regard compared to other systems located at lower latitudes (e.g., Opsahl and Benner 2003, McCallister *et al* 2006ab). This last point is important because it may imply that estuaries located in the northern temperate regions are more efficient exporters of riverine DOC to the ocean, especially considering the lower direct sunlight and seasonal ice cover tempering UV intensity.

---

[6] The pulse-chase experiment involves adding some amount of isotopically enriched inorganic nutrient (e.g., $H_2{}^{13}CO_3$) to the surface waters for a regular period of time (e.g., daily for 10 days) and collecting samples throughout the water column (DOC, POC and SOC) for the duration of the addition, and a given period of time after the addition has ended. In this manner it is possible to trace the ^{13}C as it flows from one pool of carbon into another and eventually remineralization.

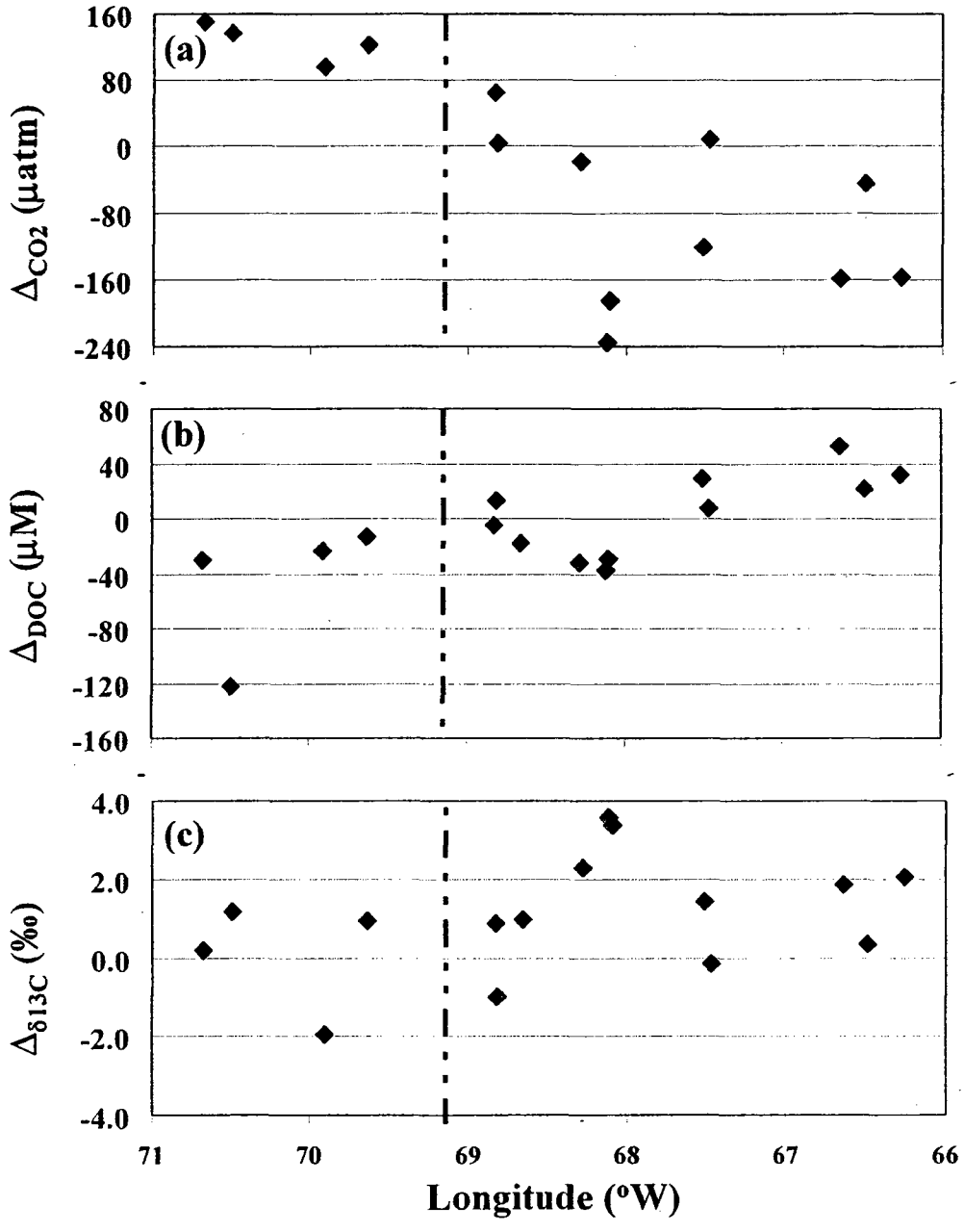

Figure 5-8 Spatial distribution and deviations from conservative behaviour. (a) pCO_2, (b) DOC and (c) $\delta^{13}C_{DOC}$ (Δ_{DOC}, Δ_{CO2}, and $\Delta_{\delta 13C}$, respectively) in surface waters of the St. Lawrence Estuary. The dashed line is the demarcation between the Upper and Lower estuaries.

5.4.2 A spatial trophic shift and DOC oxidation

To better understand relationships between dissolved pools in the water column, deviations from conservative mixing in pCO_2 and DOC quantitative and isotopic data was modeled from two-end-member mixing curves (see supporting information for details). The role of POC is excluded from the modelling exercise because it is not a dissolved entity and thus not governed by the same physical controls on mixing. Quantitative deviations from conservative behaviour occur only near the surface, indicating that the bottom waters of the Lower Estuary are balanced (i.e. no net surplus or deficit) with respect to DOC and pCO_2 fluxes. Taking only surface waters (< 5 m) into account, a striking spatial trend for the quantitative parameters is found across the estuarine transect (Figure 5-8a-b). Firstly, pCO_2 exceeds the conservative estimate through the length of the upper estuary during both sampling seasons and falls below it in the lower estuary for 2007. Note the extreme values located at longitude ~68.1 (Figure 5-8b) correspond to sites of production at the time of sampling. DOC concentrations show the opposite trend – below the conservative estimate in the Upper estuary and exceeding it in the Lower in 2007. In other words an apparent shift from net heterotrophy to net autotrophy is evident in the surface waters of the St. Lawrence Estuary transition, in line with the finding of near-shore ecosystems as net sources, and coastal areas as net sinks of CO_2 (Chen and Borges 2009).

The surface waters of the Lower Estuary are net autotrophic in May 2007, but approximately balanced (with respect to heterotrophy) in June 2006 and is thus subject to more seasonal variability than the lower estuary, as shown in the Gulf in a previous study (Packard *et al* 2000). Certainly the phytoplankton bloom

occurring in early spring following the freshet defines the net trophic state of the surface waters, as the largest pCO_2 deficits, DOC concentration surpluses and $\delta^{13}C_{DOC}$ enrichments occur where POC measurements (N/C, $\delta^{13}C_{POC}$) carry the strongest phytoplankton signal. The overall enrichment of $\delta^{13}C_{DOC}$ relative to the conservative estimate in the Lower Estuary in May 2007 certainly supports primary production. Note that causes for deviations from conservative behaviour through the system (photo-oxidation of riverine DOC and phytoplankton production) both result in $\delta^{13}C$ enrichments (Vähätalo and Wetzel 2008, Bauer *et al* 2002, respectively) thus resulting in isotope enrichment in both zones (Figure 5-8c). Taken together, the upper estuary is a net source of CO_2 mainly via photo-oxidation of organic matter in surface waters, and the Lower estuary is a seasonally variable system that is a net sink during the phytoplankton bloom.

5.4.3 From surface to sediments... and back?

Though POC is not here modelled using the same approach as the dissolved carbon pools, it is still possible to evaluate its extent of degradation in the system. Most striking are the differences in value and variability of elemental and isotopic composition between POC and SOC, indicating significant dynamism in the water column with stabilization in the sediments, particularly with respect to N/C. Comparing surface water POC through the Lower Estuary (averaged values for all samples) and surface sediment elemental (SOC and TN) compositions (mmol g^{-1}) shows decreases of ~90 % and ~85 % in carbon and nitrogen, respectively, from the surface to the seafloor. This estimate is higher than one other made in the Lower Estuary with ~70 % of POC mineralized

(Lucotte *et al* 1991) and is closer in magnitude to a previous assessment for the Gulf (Silverberg *et al* 2000). To the best of our knowledge this is the first rough estimation of relative particulate nitrogen consumption in the water column of the estuary.

One of the more intriguing results is the possible indication from isotopic and elemental evidence of cyanobacteria in the deep Lower Estuary. The benthic layer is very well developed in this area and can extend to 50 m from the sea floor as a result of strong tidal shear in the bottom waters (Syvitski and Hutton 1996), however no reports of their organic geochemistry can be found in the literature. Stable carbon isotopes clearly show very little of this isotopically depleted carbon is transferred to and preserved in the sediments. Since the benthic nepheloid layer was not initially a primary objective of this work its collection at the time of sampling was patchy, but as results suggest microbial biomass, this layer may be a very important site of O_2 consumption. Future work certainly should include a closer investigation of the carbon and nitrogen cycling in this layer, including microbiological characterization.

Sedimentary elemental and isotopic profiles show a clear diagenetic pattern (Berner, 1982, Goñi and Hedges 1995, Rothman and Forney 2007) with rapid degradation of organic matter in the upper few cm of all sediments, followed by an apparent stabilization. Mucci *et al* (2000) quantitatively demonstrated the production of DIC in sediment pore-waters in the Gulf as a result of organic matter mineralization, and the stable isotopes here clearly point to dissolution of SOC into the pore-waters (Figure 5-7b). Quantitative pwDOC

profiles do not inherently reflect such a relationship due to the natural variability and dynamic nature of this pool (Alperin *et al* 1999). The quantitative pattern reported here is usually interpreted as a flux of pwDOC out of the sediments (Alperin *et al* 1999), but may also reflect the surface reactivity of pwDOC with a fraction sorbing to oxic mineral surfaces (Arnarson and Keil 2000,Lalonde, unpublished results) prior to fluxing out. The fact that the relationship in Figure 5-7b does not fall on a 1:1 line, with the pwDOC on average 1.1 ± 0.5 ‰ more enriched than SOC in all samples, indicating isotopic and by extension biochemical compositional fractionation. Preferential dissolution of carbohydrates and/or amino acid-based compounds from sediments is the likeliest reason for the enrichment, as these biochemicals tend to be $\delta^{13}C$ enriched compared to other components of bulk natural organic matter (e.g., Wang *et al* 1998). The fractionation can be controlled by solubility properties, microbial processes within the sediments, or mineral-organic matter associations with all three most likely playing a role.

The return of carbon from sediments to the water column as DOC fluxes can explain the slight increase in DOC concentration in the deepest water sample of Stn 23 (65 μM at 330 m *vs.* 58 ± 1.0 μM in four samples between 150 and 300 m), however the same samples are isotopically invariant (Figure 5-6). Thus, if a flux of pwDOC is occurring, it is apparently isotopically indistinct from marine DOC, or that the isotopically unique fraction is rapidly degraded. Lignin phenols in UDOC argue for a flux of DOC into the bottom waters at the hypoxic zone as Σ_6 is about quadruple the concentration in the benthic layer relative to

the North Atlantic, which serves as the source of deep waters for the St. Lawrence; it is however impossible to say from this single measurement whether it is the result of sediment flux or POC degradation within the water column. More detailed investigations, involving direct time-lapse measurements of bulk as well as relevant molecular markers (lignin phenols, amino acids and carbohydrates) to compare fluxes from sediments to desorption from particulate matter will certainly shed light on this topic, as it might pertain strongly to O_2 consumption in the hypoxic zone.

5.5 Summary

The extensive elemental and isotopic analyses of five pools of carbon broadly show strong conservativeness and simple depositional patterns. However, spatial distribution of production, consumption and compositional control emerge when pools are compared, revealing; (1) a clear spatial shift in trophic state with photo-oxidation of DOC resulting in Upper estuarine net heterotrophy and primary production resulting in Lower Estuarine net autotrophy; (2) isotopic evidence for common sources of DOC and POC exists but the two pools appear decoupled because physical mixing outpaces phase transfer; (3) between 85-90 % of primary produced particulate carbon and nitrogen is consumed prior to sedimentary deposition in the Lower Estuary; (4) stable isotopes indicate the export of riverine DOC is more efficient than estuarine systems from lower latitudes perhaps making similarly located estuaries important sources of terrestrial DOC to the world's oceans; (5) the benthic nepheloid layer may be a site of microbial activity in the hypoxic Lower Estuary;

(6) isotopic fractionation between pwDOC and SOC implies compositionally-driven *in situ* sedimentary fractionation; and (7) a net flux of dissolved carbon into the benthic layer of the hypoxic zone is occurring, but the exact magnitude and source(s) are still not certain.

Chapter 6.

Organic Carbon the St. Lawrence: Analytical and Geochemical Advances

6.1 St. Lawrence Estuarine Carbon Cycle

The goals of this work hinge about better understanding the carbon cycle in the St. Lawrence Estuary and what discernable anthropogenic perturbations has the system experienced. Two areas within the estuary are of particular interest, the Upper Estuarine maximum turbidity zones (MTZ) and Lower Estuarine hypoxic zone. Two approaches to interpret these changes are taken; the analysis of bulk pools of organic carbon throughout the system and the targeted analysis of molecules specific to anthropogenic activity (polycyclic aromatic hydrocarbons (PAH)) and vascular terrestrial plant inputs (lignin phenols). Here the most significant contributions towards this end are briefly summarized.

6.1.1 Analytical Advances

In order to properly fulfill the requirements for the bulk analyses and give insight into the sources and dynamics of the pool of DOC, a total organic carbon analyzer was coupled to an isotope ratio mass spectrometer. The on-line HTC-IRMS system described (Chapter 2, Panetta *et al* 2008) can withstand a large number (~300) of difficult sample matrices (high salinity and/or high DOC) before catalyst regeneration or fouling by salt deposition occurs and is at least as accurate and precise as other methods for $\delta^{13}C_{DOC}$ for a diverse range of sample types. It has allowed large-scale routine $\delta^{13}C_{DOC}$ analysis of saline natural samples, and can be extended to allow a more complete understanding of DOC sources and cycling in complex environments with large DOC concentration gradients such as estuaries, coastal zones, and interstitial boundaries (e.g., sediment-water interfaces). Though standard reference materials do not yet

exist, unprocessed natural samples that cover DOC freshwater and marine end-members were suggested; Deep Sargasso Sea DOC Certified Reference Material is easily suggested as the low-DOC high-salinity anchor. Future directions in HTC-IRMS system development should focus on further reducing the background signal of the TOC instrument to lessen the impact of blank correction on natural-abundance stable isotope analyses, which would also aid in reducing total analysis time and material consumption. One reviewer suggested that if used in concert with the IRMS sensitivity increase reported in Osburn and St-Jean (2007) the sample throughput of HTC-IRMS could potentially increase as much as two-fold, and is thus certainly worth investigating further.

6.1.2 Perturbation State of the St. Lawrence

The water column of the St. Lawrence estuary falls within the range of relatively pristine, conservative systems (Maybeck 1982, Abril *et al* 2002 and references therein) especially when compared to the heavily perturbed systems such as the Scheldte estuary in Northern Europe (Abril *et al* 2002). Sediments demonstrate a clear depositional pattern in agreement with previous assessments (Dufour and Ouellet 2007 and ref. therein), and follow down-core trends consistent with natural sediments in coastal and marine systems (Berner, 1982, Goñi and Hedges 1995, Rothman and Forney 2007). The effects of the northern tributaries on the depositional profile of the Lower Estuary are confirmed. Thus, in terms of bulk measurements the St. Lawrence presents itself as a natural system that has not been perturbed by (direct) anthropogenic inputs of organic carbon.

Markers specific to anthropogenic activity (PAHs) were analysed as well and easily support the conclusions of little anthropogenic impact on the system. Sedimentary PAH are below levels considered toxic to marine life in the St. Lawrence Estuary, attesting to the relatively low particle loads from the St. Lawrence River as well as the effectiveness of the heavily contaminated Saguenay Fjord at trapping particulate matter due to a sill at its mouth (Louchouarn *et al* 1999). In terms of PAH deposition to the systems, three main sources appear to dominate: low-level atmospheric deposition from long distances reflecting mostly petroleum burning, low-level direct inputs from industrial activities (mainly metal smelting and pulp and paper) that settle very rapidly, and possibly run-off from agricultural soils mixing with urban/industrial inputs from the Great Lakes watersheds in the maximum turbidity zone. Despite the industry in the region, the dominance of perylene in all samples might indicate agricultural run-off as an important source of natural PAH to the system. The clear association of perylene with the pyrogenic PAH certainly warrants further investigation into the role played by run-off from agricultural lands, not just as conduit for export, but in the distribution and reactivity of organic pollutants as well as the potentially larger significance on organic geochemical processes in estuarine systems as a whole.

6.1.3 Carbon sources and processing in the St. Lawrence Estuary

Though the extensive elemental and isotopic analyses of five pools of carbon, as well as PAH analyses show strong conservative tendencies and simple depositional patterns of a natural signature, main characteristics are

identified; (1) a clear spatial shift in trophic state with photo-oxidation of DOC resulting in Upper estuarine net heterotrophy and primary production resulting in Lower Estuarine net autotrophy; (2) isotopic evidence for common sources of DOC and POC exists but the two pools appear decoupled because physical mixing outpaces transfer; (3) approximately 90 % of primary produced particulate carbon and nitrogen is consumed prior to sedimentary deposition in the Lower Estuary; (4) stable isotopes indicate the export of riverine DOC is more efficient than estuarine systems from lower latitudes perhaps making similarly located estuaries important sources of terrestrial DOC to the world's oceans; (5) the benthic nepheloid layer may be a site of microbial activity in the hypoxic Lower Estuary; (6) isotopic fractionation between pwDOC and SOC implies compositionally-driven *in situ* sedimentary fractionation; and (7) a net flux of dissolved carbon into the benthic layer of the hypoxic zone is occurring, but the exact magnitude and source(s) are still not certain.

Physicochemical partitioning is shown to be very important in defining pools of estuarine organic carbon (e.g., Hernes and Benner), and DOC (bulk and UDOC) measurements of the St. Lawrence Estuary do indicate removal from the water column in the maximum turbidity zone. However, direct comparison between POC and DOC results does not directly confirm such partitioning, as noted above. PAH and lignin phenol sedimentary results can be explained by partitioning, with low mass volatile PAH for the most part below detection limits, thus the main transport mechanism being from those PAH that are typically sorbed onto particles. Sorption of some PAH to organic rich particles, such as

lignin-rich solid effluents was also not directly observed. Rather PAH putatively linked to the pulping process appear to associate with the pulp and paper effluents.

6.1.4 Photo-oxidation and Microbial Activity

Estuaries are zones where carbon dynamics are dominated by photochemistry and microbial activity (Benner and Opsahl 2001, Raymond and Bauer 2001, Otero *et al* 2003, Hernes and Benner 2003, Bianchi *et al* 2004, Mayorga *et al.* 2005, McCallister *et al* 2006a-b, Guo *et al* 2009). Bacterial activity in the water column of the Upper Estuary has been reported highest just upstream the maximum turbidity zone (but still an order of magnitude lower than other similar systems) and decreases significantly until the Lower Estuary (Painchaud *et al* 1995, Vincent *et al* 1996) and microbial degradation experiments carried over the time span of estuarine water residence (14 days) resulted in no net DOC changes. When compared to conservative estuarine mixing models show two sites of DOC removal: at the maximum turbidity zone suggesting mineral surface changes (Abril *et al* 1999) or microbial degradation (Middelburg and Herman 2007, McCallister *et al.* 2006b); and in surface waters through the Upper Estuary implicating photo-oxidation as a dominant driver of DOC degradation and by extension CO_2 efflux from the system. Synergy between photo-oxidation and microbial degradation in estuaries has been demonstrated (e.g., Amon and Benner 1996) but no such relationship is clearly demonstrated with these results.

Though microbial activity in the Upper Estuarine water column is not clearly indicated with these results, sediments in the maximum turbidity zone do show evidence for microbial sources of carbon; the abundance of the PAH perylene, speculated in Chapter 4 as a possible indicator of agricultural runoff, could just as well be of bacterial origin, though the oxidation conditions of these sediments was not investigated. Relatively low levels of PAH and lignin phenols throughout the system lead to a conclusion that natural sources

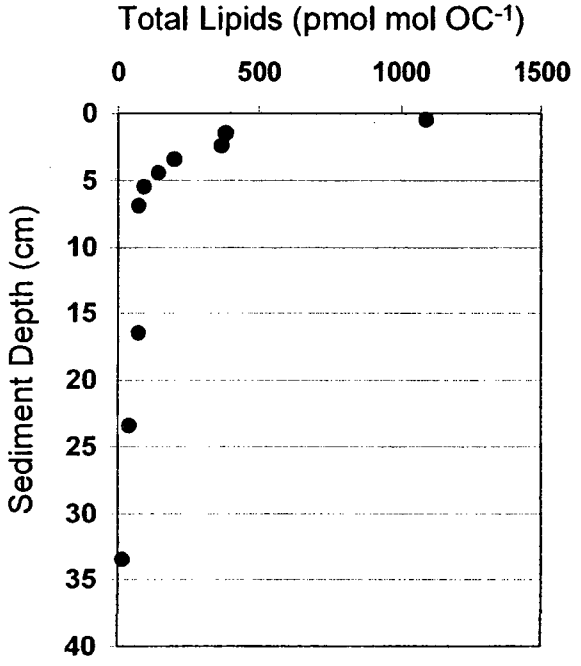

Figure 6-1 Total lipid profile in Station 23 sediments.

(planktonic/terrestrial primary and microbial secondary productivity) dominate organic carbon in the St. Lawrence Estuary. Such is supported by down-core sedimentary profiles of lipid biomarkers (Figure 6-1, manuscript in preparation). Fatty acids commonly attributed exclusively to bacteria (Parkes and Taylor 1983)

such as pentadecanoic and heptadecanoic acids are the most dominant in the system, decreasing rapidly with depth. Following the Downcore trends for OC, a conclusion that bacteria is an important source of organic carbon in the lower estuary can be postulated. Much of this material, at least the lipids, is consumed in the upper few centimetres of the sediments. Whether the sedimentary community is related to the supposed benthic community described above is not certain, but stable carbon isotopes indicate the two are distinct and do not exchange carbon. Also of importance is the question of which of these communities is responsible for the bulk of the O_2 consumption in the bottom of the St. Lawrence Estuary.

6.2 Perspective and Future Directions

6.2.1 Contributions

Evaluated against the sphere of organic geochemistry the most significant contribution of this dissertation to the field is the development of an instrument capable of obtaining $\delta^{13}C_{DOC}$ in high-salinity samples providing only the third large-scale data set of this measurement in riverine/estuarine systems (Mayorga *et al* 2005, Bouillon *et al* 2006). It also allowed additional insight into the cycling of carbon in the St. Lawrence water column that would not otherwise have been evident using quantitative measures alone. It provides a demonstration of the value of collecting $\delta^{13}C_{DOC}$, not just in water column samples but also sedimentary interstitial waters and adds to the work of other $\delta^{13}C_{DOC}$ instrumentation developments (St-Jean 2003, Osburn and St-Jean 2006, Lang *et al* 2006, Bouillon *et al* 2006) by accomplishing the analysis low-DOC high saline

waters within a reasonable analysis time. Future improvements to this first coupling should focus on reducing analysis time as ~20 – 30 minutes per sample is currently required. Automation of the trapping and releasing would also be greatly beneficial to the analysis. The data set presented in Chapter 5 joins that of Bouillon *et al* (2007a and b) in being one of the few recent high-throughput stable carbon isotope analyses of multiple pools of carbon (including DOC) in a complex system. Hopefully it will spur others in the field to add to the scant body of $\delta^{13}C_{DOC}$ knowledge to push further the survey and review conducted by Raymond and Bauer 2001 to gain more insight into the fate of riverine DOC.

6.2.2 Future Work in the St. Lawrence

One of the more surprising results from the analyses is the seemingly lack of direct anthropogenic inputs of carbon. Looking at the hydrography of the fluvial St. Lawrence and surrounding industrialized tributaries it is easy to see why with sills and fluvial lakes trapping particles and anthropogenic inputs (pollutants, sewage, etc.). This coupled to the relative simplicity of the processing of carbon in the system make the St. Lawrence Estuary an ideal location to study estuarine carbon cycling in natural systems. A good deal of information will be revealed through participation with the "Big Rivers Project" led by Anssi Vähätalo at the Univeristy of Helsinki to investigate the coupled effects of long-term UV oxidation and microbial degradation to understand the long-term sinks and cycling of riverine DOC in several major rivers in the world. A more local investigation that is strongly advocated centers on the role played by the maximum turbidity zone in regulating organic carbon dynamics. Since the only process which is strongly

implicated within the Upper Estuary is photo-oxidation different approaches are here recommended; either more experimental which would involve incubations with suspended matter, for example, or extended field observations so that more than a single "snapshot" is obtained at locations deemed to be zones of DOC dynamic changes to improve temporal dynamics at the expense of spatial coverage.

Work on microbial biomarkers has revealed bacterial biomass makes up a significant portion of organic matter in rivers (Tremblay and Benner 2009) and oceans (Kaiser and Benner 2008). The role of this secondary production in controlling and regulating the carbon cycle in the two relevant zones of the St. Lawrence Estuary (MTZ and hypoxic zone) warrants close attention. A pertinent question to both areas is the extent to which the microbial loop acts as a sink, effectively trapping carbon and nitrogen and how long does this cycle prior before remineralization? Testing this within a natural system is not a simple task, but can be most unambiguously defined with a pulse-chase experiment. Here, microbial markers, such as amino acids and the fatty acids indicated earlier can be analyzed by simple GC-MS to determine a time-series of carbon integration and turnover throughout the water column.

Though an undercurrent of the work has been no *direct* anthropogenic inputs of carbon, the carbon cycle itself has been perturbed by eutrophication of the system from agricultural run-off of nutrients. Important changes have been noted in the benthic communities of this system since the onset of hypoxia (L. Genovesi, unpublished results). Regular monitoring of elemental and isotopic

parameters of organic matter in the hypoxic bottom waters and underlying sediments coupled to changes in O_2 and physical oceanographic measurements (e.g., salinity, temperature) would help in being able to understand and quantify the oxygen consumption process. The quandary of the benthic layer must also be resolved. If it is a location of intense microbial activity then surely it must be the prime agent in effectuating hypoxia and the biogeochemical cycling by this community should be investigated.

References

Abril, G., M. Nogueira, H. Etcheber, G. Cabeçadas, E. Lemaire, and M.J. Brogueira (2002) Behaviour of organic carbon in nine contrasting European estuaries. *Est. Coast. Shelf Sci.*, **54**, 241 – 262.

Alperin, M.J., C.S. Martens, D.B. Albert, I.B. Suayah, L.K. Benninger, N.E. Blair, and R. Jahnke (1999) Benthic fluxes and porewater concentration profiles of dissolved organic carbon in sediments from the North Carolina continental slope, *Geochim. Cosmochim. Acta,* **63**, 427 – 448.

Amon, R.W.M. and R. Benner (1996) Photochemical and microbial consumption of dissolved organic carbon and dissolved oxygen in the Amazon River system. *Geochim. Cosmochim. Acta*, **60**, 1783 – 1792.

Arnarson, T.S., and R.G. Keil (2000) Mechanisms of pore water organic matter adsorption to montmorillonite, *Mar. Chem.*, **71**, 309 – 320.

Aufdenkampe, A.K., J.I. Hedges, A.V. Krusche, C. Llerena and J. E. Richey. (2001) Sorptive fractionation of dissolved organic nitrogen and amino acids onto sediments within the Amazon Basin. *Limnol. Oceanogr.*, **46**, 1921 – 1935.

Azam, F. (1998) Microbial control of oceanic carbon flux: The plot thickens, *Science*, **280**, 694 – 696.

Barra, R., R. Quiroz, K. Saez, A. Araneda, R. Urrutia, and P. Popp (2008) Sources of polycyclic aromatic hydrocarbons PAHs in sediments of the Biobio River in south central Chile. *Environ. Chem. Lett.*, DOI, 10.1007/s10311-008-0148-z.

Barthe, M., E. Pelletier, G.D. Breedveld, and G. Cornelissen (2008) Passive samplers versus surfactant extraction for the evaluation of PAH availability in sediments with variable levels of contamination. *Chemosphere*, **71**, 1486 - 1493.

Bauer, J. E., E.R.M. Druffel, and P.M. Williams (1992) Recovery of submilligram quantities of carbon dioxide from gas streams by molecular sieve for subsequent determination by carbon-13 and carbon-14 natural abundances. *Anal. Chem.*, **64**, 824 – 827.

Bauer, J. E., E.R.M. Druffel, D.M. Wolgast, and S. Griffin (2001) Sources and cycling of dissolved and particulate organic radiocarbon in the northwest Atlantic continental margin. *Global Biogeochem. Cycles*, **15**, 615 – 636.

Bauer, J. E.; M.L. Occelli, P.M. Williams, and P.C. McCaslin (1993) Heterogeneous catalyst structure and function: review and implications for the analysis of dissolved organic carbon and nitrogen in natural waters. *Mar. Chem.* **41**, 75 – 89.

Bauer, J.E., E.R.M. Druffel, D.M. Wolgast, and S. Griffin (2002) Temporal and regional variability in sources and cycling of DOC and POC in the northwest Atlantic continental shelf and slope, *Deep-Sea Res. II*, **49**, 4387 – 4419.

Bekker, A., H.D. Holland, P.L. Wang, D. Rumble, H.J. Stein, J.L. Hannah, L.L. Coetzee, and N.J. Beukes (2004) Dating the rise of atmospheric oxygen, *Nature*, **427**, 117 – 120.

Belicka, L.L., R.W. Macdonald, and H.R. Harvey (2002) Sources and transport of organic carbon to shelf, slope, and basin surface sediments of the Artic Ocean. *Deep-Sea Res. I*, **49**, 1463 – 1483.

Benner, R. (2002) Chemical composition and reactivity, in Biogeochemistry of Marine Dissolved Organic Matter, edited by D. Hansell and C. Carlson, pp. 59 – 90, Academic Press.

Benner, R. (2004) What happens to terrestrial organic matter in the ocean? *Mar. Chem.*, **92**, 307 – 310.

Benner, R. and S. Opsahl (2001) Molecular indicators of the sources and transformations of dissolved organic matter in the Mississippi river plume, *Org. Geochem.*, **32**, 597 – 611.

Benoit, P., Y. Gratton, and A. Mucci (2006) Modeling of dissolved oxygen levels in the bottom waters of the Lower St. Lawrence Estuary: Coupling of benthic and pelagic processes, *Mar. Chem*, **102**, 13 – 32.

Benson, J.R., and P.E. Hare (1975) o-Phthalaldehyde: Fluorogenic detection of primary amines in the picomole range. Comparison with fluorescamine and ninhydrin. *Proc. Nat. Acad. Sci.* **72**, 619 – 622.

Berner, R.A. (1982) Early Diagenesis: A Theoretical Approach, Princeton.

Bianchi, T.S., T. Filley, K. Dria, and P.G. Hatcher (2004) Temporal variability in sources of dissolved organic carbon in the lower Mississippi River, *Geochim. Cosmochim. Acta*, **68**, 959 – 967.

Bouillon, S., F. Dehairs, L.-S. Schiettecatte, and A.V. Borges (2007b) Biogeochemistry of the Tana estuary and delta (northern Kenya), *Limnol. Oceanogr.*, **52**, 46 – 59.

Bouillon, S., J.J. Middelburg, F. Dehairs, A.V. Borges, G. Abril, M.R. Flindt, S. Ulomi, and E. Kristensen (2007a) Importance of intertidal sediment processes and porewater exchange on the water column biogeochemistry in a pristine mangrove creek (Ras Dege, Tanzania), *Biogeosciences*, **4**, 311 – 322.

Bouillon, S., M. Korntheuer, W. Baeyens, and F. Dehairs (2006) A new automated setup for stable isotope analysis of dissolved organic carbon, *Limnol. Oceanogr.: Methods*, **4**, 216 – 226.

Bourbonniere, R.A., and P.A. Meyers (1996) Sedimentary geolipid records of historical changes in the watersheds and productivities of Lakes Ontario and Erie. *Limnol. Oceanogr.*, **41**, 352 – 359.

Breger, I.A. (1960). Diagenesis of metabolites and a discussion on the origin of petroleum hydrocarbons. *Geochim. Cosmochim. Acta*. **19**, 297 – 308.

Brion, D. and E. Pelletier (2005) Modelling PAHs adsorption and sequestration in freshwater and marine sediments. *Chemosphere*, **61**, 867 – 876.

Brown, F.S., M.J. Baedecker, A. Nissenbaum, and I.R. Kaplan (1972) Early diagenesis in a reducing fjord, Saanich Inlet, British Columbia – III. Changes in organic constituents of sediment. *Geochim. Cosmochim. Acta.* **36**, 1185 – 1208.

Bruland, K.W., E.L. Rue, G.J. Smith, and G.R. DiTullio (2005) Iron, macronutrients and diatom blooms in the Peru upwelling regime: brown and blue waters of Peru. *Mar. Chem.*, **93**, 81 – 103.

Burdige, D., W. Berleson, K. Coale, J. McManus and K. Johnson (1999) Fluxes of dissolved organic carbon from continental margin sediments. *Geochim. Cosmochim. Acta*, **63**, 1507 – 1515.

Catling, D.C. and M.W. Claire (2005) How Earth's atmosphere evolved to an oxic state: A status report. *EPS Lett.*, **237**, 1 – 20.

Chefetz, B. and B. Xing (2009) Relative role of aliphatic and aromatic moieties as sorption domains for organic compounds: A review. *Environ. Sci. Technol*, **43**, 1680 – 1688.

Chen, C-T C., and A.V. Borges (2009) Reconciling opposing views on carbon cycling in the coastal ocean: Continental shelves as sinks and near-shore ecosystems as sources of atmospheric CO2, *Deep-Sea Res. II*, **56**, 578 – 590.

Chen, W., Z. Zhao, J-F Koprivnjak, and M.E. Perdue (2002) A mechanistic study of the high-temperature oxidation of organic matter in carbon analyzer. *Mar. Chem.*, **78**, 185 – 196.

Cifuentes, L. A., and P.M. Eldridge (1998) A mass- and isotope-balance model of DOC mixing in estuaries. *Limnol. Oceanogr.* **43**, 1872 – 1882.

Coakley, J.P., E. Nagy, and J.B. Sérodes (1993) Spatial and vertical trends in sediment-phase contaminants in the Upper Estuary of the St. Lawrence River. *Estuaries*, **16**, 653 – 669.

Colombo, J.C., N. Silverberg, and J.N. Gearing (1996a) Biogeochemistry of organic matter in the Laurentian Trough, I. Composition and vertical fluxes of rapidly settling particles, *Mar. Chem*, **51**, 277 – 293.

Colombo, J.C., N. Silverberg, and J.N. Gearing (1996b) Biogeochemistry of organic matter in the Laurentian Trough, II. Bulk composition of the sediments and relative reactivity of major components during early diagenesis, *Mar. Chem,* **51**, 295 – 314.

Colombo, J.C., N. Silverberg, and J.N. Gearing (1997) Lipid biogeochemistry in the Laurentian Trough – II. Changes in composition of fatty acids, sterols and aliphatic hydrocarbons during early diagenesis, *Org. Geochem.*, **26**, 257 – 274.

Coplen, T. B., W.A. Brand, M. Gehre, M. Groening, H.A.J. Meijer, B. Toman, and R.M. Verkoutren (2006) New guidelines for $\delta^{13}C$ measurements. *Anal. Chem.*, **78**, 2439 – 2441.

Cossa, D., M. Picard-Bérubé, and J.P. Gouygou (1983) Polynuclear aromatic hydrocarbons in mussels from the Estuary and Northern Gulf of St. Lawrence. *Canada Bull. Environ. Contam. Toxicol.*, **37**, 133 – 140.

Countway, R.E., R.M. Dickhut, and E.A. Canuel (2003) Polycyclic aromatic hydrocarbon PAH distributions and associations with organic matter in surface waters of the York River, VA, Estuary. *Org. Geochem.*, **34**, 209 – 244.

d'Angelan, B. (1990) Recent sediments and sediment transport processes in the St. awrence Estuary, in Oceanography or a Large-Scale Estuarine System, the St. Lawrence, Eds. M.I. El-Sabh and N.S. Silverberg, pp. 109 – 129. Springer-Verlag.

Dauwe, B., and J.J. Middelburg (1998) Amino acids and hexosamines as indicators of organic matter degradation state in North Sea sediments. *Limnol. Oceanogr.* **43**, 782 – 798.

De Troyer, I., K. Coorevits, S. Barker, C. Perry, and R. Merckx, (2007) Isotopic analysis of dissolved organic carbon using a catalytic combustion TOC analyser coupled with an IRMS, BASIS, Ghent, Belgium.

Diaz, R.J., and Rosenberg R. (1995) Marine benthic hypoxia: A review of its ecological effects and the behavioural responses of benthic macrofauna Oceanogr. *Mar. Biol. Ann. Rev.* **33**, 245 – 303.

Dittmar, T., K. Whitehead, E.C. Minor, and B.P. Koch (2007) Tracing terrigenous dissolved organic matter and its photochemical decay in the ocean by using liquid chromatography/mass spectrometry. *Mar. Chem.* **107**, 378 – 387.

Dreyer, A., C. Blodau, J. Turunen, and M. Radke (2005a) The spatial distribution of PAH depositions to peatlands of Eastern Canada. *Atmos. Environ.*, **39**, 3725 – 3733.

Dreyer, A., M. Radke, J. Turunen, and C. Blodau (2005b) Long-term change of polycyclic aromatic hydrocarbon deposition to peatlands of Eastern Canada. *Environ. Sci. Technol.*, **39**, 3918 – 3924.

Druffel, E.R.M., P.M. Williams, J.E. Bauer, and J.R. Ertel (1992) Cycling of dissolved and particulate organic matter in the open ocean, *J. Geophys. Res.*, **97**, 15639 – 15659.

Dufour, R. and P. Ouellet (2007) Estuary and Gulf of St. Lawrence marine ecosystem overview and assessment report, *Can. Tech. Rep. Fish. Aquat. Sci.*, 2744E, 112p.

Eglinton, T.I., and G. Eglinton (2008) Molecular proxies for paleoclimatology. *EPSL*, **275**, 1 – 16.

Feakins, S.J., T.I. Eglinton, and P.B. deMenocal (2007) A comparison of biomarker records of northeast African vegetation from lacustrine and marine sediments ca. 3.40 Ma. *Org. Geochem.* **38**, 1607 – 1624.

Frankignoulle, M., G. Abril, A. Borges, I. Bourge, C. Canon, B. Delille, E. Libert, and J.M. Théate (1998) Carbon dioxide emission from European estuaries, *Science*, **282**, 434 – 436.

Fry , B., S. Saupe, M. Hullar, M. and B.J. Peterson (1993) Platinum-catalyzed combustion of DOC in sealed tubes for stable isotopic analysis. *Mar. Chem.*, **41**, 187 – 193.

Fry, B. W. Brand, F.J. Mersch, K. Tholke, and R. Garritt, R. (1992) Automated analysis system for coupled $\delta^{13}C$ and $\delta^{15}N$ measurements. *Anal. Chem.*, **64**, 288 – 291.

Fry, B., C.S. Hopkinson, A. Nolin, and S.C. Wainright (1998) $^{13}C/^{12}C$ composition of marine dissolved organic carbon. *Chem. Geol.* **152**, 113 – 118.

Gälman, V., J. Rydberg, and C. Bigler (2009) Decadal diagenetic effects on d13C and d15N studied in varved lake sediment, *Limnol. Oceanogr.*, **54**, 917 – 924.

Gandhi, H., T.N. Wigner, P.H. Ostrom, L.A. Kaplan, and N.E. Ostrom (2004) Isotopic (^{13}C) analysis of dissolved organic carbon in stream water using an elemental analyzer coupled to a stable isotope ratio mass spectrometer. *Rapid Commun. Mass Spectrom.*, **18**, 903 – 906.

Gearing, J. N., and R. Pocklington (1990) Organic geochemical studies in the St. Lawrence Estuary, in Oceanography or a Large-Scale Estuarine System, the St. Lawrence, Eds. M.I. El-Sabh and N.S. Silverberg, pp. 170 – 201. Springer-Verlag.

Gilbert, D., B. Sundby, C. Gobeil, A. Mucci, and G.H. Tremblay (2005) A seventy-two year record of diminishing deep-water oxygen in the St. Lawrence estuary: The northwest Atlantic connection. *Limnol. Oceanogr.*, **50**, 1654 – 1666.

Gocht, T., J.A.C. Barth, M. Epp, M. Jochmann, M. Blessing, T.C. Schmidt, and P. Grathwohl (2007) Indications for pedogenic formation of perylene in a terrestrial soil profile, depth distribution and first results from stable carbon isotope ratios. *Appl. Geochem.*, **22**, 2652 – 2663.

Goñi, M. and J.I. Hedges (1995) Sources and reactivities of marine-derived organic matter in coastal sediments as determined by alkaline CuO oxidation, *Geochim. Cosmochim. Acta*, **59**, 2965 – 2981.

Goodwin, P., R.G. Williams, A. Ridgewell, and M.J. Follows (2009) Climate sensitivity to the carbon cycle modulated by past and future changes in ocean chemistry, *Nature Geoscience*, **2**, 145 – 150.

Görs, S., D. Rentsch, U. Schiewer, U. Karsten, and R. Schumann (2007) Dissolved organic matter along the eutrophication gradient of the Darβ – Zingst Bodden Chain, Southern Baltic Sea: I. Chemical characterization and composition. *Mar. Chem*, **104**, 125 – 142.

Gray, J.S., R.S. Wu, and Y.Y. Or (2002) Effects of hypoxia and organic enrichment on the coastal marine environment *Mar. Ecol. Prog. Ser.* **238**: 249 – 279.

Guo, L., D.M. White, C. Xu, and P.H. Santschi (2009) Chemical and isotopic composition of high-molecular-weight dissolved organic matter from the Mississippi River plume, *Mar. Chem*, **114**, 63 – 71.

Hansell, D. A., and C.A. Carlson (2001) Marine dissolved organic matter and the carbon cycle. *Oceanography*, **14**, 41 – 49.

Hansell, D.A. and C.A. Carlson (1998) Deep-ocean gradients in the concentration of dissolved organic carbon. *Nature*, **395**, 263 – 266.

Hansell, D.A. and C.A. Carlson, Eds. (2002) Biogeochemistry of Marine Dissolved Organic Matter. Academic Press.

Hedges, J. and P.L. Parker (1976) Land-derived organic matter in surface sediments from the Gulf of Mexico. *Geochim. Cosmochim. Acta.*, **40**, 1019 – 1029.

Hedges, J.I. (1992) Global biogeochemical cycles: progress and problems, *Mar. Chem.*, **39**, 67 – 93.

Hedges, J.I. and J.M. Oades (1997) Comparitive organic geochemistries of soils and marine sediments. *Org. Geochem.*, **27**, 319 – 361.

Hélie, J.-F. and C. Hillaire-Marcel (2006) Sources of particulate and dissolved organic carbon in the St. Lawrence River: isotopic approach, *Hydrol. Process.*, **20**, 1945 – 1959.

Hellou, J., P.V. Hodson, and C. Upshall (1995) Contaminants in muscle of plaice and halibut collected from the St. Lawrence Estuary and northwest Atlantic. *Chem. Ecol.*, **11**, 11 – 24.

Hernes, P.J. and R. Benner (2003) Photochemical and microbial degradation of dissolved lignin phenols: Implications for the fate of terrigenous dissolved organic matter in marine environments, *J. Geophys. Res.*, **108**, doi: 10.1029/2002JC001421.

Holcombe, B.L., R.G. Keil, and A.H. Devol (2001) Determination of pore-water dissolved organic carbon fluxes from Mexican margin sediments, *Limnol. Oceanogr.*, **46**, 298 – 308.

Hung, C-C, K.W. Warnken, and P.H. Santschi (2005) A seasonal survey of carbohydrates and uronic acids in the Trinity River, Texas, *Org. Geochem.*, **36**, 463 – 472.

Huygens, D., P. Boeckx, J. Vermeulen, X. De Paepe, A. Park, S. Barker, and O. Van Cleemput, (2007) On-line technique to determine the isotopic composition of total dissolved nitrogen. *Anal. Chem.*, **79**, 8644 – 8649.

IPCC; Core Writing Team, Pachauri RK, Reisinger A, eds (2007) Climate Change 2007: Synthesis Report. Contribution of Working Groups I, II and III to the Fourth Assessment Report of the Intergovernmental Panel on Climate Change (IPCC, Geneva).

Kaiser, K., and R. Benner (2008) Major bacterial contribution to the ocean reservoir of detrital organic carbon and nitrogen. *Limnol. Oceanogr.*, **53**, 99 – 112.

Kaldy, J. E., L.A. Cifuentes, and D. Brock (2005) Using stable isotope analyses to assess carbon dynamics in a shallow subtropical estuary. *Estuaries*, **28**, 86 – 95.

Katsev, S., G. Chaillou, B. Sundby, and A. Mucci (2007) Effects of progressive oxygen depletion on sediment diagenesis and fluxes: A model for the lower St. Lawrence River Estuary, *Limnol. Oceanogr.*, **52**, 2555 – 2568.

Keiluweit, M. and M. Kleber (2009) Molecular-level interactions in soils and sediments: The role of aromatic p-systems. *Environ. Sci. Technol.*, **43**, 3421 – 3429.

Killops, S.D., and V.J. Killops (2004). An introduction to organic geochemistry. Wiley-Blackwell.

Lang, S.Q., M.D. Lilley, and J.I. Hedges (2007) A method to measure the isotopic (13C) composition of dissolved organic carbon using a high temperature combustion instrument, *Mar. Chem.*, **103**, 318 – 326.

Lee, K., J.J. Nagler, M. Fournier, M. Lebeuf, and D.G. Cyr (1999) Toxicological characterization of sediments from Baie des Anglais on the St. Lawrence Estuary. *Chemosphere*, **39**, 1019 – 1035.

Lehmann, M., B. Barnett, Y. Gélinas, D. Gilbert, RJ. Maranger, A. Mucci, B. Sundby, and B. Thibodeau (2009) Aerobic respiration and hypoxia in the Lower St. Lawrence Estuary: stable isotope ratios of dissolved oxygen constrain oxygen sink partitioning. *Limnol. Oceanogr.*, in press.

Lima, A.L.C., J.W. Farrington, and C.M. Reddy (2005) Combustion-derived polycyclic aromatic hydrocarbons in the environment—A review. *Environ. Forensics*, **6**, 109 – 131.

Loh, A.N., J.E. Bauer, and E.R.M. Druffel (2004) Variable ageing and storage of dissolved organic components in the open ocean, *Nature*, **430**, 877 – 881.

Louchouarn, P., M. Lucotte, and N. Farella (1999) Historical and geographical variations of sources and transport of terrigenous organic matter within a large-scale coastal environment, *Org. Geochem.*, **30**, 675 – 699.

Lucotte, M., C. Hillaire-Marcel, and P. Louchouarn (1991) First-order organic carbon budget in the St. Lawrence Lower Estuary from 13C data, *Estuar. Coast. Shel Sci.*, **32**, 297 – 312.

Madureira, L.A.S., M.H. Conte, and G. Eglinton (1995) Early diagenesis of lipid biomarker compounds in North Atlantic Sediments. *Paleoceanogr.*, **10**, 627 – 642.

Martel L., M.J. Gagnon, R. Massé, A. Leclerc, and L. Tremblay (1986) Polycyclic aromatic hydrocarbons in sediments from the Saguenay Fjord. *Canada Bull. Environ. Contam. Toxicol.*, **37**, 133 – 140.

Martineau, D., K. Lemberger, A. Dallaire, P. Labelle, T.P. Lipscomb, P. Michel, and I. Mikaelian (2002) Cancer in wildlife, a case study, beluga from the St. Lawrence Estuary, Québec, Canada. *Environ. Health Perspect.*, **110**, 285 – 292.

Maybeck, M. (1982) Carbon, nitrogen and phosphorus transport by world rivers, *Amer. J. Sci.*, **282**, 401 – 450.

McCallister, S.L., J.E. Bauer, H.W. Ducklow, and E.A. Canuel (2006a) Sources of estuarine dissolved and particulate organic matter: A multi-tracer approach, *Org. Geochem.*, **37**, 454 – 468.

McCallister, S.L., J.E. Bauer, H.W. Ducklow, and E.A. Canuel (2006b) Bioreactivity of estuarine dissolved organic matter: A combined geochemical and microbiological approach, *Limnol. Oceanogr.*, **51**, 94 – 100.

McVeety, B.D. and R.A. Hites (1988) Atmospheric deposition of polycyclic aromatic hydrocarbons to surface waters: a mass balance approach. *Atmos. Sci.*, **22**, 511 – 536.

Meyers, P.A. (2003) Applications of organic geochemistry to paleolimnological reconstructions: a summary of examples from the Laurentian Great Lakes. *Org. Geochem.* **34**, 261 – 289.

Middelburg, J. J. and P.M.J. Herman (2007) Organic matter processing in tidal estuaries. *Mar. Chem.*, **106**, 127 – 147.

Miller, A.E.J. (1999) Seasonal investigations of dissolved organic carbon dynamics in the Tamar Estuary, U.K. Est. *Coast. Shelf Sci*, **49**, 891 – 908.

Mitra, S., R.M. Dickhut, S.A. Kuehl, K.L. Kimbrough (1999) Polycyclic aromatic hydrocarbon PAH source, sediment deposition patterns, and particle geochemistry as factors influencing (PAH) distribution coefficients in sediments of the Elizabeth River, VA, USA. *Mar. Chem.*, **66**, 113 – 127.

Mucci, A., B. Sundby, M. Gehlen, T. Arakaki, S. Zhong, and N. Silverberg (2000) The fate of carbon in continental shelf sediments of eastern Canada: a case study, *Deep-Sea Res. II*, **47**, 733 – 760.

Nixon, S.W. (1995) Coastal marine eutrophication: a definition, social causes and future concerns, *Ophelia,* **41**, 199 – 220.

Opsahl, S. and R. Benner (1997) Distribution and cycling of terrigenous dissolved organic matter in the ocean, *Nature*, **386**, 480 – 482.

Oros, D.R., and B.R.T. Simoneit (2000) Identification and emission rates of molecular tracers in coal smoke particulate matter. *Fuel*, **79**, 515 – 536.

Osburn, C.L. and G. St-Jean (2007) The use of wet chemical oxidation with high-amplification isotope mass spectrometry (WCO-IRMS) to measure stable isotope values of dissolved organic carbon in seawater, *Limnol. Oceanogr.: Methods*, **5**, 296 – 308.

Otero, E., C. Randolph, J.E. Noakes, and R.E. Hodson (2003) The distribution and $\delta^{13}C$ of dissolved organic carbon and its humic fraction in estuaries of southeastern USA, *Est. Coast. Shelf Sci.*, **56**, 1187 – 1194.

Packard, T., W. Chen, D. Blasco, C. Savenkoff, A.F. Vézina, R. Tian, L. St-Amand, S.O. Roy, C. Lovejoy, B. Klein, J.-C. Therriault, L. Legendre, and R.G. Ingram (2000) Dissolved organic carbon in the Gulf of St. Lawrence, *Deep-Sea Res. II*, **47**, 435 – 459.

Painchaud, J., D. Lefaivre, J.C. Therriault, and L. Legendre (1995a) Physical processes controlling bacterial distribution and variability in the Upper St. Lawrence Estuary. *Estuaries*, **18**, 433 – 444.

Painchaud, J., J-C Therriault, and L. Legendre (1995b) Assessment of salinity-related mortality of freshwater bacteria in the St. Lawrence Estuary, *Appl. Environ. Microbiol.*, **61**, 205 – 208.

Panetta, R.J., M. Ibrahim, and Y. Gélinas (2008), Coupling a high-temperature catalytic oxidation total organic carbon analyzer to an isotope ratio mass spectrometer to measure natural–abundance $\delta^{13}C$–dissolved organic carbon in marine and freshwater samples, *Anal. Chem.*, **80**, 5232 – 5239.

Panetta, R.J. and Y. Gélinas (2009) Expressing biomarker data in stoichiometric terms, shifts in distribution and biogeochemical interpretation. *Limnol. Oceanogr: Methods*, **7**, 269 – 276.

Parkes, R.J., and J. Taylor (1983) The relationship between fatty acid distributions and bacterial respiratory types in contemporary marine sediments. *Estuar. Coast. Shelf Sci.*, **16**, 173 – 189.

Peltzer, E. T., B. Fry, P.H. Doering, J.H. McKenna, B. Norrman, and U.L. Zweifel (1996) A comparison of methods for the measurement of dissolved organic carbon in natural waters. *Mar. Chem.*, **54**, 85 – 96.

Perdue, E.M. and Koprivnjak, J-F. (2007) Using the C/N ratio to estimate terrigenous inputs of organic matter to aquatic environments, *Est. Coast. Shelf Sci.*, **73**, 65 – 72.

Peterson, B. J., R.W. Howarth, and R.H. Garritt (1985) Multiple stable isotopes used to trace the flow of organic matter in estuarine food webs. *Science*, **227**, 1361 – 1363.

Peterson, B., B. Fry, M. Hullar, and S. Saupe (1994) The distribution and stable carbon isotopic composition of dissolved organic carbon in estuaries, *Estuaries*, **17**, 111 – 121.

Polizzotto, M.L., B.D. Kocar, S.G. Benner, M. Sampson and S. Fendorf (2008) Near-surface wetland sediments as a source of arsenic release to ground water in Asia. *Nature*, **454**, 505 – 509.

Poynter, J., and G. Eglinton (1990) Molecular composition of three sediments from hole 717C: the Bengal Fan. In J.R. Cochran and D.A.V. Stow [eds.], *Proc. ODP, Sci. Results* **116**: 155 – 161.

Prahl, F.G. and R. Carpenter (1983) Polycyclic aromatic hydrocarbon PAH-phase associations in Washington coastal sediments. *Geochim. Cosmochim. Acta*, **47**, 1013 – 1023.

Qian, J. and K. Mopper, (1996) Automated high-performance, high-temperature combustion total organic carbon analyzer. *Anal. Chem.*, **68**, 3090 – 3097.

Ramanathan, V. and Y. Feng (2008) On avoiding dangerous anthropogenic interference with the climate system: Formidable challenges ahead *PNAS*, **105**, 14245 – 14250.

Raymond, P.A., and J.E. Bauer (2001) Use of 14C and 13C natural abundances for evaluating riverine, estuarine, and coastal DOC and POC sources and cycling: a review and synthesis, *Org. Geochem.*, **32**, 469 – 485.

Rennie, M. J., W. Meier-Augenstein, P.W. Watt, A. Patel, I.S. Begley, and C.M. Scrimgeour (1996) Use of Continuous Flow - Combustion - Isotope Ratio Mass Spectrometry in Studies of Human Metabolism. *Biochem. Soc. Trans.*, **24**, 927 – 932.

Rommerskirchen, F., A. Plader, G. Eglinton, Y. Chikaraishi, and J. Rullkötter (2006) Chemotaxonomic significance of distribution and stable carbon isotopic composition of long-chain alkanes and alkan-1-ols in C4 grass waxes. *Org. Geochem.*, **37**, 1303 – 1332.

Rothman, D.H. and D.C. Forney (2007) Physical model for the decay and preservation of marine organic carbon, *Science*, **316**, 1325 – 1328.

Roy, S., B. Sundby, A.F. Vézina, and L. Legendre (2000) A Canadian JGOFS process study in the Gulf of St. Lawrence. Introduction, *Deep-Sea Res. II*, **47**, 377 – 384.

Salau, J.S.I., R. Tauler, J.M. Bayona, and I. Tolosa (1997) Input characterization of sedimentary organic contaminants and molecular markers in the northwestern Mediterranean Sea by exploratory data analysis. *Environ. Sci. Tech.*, **31**, 3482 – 3490.

Schlünz, B., R.R. Schneider, P.J. Müller, W.J. Showers, and G. Wefer (1999) Terrestrial organic carbon accumulation on the Amazon deep sea fan during the last glacial sea level low stand. *Chem. Geol.*, **159**, 263 – 281.

Schrope, M. (2006) The dead zones. *New Scientist,* **192**, 38 – 42.

Schubert, C., J. Niggemann, G. Klockgether, and T. Fedelman (2005) Chlorin Index: A new paramter for organic matter freshness in sediments. *Geochem. Geophys. Geosyst.*, **6**, Q03005, doi: 10.1029/2004GC000837.

Schwarzenbach, R.P. and J. Westall (1981) Transport of nonpolar organic compounds from surface water to groundwater, laboratory sorption studies. *Environ. Sci. Technol.*, **15**, 1360 – 1367.

Sharp, J.; C.A. Carlson, E.T. Peltzer, D.M. Castle-Ward, K.B. Savidge, and K.R. Rinker, (2002) Final dissolved organic carbon broad community intercalibration and preliminary use of DOC reference materials. *Mar. Chem.*, **77**, 239 – 253.

Silliman, J.E., P.A. Meyers, P.H. Ostrom, N.E. Ostrom, and B.J. Eadie (2000) Indications for pedogenic formation of perylene in a terrestrial soil profile: Depth distribution and first results from stable carbon isotope ratios. *Org. Geochem.*, **31**, 1133 – 1142.

Simpson, M.J., B. Chefetz, A.P. Deshmukh, and P.G. Hatcher (2005) Comparison of polycyclic aromatic hydrocarbon distributions and sedimentary organic matter characteristics in contaminated, coastal sediments from Pensacola Bay, Florida. *Mar. Environ. Res.*, **59**, 139 – 163.

Sluijs, A., S. Schouten, M. Pagani, M. Woltering, H. Brinkhuis, J.S. Sinninghe Damste', G.R. Dickens, M. Huber, G-R. Reichart, R. Stein, J. Matthiessen, L.J. Lourens, N. Pedentchouk, J. Backman, K. Moran, K., and Expedition 302 Scientists (2006) Subtropical Arctic Ocean temperatures during the Palaeocene/Eocene thermal maximum. *Nature*, **44**, 610 – 613.

Smith, J.N. and C.T. Schafer (1999) Sedimentation, bioturbation, and Hg uptake in the sediments of the estuary and Gulf of St. Lawrence. *Limnol. Oceanogr.*, **44**, 207 – 219.

Smith, J.N. and E.M. Levy (1990) Geochronology for polycyclic aromatic hydrocarbon contamination in sediments of the Saguenay Fjord. *Environ. Sci. Technol.*, **24**, 874 – 879.

Spyres, G., M. Nimmo, P.J. Worsfold, E.P. Achterberg, and A.E.J. Miller (2000) Determination of dissolved organic carbon in seawater using high temperature catalytic oxidation techniques. *TrAC*, **19**, 498 – 506.

Stark, A., T. Abrajano, J. Hellou, and J.L. Metcalf-Smith (2003) Molecular and isotopic characterization of polycyclic aromatic hydrocarbon distribution and sources at the international segment of the St. Lawrence River. *Org. Geochem.*, **34**, 225 – 237.

St-Jean, G. (2003) Automated quantitative and isotopic (^{13}C) analysis of dissolved inorganic carbon and dissolved organic carbon in continuous-flow using a total organic carbon analyser, *Rapid Commun. Mass Spec.*, **17**, 419 – 428.

Strumm, W. and J.J. Morgan (1996) Aquatic chemistry, chemical equilibriua and rates in natural waters, 3rd Ed. Wiley.

Syvitski, J.P.M., and E.W.H. Hutton (1996) In situ characteristics of suspended particles as determined by the floc camera assembly FCA, *J. Sea Res.*, **36**, 131 – 142.

Thibodeau, B., A. de Vernal, and A. Mucci (2006) Recent eutrophication and consequent hypoxia in the bottom waters of the Lower St. Lawrence Estuary: Micropaleontological and geochemical evidence, *Mar. Geol.*, **231**, 37 – 50.

Treibs, A.E. (1936) Chlorophyll-und Häminderivate in organischen mineralstoffen. *Angewandte Chemie.*, **49**, 682 – 686.

Tremblay, L, and R. Benner (2009) Organic matter diagenesis and bacterial contributions to detrital carbon and nitrogen in the Amazon River system. *Limnol. Oceanogr.*, **54**, 681 – 691.

Unesco (1981) The Practical Salinity Scale 1978 and the International Equation of State of Seawater 1980. *Tech. Pap. Mar. Sci.*, **36**: 25 pp.

Vähätalo, A. and R.G. Wetzel (2008) Long-term photochemical and microbial decomposition of wetland-derived dissolved organic matter with alteration of 13C:12C mass ratio, *Limnol. Oceanogr.*, **53**, 1387 – 1392.

Vincent, W., J.J. Dodson, N. Bertrand, and J-J Frenette (1996) Photosynthetic and bacterial production gradients in a larval fish nursery: the St. Lawrence River transition zone, *Mar. Ecol. Prog. Ser.*, **139**, 227 – 238.

Volkman, J.K., A.T. Revill, D.G. Holdsworth, and D. Fredricks, D. (2008) Organic matter sources in an enclosed coastal inlet assessed using lipid biomarkers and stable isotopes. *Org. Geochem.*, **39**, 689 – 710.

Wade, T.L., Y. Soliman, S.T. Sweet, G.A. Wolff, and B.J. Presley (2008) Trace elements and polycyclic aromatic hydrocarbons PAHs concentrations in deep Gulf of Mexico sediments. *Deep-Sea Res. II*, **55**, 2585 – 2593.

Wakeham, S.G. (1996) Aliphatic and polycyclic aromatic hydrocarbons in Black Sea sediments. *Mar. Chem.*, **53**, 187 – 205.

Wakeham, S.G., C. Lee, J.I. Hedges, P.J. Hernes, and M.L. Peterson (1997) Molecular indicators of diagenetic status in marine organic matter. *Geochim. Cosmochim. Acta*, **61**, 5363 – 5369.

Wakeham, S.G., C. Schaffner, and W. Geiger (1980) Polycyclic aromatic hydrocarbons in recent lake sediments – II. Compounds derived from biogenic precursors. *Geochim. Cosmochim. Acta*, **44**, 415 – 429.

Woulds, C., J.H. Andersson, G.L. Cowie, J.J. Middelburg, and L.A. Levin (2009) The short-term fate of organic carbon in marine sediments: Comparing the Pakistan margin to other regions, *Deep-Sea Res. II*, **56**, 393 – 402.

Wu, Y., J. Zhang, M. Tie-zhu, and B. Li (2001) Occurence of n-alkanes and polycyclic aromatic hydrocarbons in the core sediments of the Yellow Sea. *Mar. Chem.*, **76**, 1 – 15.

Yunker, M.B. and R. MacDonald (2003) Alkane and PAH depositional history, sources and fluxes in sediments from the Fraser River Basin and Strait of Georgia, Canada. *Org. Geochem.*, **34**, 1429 – 1454.

Yunker, M.B., L.L. Belicka, H.R. Harvey, and R.W. Macdonald (2005) Tracing the inputs and fate of marine and terrigenous organic matter in Arctic Ocean sediments: A multivariate analysis of lipid biomarkers. *Deep Sea Res. II*, **52**, 3478 – 3508.

Zimmerman, A.R., and E.A. Canuel (2001) Bulk organic matter and lipid biomarker composition of Chesapeake Bay surficial sediments as indicators of environmental processes. *Est. Coast. Shelf Sci.*, **53**, 319 – 341.

Appendix 1. Cover Pages of Published Chapters

The following are reprint cover pages of the two chapters in this thesis which have appeared in print. Chapter 2, "Coupling a high-temperature catalytic oxidation total organic carbon analyzer to an isotope ratio mass spectrometer to measure natural-abundance δ^{13}C-DOC in marine and freshwater samples" appeared in the July 1, 2008 issue of *Analytical Chemistry*, (Volume 80) under the heading of a Technical Note. Chapter 3, "Expressing biomarker data in stoichiometric terms: shifts in distribution and biogeochemical interpretation" was published on-line in April 2009 in *Limnology and Oceanography: Methods* (Volume 7).

Anal. Chem. 2008, 80, 5232–5239

Technical Notes

Coupling a High-Temperature Catalytic Oxidation Total Organic Carbon Analyzer to an Isotope Ratio Mass Spectrometer To Measure Natural-Abundance δ^{13}C-Dissolved Organic Carbon In Marine and Freshwater Samples

Robert J. Panetta, Mina Ibrahim, and Yves Gélinas*

GEOTOP and Department of Chemistry and Biochemistry, Concordia University, 7141 Sherbrooke Street West, Montréal, Québec, Canada, H4B 1R6

The stable isotope composition of dissolved organic carbon (δ^{13}C-DOC) provides powerful information toward understanding carbon sources and cycling, but analytical limitations have precluded its routine measurement in natural samples. Recent interfacing of wet oxidation-based dissolved organic carbon analyzers and isotope ratio mass spectrometers has simplified the measurement of δ^{13}C-DOC in freshwaters, but the analysis of salty estuarine/marine samples still proves difficult. Here we describe the coupling of the more widespread high-temperature catalytic oxidation-based total organic carbon analyzer to an isotope ratio mass spectrometer (HTC-IRMS) through cryogenic trapping of analyte gases exiting the HTC analyzer for routine analysis of δ^{13}C-DOC in aquatic and marine samples. Targeted elimination of major sources of background CO_2 originating from the HTC analyzer allows for the routine measurement of samples over the natural range of DOC concentrations (from 40 μM to over 2000 μM), and salinities (<0.1–36 g/kg). Because consensus reference natural samples for δ^{13}C-DOC do not exist, method validation was carried out with water-soluble stable isotope standards as well as previously measured natural samples (IAEA sucrose, Suwannee River Fulvic Acids, Deep Sargasso Sea consensus reference material, and St. Lawrence River water) and result in excellent δ^{13}C-DOC accuracy (±0.2‰) and precision (±0.3‰).

Measurement of the stable isotope composition of carbon (δ^{13}C) has proven a powerful approach for deciphering the sources and cycling of dissolved organic carbon (DOC) in freshwater and marine systems.[1–5] The methods employed to measure δ^{13}C-DOC in marine samples tend to be long and tedious usually requiring highly specialized, expensive equipment, large sample volumes, and a number of steps to remove carbonates and quantitatively convert DOC into CO_2 (by UV oxidation or combustion in an O_2 atmosphere) for eventual offline analysis by mass spectrometry.[6,7] Alternatively, concentrating a sample (by lyophilization or evaporation) to obtain δ^{13}C-DOC by solid-state elemental analysis coupled to an isotope ratio mass spectrometer (EA-IRMS) is a frequently chosen option. This approach works well when the ratio of DOC to inorganic salt is relatively high;[8] however, the low DOC to salt ratios that characterize estuarine/marine samples introduce a high degree of uncertainty and poor reproducibility in the measurement,[10] limiting this approach to freshwaters. Considering the importance of coastal zones to the general health of the global ocean as well as the significant role they play in the global economy, understanding how coastal phenomena are related to the carbon cycle is of growing importance.

Generally δ^{13}C-DOC is more depleted in freshwater systems (−26 to −30‰) and more enriched toward marine sites (−22 to −20‰) and the signature in the open ocean is relatively invariant with depth or location.[6] δ^{13}C-DOC mixing behavior between the fresh and marine end-members in estuaries and coasts has been modeled,[4] and when unperturbed, most systems can be predicted to a good degree. However when a coastal zone or estuary has been perturbed due to either climate change or land-use changes, the organic carbon dynamics may also be altered in a number of

* To whom correspondence should be addressed: Tel: 514-848-2424 (ext 3337). Fax: 514-848-2643. E-mail: ygelinas@alcor.concordia.ca.

(1) Raymond, P. A.; Bauer, J. E. *Org. Geochem.* **2001**, *32*, 469–485.
(2) Bauer, J. E.; Druffel, E. R. M.; Wolgast, D. M.; Griffin, S. *Global Biogeochem. Cycles* **2001**, *15*, 615–636.
(3) Druffel, E. R. M.; Williams, P. M.; Bauer, J. E.; Ertel, J. R. *J. Geophys. Res. C* **1992**, *97*, 15639–15659.
(4) Cifuentes, L. A.; Eldridge, P. M. *Recent Oceanogr.* **1998**, *43*, 1672–1688.
(5) Boutton, S.; Dehairs, F.; Schiettecatte, L-S; Borges, A. V. *Recent Oceanogr.* **2007**, *52*, 46–70.
(6) Fry, B.; Hopkinson, C. S.; Nolin, A.; Wainright, S. C. *Chem. Geol.* **1998**, *152*, 113–116.
(7) Bauer, J. E.; Druffel, E. R. M.; Williams, P. M. *Anal. Chem.* **1992**, *64*, 824–827.
(8) Fry, B.; Snape, S.; Holder, M.; Peterson, B. J. *Mar. Chem.* **1993**, *42*, 189–193.
(9) Gandhi, H.; Wigner, T. N.; Cotrom, P. H.; Raphan, L. A.; Cotrom, N. E. *Rapid Commun. Mass Spectrom.* **2004**, *18*, 903–906.
(10) St-Jean, G. *Rapid Commun. Mass Spectrom.* **2003**, *17*, 419–428.

10.1021/ac702481t CCC: $40.75
Published on Web 06/05/2008

LIMNOLOGY
and
OCEANOGRAPHY: METHODS

Limnol. Oceanogr.: Methods 7, 2009, 259–276
© 2009, by the American Society of Limnology and Oceanography, Inc

Expressing biomarker data in stoichiometric terms: shifts in distribution and biogeochemical interpretation

Robert J. Panetta and Yves Gélinas*
GEOTOP and Department of Chemistry and Biochemistry, Concordia University, Montréal, Québec, Canada

Abstract

Quantitative biomarker analysis is an invaluable tool used routinely by organic geochemists to interpret and explain environmental processes. Since the advent of organic geochemistry, all levels of biomarker methodology from wet chemistry to data interpretation have significantly advanced; however, an important aspect of data analysis has remained constant and that is the expression of biomarkers in terms of mass (e.g., mg gOC^{-1}). We argue that biomarkers are more appropriately expressed in terms of moles (e.g., mmol $molOC^{-1}$) to better reflect molecular-level distribution of compounds of interest, as well as introducing a chemical consistency for better comparability and transferability between data sets. Using modeled and real data culled from the literature, we demonstrate that the use of moles is not a trivial conversion and that distribution and relative weighting of biomarker data sets are shifted and affect the total data structure. The shift is sometimes strong enough to exert changes in interpretation (e.g., microbial abundance in an estuarine system), alter proxies (e.g., terrestrial-to-aquatic ratio), and potentially influence the use of multivariate statistical methods (e.g., principal components analysis).

Introduction

Compound-specific identification, or biomarker analysis, in organic geochemistry lends an added dimension to the understanding of the carbon cycle in environmental systems, in many cases highlighting subtle yet important details not revealed by bulk analyses alone. For example, the stable carbon isotopic signature of estuarine organic matter is generally proportional to the fraction of terrestrially derived material; however, the analysis of lignin oxidation products can shed light on its degradation state and provide more specificity on the origins of the terrestrial matter (e.g., Louchouarn et al. 1999). This higher level of understanding is invariably linked to the quantitative analysis of target biomarkers, and in particular to the calculation of the relative abundance of individual or groups of molecules to the total mass of quantified biomarkers. The analysis of source material (without which biomarker interpretation is extremely limited, as explained in Volkman et al. 2008), and its comparison to natural samples, has led to the development of a number of effective, simple, and robust biomarker-derived proxies that have advanced the understanding of carbon dynamics in environmental systems, including the terrestrial to aquatic ratio (TAR), the alkenone paleothermometer ($U^{K'}_{37}$), and average chain length (ACL), among several others (see Meyers 2003 and Eglinton and Eglinton 2008 for two thorough reviews on the topic).

The use of biomarker analysis in organic geochemistry arose from the overlapping interests of petrochemistry, geology, and ecology through the link between current biological production of organic matter to its deposition, diagenesis, and ultimate transformations to petroleum products. Alkanes, fatty acids, amino acids, polycyclic aromatic hydrocarbons, lignin, pigments, etc., were identified in a number of studies attempting to address the source of natural organic matter (e.g., Treibs 1936), its transformations in the environment (e.g., Brown et al. 1972), and how it might be converted to petroleum through geological processes (e.g., Breger 1960).

Historically, the most widely studied group of biomarkers are lipids, broadly defined as any compounds extractable with organic solvents such as dichloromethane or hexane, which comprise hundreds of distinct organic chemicals. For simplicity, lipids can be liberally separated into three branches: (1) hydrocarbons, (2) alkanoic acids, and (3) sterols. Other biomarkers that are routinely reported in biogeochemical studies

*Corresponding author: E-mail: rpanetta@live.concordia.ca

Acknowledgments

This work was funded by the National Science and Engineering Research Council of Canada (NSERC), the Fonds québécois de la recherche sur la nature et les technologies (FQRNT), and the Canadian Foundation for Innovation (CFI). The authors extend thanks to Karine Lalonde, Alexandre Ouellet, and Mina Ibrahim for helpful discussion and comments on the concept presented in this paper. This is GEOTOP publication number 2009-0003.

Appendix 2. Supporting Information for Chapter 2

Published online at http://pubs.acs.org as the accompanying Supporting Information to:

Coupling a high-temperature catalytic oxidation total organic carbon analyzer to an isotope ratio mass spectrometer to measure natural-abundance δ^{13}C-DOC in marine and freshwater samples

This Supporting Information section contains details on IRMS operating conditions, including results on signal-to-noise and linearity at low signal intensities of the mass spectrometer for the m/z 45 ion ($^{13}CO_2$). Natural sample collection and processing is detailed as well as the procedure and quantitative results for the standard addition of IHSS Suwannee River Fulvic Acids (SRFA) to a natural marine sample. Results and a representative TIC of an IAEA-CH-6 sample from the direct coupling between the unmodified TOC analyzer and the IRMS are also shown.

Isotope Ratio Mass Spectrometer

Source parameters for carbon are; magnet current 4000 mA, electron volts set to 87.5 eV and trap current held at 100 μA. Other parameters varied within normal limits throughout the analysis period and were fine-tuned regularly, including; accelerating voltage 3522-3526 V, extraction voltage 86-88 %AV, half plate differential 33-50 V, Z-plates voltage -62 to -57 V and ion repeller voltage at 0.45-0.55 V. Figure A2-1(a) shows some typical m/z 45 ion chromatograms demonstrating background noise of the IRMS is insignificant compared to analyte. Here, the trace for m/z 45 ion (^{13}C) of a representative HTC blank is clearly distinguishable from baseline and the DSS-CRM at 46 μM C is significantly larger than the HTC blank. Ion ratio (45/44) traces for samples clearly demonstrate the benefit of cryogenic trapping of HTC gases compared to direct injection, resulting in peak shape equivalent to EA-IRMS (Figure A2-1(b)). A demonstration of the stability and precision of the instrument is given for multiple low-intensity injections of CO_2 reference gas in a design simulating a regular analysis (Table A2-1, Figure A2-2). The different peak intensities are obtained by varying the time the reference gas valve is open; 30 sec. for a reference peak and 1-4 sec. to obtain the simulated analyte peaks.

Sample Collection and Storage

The St. Lawrence River was sampled near Québec City in June 2006 and at Station 23, located ~300 km downstream from Québec City in May 2007 on board the *R/V Coriolis II* representing fresh and marine end-members of the estuary, respectively. All water samples were collected with Niskin bottles

mounted on a rosette equipped with a CTD to measure *in-situ* salinity, temperature, pH, oxygen, and fluorescence. Once on board samples were immediately filtered over pre-combusted (500 °C, 4 hours) GF/F filters, transferred to pre-cleaned, pre-combusted 30-mL amber bottles and acidified with 100 μL of 12 N HCl. All samples were stored at 4 °C until time of analysis.

SRFA Standard Addition experiments

SRFA was analyzed because humic substances required strong base to dissolve and would precipitate out of solution, sometimes even before acidification. Precipitation of SRFA out of acidified, high ionic-strength solutions is also of concern as the pKa of the bulk sample is 3.80[1]. Volumetric glassware was sonicated in a concentrated KOH/30% H_2O_2 mixture for 60 minutes to oxidize organics. Other glassware was combusted at 500 °C for at least 4 hours. 1.253 mg of SRFA was dissolved in 25.00 mL of ultra-pure water giving a stock solution of 2188 μM C. Stock solution was quantitatively spiked into a sample collected at Stn. 23, 300 m (S = 34.5 psu, [DOC] = 62.8 μM C) for a final sample volume of 10.00 mL, and spike concentrations of 54, 109 and 218 μM C prepared. The spiked sample was acidified with HCl and analyzed immediately to minimize effects caused by precipitation of SRFA. Quadruplicate solutions of each spike level were prepared and analyzed. Quantitative results are shown in Figure A2-3 with *x*-intercept equal to the negative concentration of DOC in the sample matrix, and response factor within error of KHP and β-alanine calibrations.

Direct HTC-IRMS

Direct coupling of the HTC analyzer to the IRMS with only a Cu wool halogen trap resulted in δ^{13}C-DOC of -10.89 ± 1.02 (n = 3) for a 150 μL injection of 1750 μM IAEA-CH-6, with no background correction. An example TIC of the direct coupling is shown (Figure A24). The direct coupling was tested with only this solution.

References

Ritchie, J.D. and Perdue, E.M. *Geochim. Cosmochim. Acta.*, **2003**,*67*, 85-96

Table A2-1. Stability and accuracy of the IRMS for sample intensities below 1 nA.[a]

Average Height (nA)	Average δ^{13}C (‰)	Standard Deviation	Deviation from True Value (‰)
0.22	-18.61	0.14	0.02
0.60	-18.69	0.06	0.06
0.76	-18.59	0.03	0.04
0.85	-18.63	0.05	0.00
1.03	-18.61	0.05	0.02
Average	-18.62	0.02	0.01

[a]Determined with CO_2 reference gas (δ^{13}C -18.63). Each intensity is based the average of 10 samples. See Figure A2-2 for an example chromatogram of these experiments.

Figure A2-1 (a) Ion trace of m/z 45 ($^{13}CO_2$ signal) for IRMS background (purple), HTC background trapped for 19 minutes (red), DSS-CRM trapped six times (burgundy). Only the background from the HTC analyzer is significant for background correction of low-DOC concentration samples. The full scale (100 %) on the *y*-axis represents 1.06 nA for the DOC peaks. DSS-CRM is 0.19 nA, the HTC background is 0.04 nA, and the IRMS background did not register a peak.

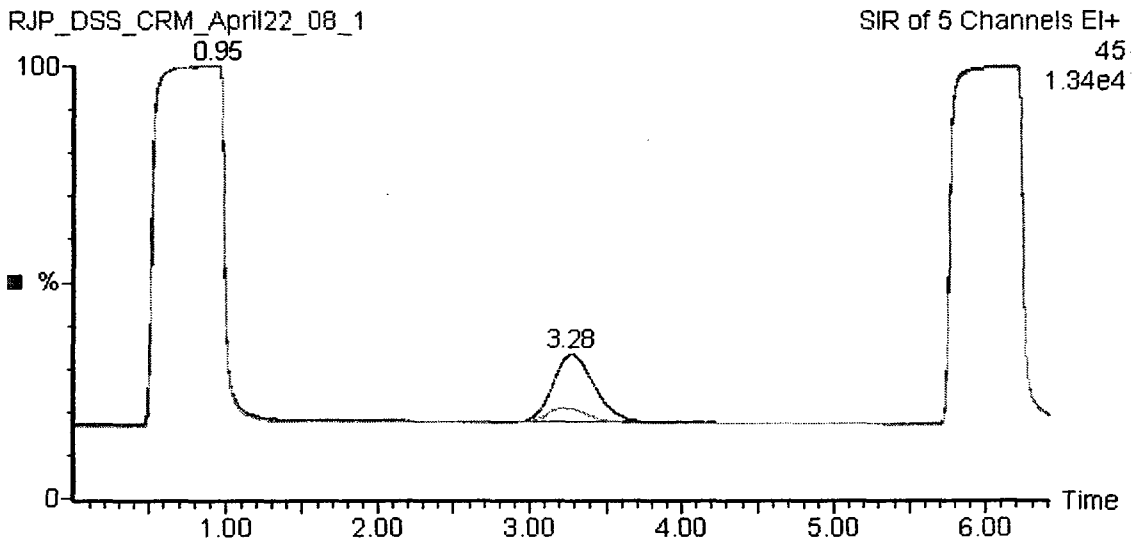

Figure A2-1 (b) Ion ratio (45/44) chromatograms for (A) 1750 μM C (0.2625 μmoles) sucrose with the unmodified HTC analyzer with no cryogenic trapping; (B) IRMS background (0.0092 μmoles C); (C) HTC analyzer background, equivalent to six trap injections; (D) DSS-CRM trapped six times (0.0414 μmoles C); (E) 2188 μM C SRFA standard trapped two times (0.6564 μmoles of carbon); (F) 2.4 μmoles of carbon from □-alanine analyzed by EA-IRMS.

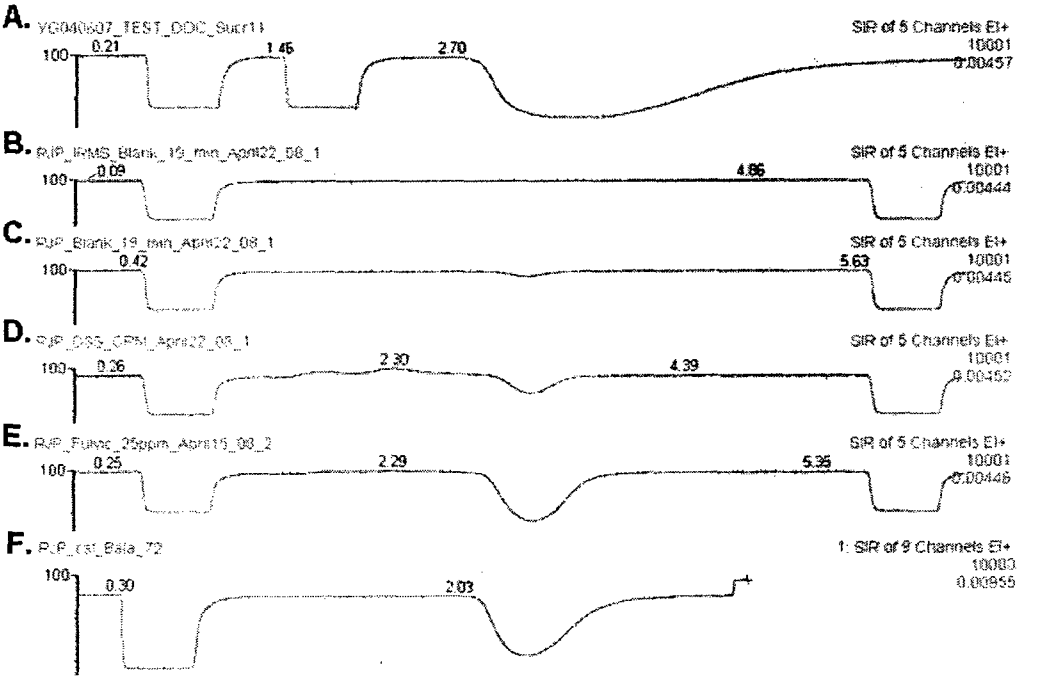

Figure A2-2. Total ion chromatogram from which stability of the IRMS is evaluated at peak intensities below 1 nA. All peaks are generated using the automatic CO_2 reference gas valve. The full scale (100 %) on *y*-axis is equivalent to 0.85 nA. All other peaks range from 0.20 to 0.75 nA, which is equivalent to six trappings of ~40 to 300 μM C respectively. See Table A2-1 for numerical data of these experiments. The sharpness of the mimicked sample peaks is due to the reference gas not passing through a chromatography column, as is the case for real sample peaks.

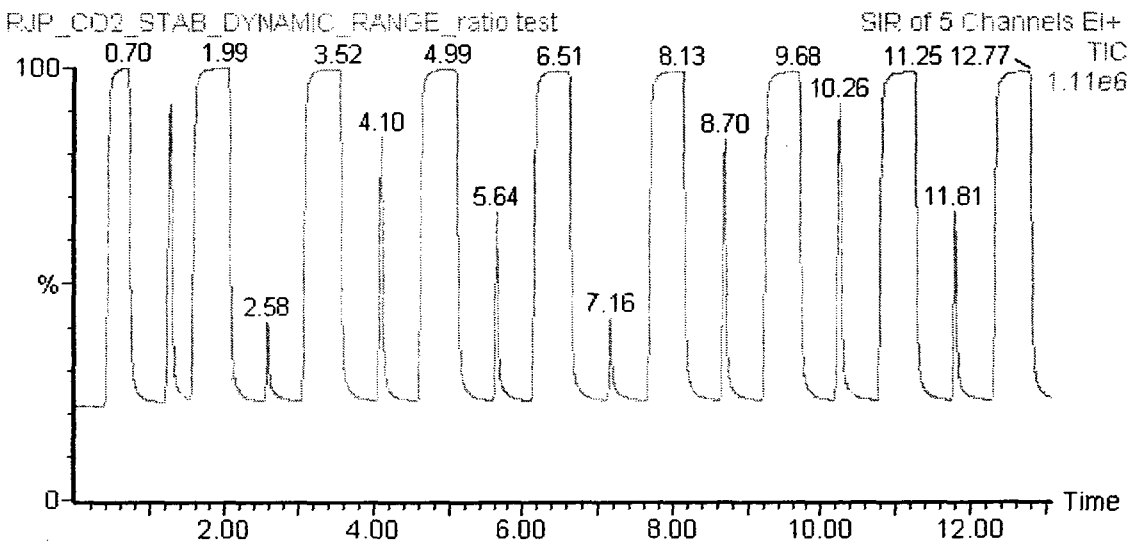

Figure A2-3. HTC Analyzer response for standard addition of IHSS SRFA to a marine end-member sample.

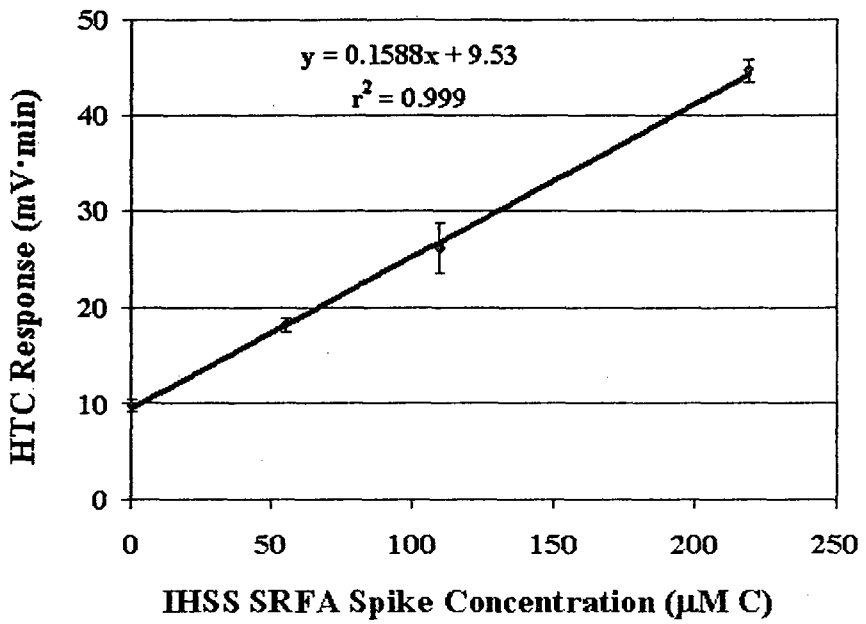

Figure A2-4. Total ion chromatogram for a 1750 μM IAEA-CH-6 sucrose solution injected into the unmodified HTC analyzer and directly into the ion source of the IRMS. The *y*-axis full scale is 2.8 nA, and the peak is integrated as -10.12 ‰.

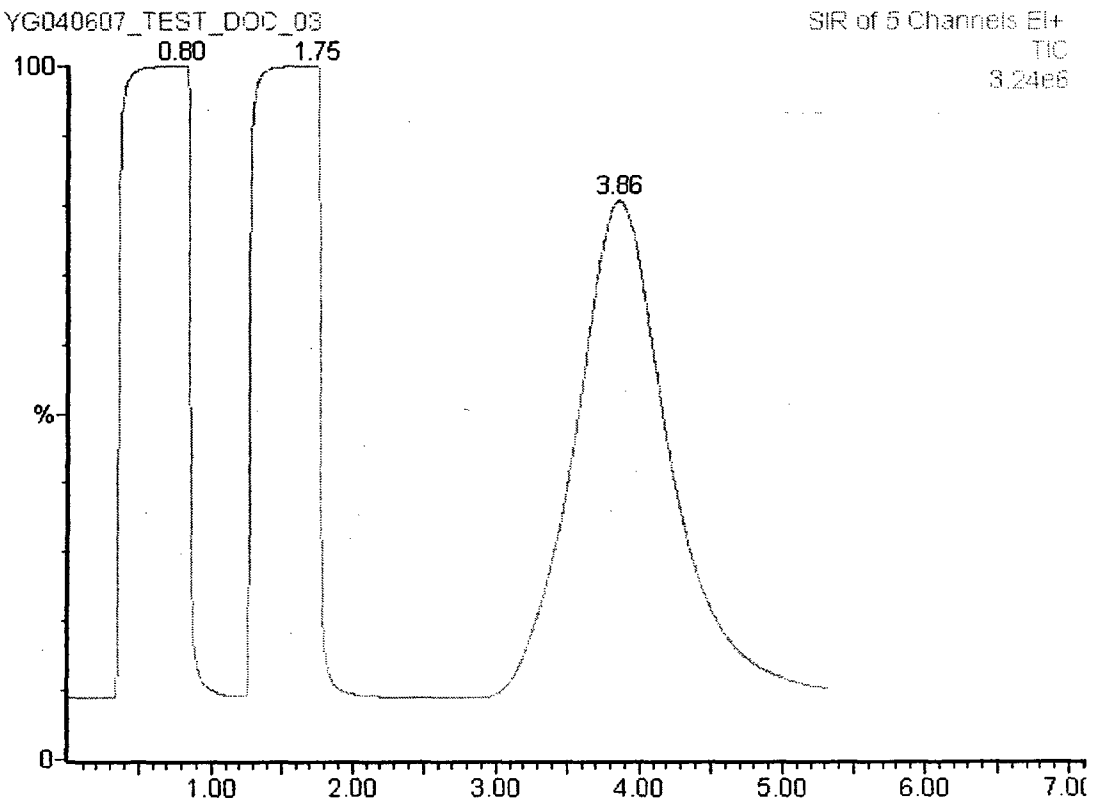

Appendix 3 Supporting Information for Chapter 3

Published as Supporting Web Material for Chapter 3:

Expressing biomarker data in stoichiometric terms: shifts in distribution and biogeochemical interpretation

Appendix 4 Supporting Information for Chapter 4

Submitted as Supporting Information for Chapter 4:

Polycyclic aromatic hydrocarbons in the St. Lawrence Estuary (QC, Canada): Transport, distribution and patterns as influenced by terrestrial organic matter

This supporting information section contains the complete data for bulk organic geochemical (total OC, $\delta^{13}C$, solvent extractable carbon), lignin phenol parameters (Σ_8, λ_8, S/V, and vanillyl acid-to-aldehyde ratios) as well as all polycyclic aromatic hydrocarbon (PAH) compounds and several commonly reported diagnostic isomer ratios.

Table A4-1. Complete bulk organic and lignin phenol parameters reported.

Stn	Depth (cm)	TOC[a]	ExC [b]	$\delta^{13}C$ (‰)	C/N	λ_8[c]	Σ_8[d]	S/V[e]	C/V[f]	$(Ac/Ad)_V$[g]
DE	0 - 2	11.3	0.53	-25.5	9.9	4.76	5.23	0.51	0.20	0.43
23	1 - 2	16.0	0.28	-23.8	11.5	2.37	3.79	0.53	0.14	0.42
	2 - 3	15.9	0.34	-23.7	11.2	2.15	3.44	0.31	0.15	0.55
	3 - 4	15.6	0.20	-23.8	11.3	1.94	3.11	0.31	0.15	0.46
	4 - 5	15.3	0.32	-24.1	12.0	2.15	3.23	0.29	0.15	0.54
	5 - 6	15.7	0.17	-23.8	11.1	2.09	3.35	0.30	0.14	0.50
	6 - 8	14.1	0.18	-23.9	11.3	2.35	3.29	0.29	0.13	0.56
	15 - 18	14.5	0.16	-24.5	12.4	2.63	3.69	0.25	0.10	0.46
	21 - 26	13.9	0.12	-24.4	12.8	2.38	3.33	0.24	0.11	0.48
	31 - 36	11.9	0.06	-24.8	12.7	1.70	2.36	0.27	0.14	0.43
	36 - 41	11.7	0.07	-24.8	12.0	1.84	2.19	0.33	0.20	0.46
20	0 - 1	6.1	0.31	-23.1		1.13	0.90	0.27	0.62	0.53
	1 - 2	6.2	0.34	-23.8	8.1	1.39	0.84	0.29	0.72	0.57
	2 - 3	8.7	0.32	-22.8	10.5	2.22	1.36	0.15	0.69	0.44
	3 - 4	8.3	0.33	-23.6		1.05	0.84	0.17	0.66	n.d.
	4 - 5	7.8	0.26	-23.7	9.4	1.05	0.84	0.19	0.70	0.54
	5 - 6	6.1	0.23	-23.8	9.4	1.35	0.81	0.30	0.68	0.51
	36 - 41	7.7	0.04	-23.1	10.9	0.47	0.57	0.46	1.62	0.52

[a]Total organic carbon (mg g^{-1}); [b]Total solvent extractable carbon (mg g^{-1}), determined by elemental analysis of dried sediment extracts; [c]Sum of eight lignin phenols normalized to 100 mg OC; [d]Sum of eight lignin phenols normalized dry mass of sediment; [e]Ratio of all syringyl to vanillyl lignin phenols; [f]Ratio of all cinnamyl to vanillyl lignin phenols; [g]Ratio of aldehydic to acid vanillyl lignin phenols.

Table A4-2. Polycyclic aromatic hydrocarbon levels (ng g^{-1}) in sediments collected in three cores of the St. Lawrence Estuary.[a]

Stn	Depth (cm)	Σ 15–PAH	Ace	Flu	Ant	Phe	Flt	Pyr	BaA	Chr	BbF	BkF	BeP	BaP	Per	DahA	BghiP
DE	0 - 2	543.2	n.d.[b]	n.d.	6.0	21.7	45.7	39.3	32.8	32.3	44.7	48.0	47.9	53.1	159.0	n.d.	12.9
23	1 - 2	237.9	10.0	n.d	3.6	6.2	26.7	22.4	32.1	39.6	15.7	12.7	11.2	10.6	28.5	2.5	16.0
	2 - 3	262.0	9.0	n.d	3.8	16.4	31.6	28.3	31.8	38.7	20.2	15.4	14.5	12.7	35.5	4.2	0.0
	3 - 4	260.4	8.9	n.d	3.5	8.9	28.5	22.7	31.1	38.8	22.7	15.8	15.4	11.8	35.1	4.3	13.0
	4 - 5	350.8	6.9	n.d	5.6	26.9	39.1	35.1	30.1	37.8	26.6	28.2	20.1	20.7	56.4	1.4	15.8
	5 - 6	237.5	5.3	n.d	2.5	12.9	21.2	17.8	19.9	24.7	28.1	22.9	19.4	16.9	31.8	3.1	11.1
	6 - 8	103.4	3.8	n.d	1.7	9.5	15.1	12.3	13.2	15.8	5.9	4.1	3.7	2.9	11.1	1.1	3.2
	15 - 18	344.3	0.6	n.d	10.8	48.2	22.2	21.9	16.6	16.3	46.1	34.2	31.0	28.3	58.7	n.d	9.4
	21 - 26	400.4	3.5	n.d	14.6	51.5	24.7	21.6	16.5	20.0	48.5	39.9	39.7	32.4	70.5	8.1	9.1
	31 - 36	140.8	2.6	n.d	2.9	17.8	20.8	n.d	11.6	14.2	11.9	10.4	8.2	8.4	15.8	9.9	6.3
	36 - 41	97.0	3.1	n.d	1.9	6.3	14.6	7.0	12.3	14.2	8.4	9.0	*	*	*	11.3	8.9
20	0 - 1	61.7	n.d	n.d	0.9	2.5	8.4	n.d	7.1	7.3	5.1	3.9	4.1	2.0	5.6	n.d	14.8
	1 - 2	131.2	1.6	1.5	1.5	6.5	16.1	n.d	8.4	8.7	12.9	7.9	11.6	5.8	24.4	4.1	20.3
	2 - 3	81.0	n.d	n.d	0.7	1.6	5.7	4.5	6.6	6.9	5.3	3.5	6.8	6.8	21.2	n.d	11.3
	3 - 4	107.7	1.4	1.5	0.9	4.5	11.6	15.3	5.8	6.0	8.4	7.1	5.9	6.6	16.3	n.d	16.4
	4 - 5	82.7	n.d	1.2	0.9	3.6	9.2	11.1	4.5	4.6	5.7	5.1	4.8	4.9	13.1	n.d	14.0
	5 - 6	51.0	1.3	n.d	0.2	0.5	7.9	8.8	4.2	4.3	1.6	1.0	1.2	1.3	2.5	3.3	12.9
	36 - 41	11.9	n.d	n.d	0.1	0.2	0.4	0.2	1.0	1.0	0.0	0.0	1.8	0.0	6.5	0.7	n.d

[a]Refer to text for abbreviations; [b]Not detected; *Instrumental error.

Table A4-3. Diagnostic PAH ratios and sums.

Stn	Depth (cm)	Σ15-PAH	Σ-Py	BaA/Chr	BaP/BeP	Phen/Ant	Flt/Pyr
DE	0 - 2	543.2	343.7	0.87	1.1	3.34	1.16
23	1 - 2	237.9	171.1	0.81	0.9	1.71	1.19
	2 - 3	262.0	193.2	0.82	0.9	4.30	1.12
	3 - 4	260.4	186.7	0.80	0.8	2.55	1.26
	4 - 5	350.8	237.8	0.80	1.0	4.82	1.12
	5 - 6	237.5	170.9	0.81	0.9	5.20	1.19
	6 - 8	103.4	73.1	0.83	0.8	5.70	1.23
	15 - 18	344.3	216.7	1.02	0.9	4.48	1.01
	21 - 26	400.4	243.2	0.82	0.8	3.52	1.15
	31 - 36	140.8	85.5	0.82	1.0	3.52	n.d
	36 - 41	97.0	65.5	0.82		6.07	2.09
20	0 - 1	61.7	37.9	0.97	0.5	2.60	n.d
	1 - 2	131.2	71.4	0.97	0.5	4.34	n.d
	2 - 3	81.0	46.1	0.97	1.0	2.26	1.26
	3 - 4	107.7	66.6	0.97	1.1	4.81	0.76
	4 - 5	82.7	49.9	0.98	1.0	4.14	0.83
	5 - 6	51.0	30.3	0.98	1.1	2.75	0.90
	36 - 41	11.9	4.4	0.98		1.95	1.79

Appendix 5 Supporting Information for Chapter 5

Supporting Information for Chapter 5:

Quantitative and natural abundance stable isotope mapping of five pools of carbon in the St. Lawrence Estuary

Modeling of DOC conservative mixing

Conservative DOC estimates were modeled ($[DOC]_M$) based on salinity following Cifuentes *et al* 1998:

$$[DOC]_{Est} = (f_R \times [DOC]_R) + (f_M \times [DOC]_M)$$

where $[DOC]_R$ and $[DOC]_M$ are experimentally measured fresh and marine water end-member concentrations of 425 and 58 μM, respectively, f_M is the fraction of marine water in the system, calculated as the ratio of measured salinity (S) to maximal salinity (34.6) and f_R is the fraction of riverine water and is $1 - f_M$ in the calculations.

$\delta^{13}C_{DOC}$ modeled from the conservative DOC estimate was modeled from Cifuentes *et al.* 1998 as well:

$$\delta_{Est} = \frac{(f_R \times [DOC]_R \times \delta_R) + (f_M \times [DOC]_M \times \delta_M)}{[DOC]_{Est}}$$

where δ_{Est} is the estimated $\delta^{13}C_{DOC}$, and δ_R and δ_M are the experimentally determined riverine and marine $\delta^{13}C_{DOC}$ endmembers (-26.8 and -20.8 ‰, respectively) and all other symbols as above.

Table A5-1. Sedimentary organic matter data

Stn	Depth (cm)	Avg (cm)	Porosity	C (mmol/g)	$\delta^{13}C_{SOC}$ (‰)	N (mmol/g)	$\delta^{15}N$ (‰)	C/N[a]	N/C	pwDOC (µmol C/L)	$\delta^{13}C$-DOC (‰)	$\Delta^{13}C$[b]
DE	5-10	4.5	0.78	1.57	-25.7	0.12	6.0	12.6	0.08	1029	-25.0	0.7
DE	0-2	0.5	0.80	0.94	-25.5	0.09	4.7	10.0	0.10			
23S	0-1	0.5	0.88	1.28	-23.8	0.12	3.6	10.8	0.09	200	-22.6	1.1
23S	10-12	11.0	0.80	1.17	-23.9	0.10	4.7	11.4	0.09			
23S	1-2	1.5	0.86	0.97	-23.4	0.11	6.1	9.1	0.11	300	-21.8	1.6
23S	12-15	13.5	0.77	1.15	-23.9	0.10	3.9	11.5	0.09			
23S	2-3	2.5	0.84	0.96	-23.8	0.10	6.1	9.7	0.10	408	-23.2	0.6
23S	3-4	3.5	0.82	1.35	-24.3	0.12	7.8	11.3	0.09	482	-23.0	1.3
23S	4-5	4.5	0.84	0.99	-23.6	0.10	5.6	9.9	0.10	644	-23.7	-0.1
23S	5-6	5.5	0.82	1.31	-24.4	0.11	7.8	11.5	0.09	833	-23.8	0.6
23S	6-8	7.0	0.80	0.92	-24.2	0.10	6.3	9.7	0.10	750	-23.0	1.2
23S	8-10	9.0	0.79	1.02	-23.9	0.10	4.9	10.4	0.10	1054	-23.5	0.4
23S	15-18	16.5	0.76	1.20	-24.4	0.10	8.0	12.2	0.08			
23S	18-21	19.5	0.75	0.87	-24.6	0.08	4.8	11.0	0.09			
23S	21-26	23.5	0.76	1.21	-24.6	0.10	7.4	12.7	0.08			
23S	26-31	28.5	0.75									
23S	31-36	33.5	0.75	0.79	-24.7	0.07	4.8	10.8	0.09			
23N	0-1	0.5	0.79	0.98	-24.1	0.08	1.2	12.5	0.08	246	-21.8	2.2
23N	10-12	11.0	0.64	0.72	-24.5	0.06	0.2	12.7	0.08			
23N	1-2	1.5	0.79	0.86	-24.1	0.07	1.9	12.1	0.08	389	-22.5	1.7
23N	12-15	13.5	0.69	0.80	-24.4	0.06	0.5	12.8	0.08	405	-23.3	1.1
23N	2-3	2.5	0.79	0.88	-24.4	0.07	1.3	12.7	0.08			
23N	3-4	3.5	0.77	0.90	-24.5	0.07	1.7	12.5	0.08	549	-22.4	2.1
23N	4-5	4.5	0.69	0.83	-24.4	0.06	0.5	13.5	0.07			
23N	5-6	5.5	0.73	0.83	-24.4	0.07	0.4	12.7	0.08	565	-23.5	0.9
23N	6-8	7.0	0.68	0.43		0.04			0.08			
23N	8-10	9.0	0.71	0.76	-24.5	0.06	-0.1	13.2	0.08	381	-23.1	1.5
23N	15-18	16.5	0.64	0.82	-24.2	0.06	0.9	12.8	0.08			
23N	18-21	19.5	0.71	0.59	-24.0	0.05	1.3	12.2	0.08	565	-23.3	0.7
23N	21-26	23.5	0.69	1.19	-24.3	0.10	2.9	12.4	0.08			
23N	26-31	28.5	0.60		-24.5		-0.3			631	-23.4	1.1

23N	31-36	33.5	0.75		-24.6		-1.4		
23N	36-41	38.5	0.76		-24.9		-0.7		
22N	0-1	0.5	0.78	0.65	-23.3	0.07	5.7	9.8	0.10
22N	10-12	11.0	0.70	0.66	-23.0	0.06	6.2	10.2	0.10
22N	1-2	1.5	0.76	0.91	-23.2	0.09	6.5	10.6	0.09
22N	12-15	13.5	0.62	0.68	-23.2	0.07	4.4	10.3	0.10
22N	2-3	2.5	0.69	0.68	-23.1	0.07	5.1	9.7	0.10
22N	3-4	3.5	0.70	0.96	-23.4	0.09	6.7	10.9	0.09
22N	4-5	4.5	0.70	0.68	-23.3	0.07	3.8	10.0	0.10
22N	5-6	5.5	0.70						
22N	6-8	7.0	0.67	0.70	-23.5	0.07	4.5	10.3	0.10
22N	8-10	9.0	0.70	0.63	-23.4	0.06	5.3	10.0	0.10
22N	15-18	16.5	0.66	0.56	-23.6	0.06	6.0	10.0	0.10
22N	18-21	19.5	0.67	0.51	-23.4	0.05	4.6	10.1	0.10
22N	21-26	23.5	0.63	0.48	-23.5	0.05	5.5	9.8	0.10
22N	26-31	28.5	0.66	0.60	-22.8	0.06	7.4	10.7	0.09
22N	31-36	33.5	0.63	0.54	-23.1	0.05	5.8	9.9	0.10
22N	36-41	38.5	0.69	0.42	-23.6	0.04	5.3	9.8	0.10
21N	0-1	0.5	0.61	0.43	-23.2	0.04	1.9	11.1	0.09
21N	10-12	11.0	0.51	0.31	-23.8	0.03	0.6	11.6	0.09
21N	1-2	1.5	0.60	0.54	-23.4	0.05	2.2	11.8	0.08
21N	12-15	13.5	0.48	0.28	-23.5	0.02	0.2	11.7	0.09
21N	2-3	2.5	0.55	0.44	-23.5	0.04	-1.1	12.0	0.08
21N	3-4	3.5	0.55	0.39	-23.6	0.03	-0.2	12.0	0.08
21N	4-5	4.5	0.55	0.37	-23.3	0.03	0.2	11.5	0.09
21N	5-6	5.5	0.54	0.32	-23.4	0.03	-3.1	11.9	0.08
21N	6-8	7.0	0.53	0.30	-23.4	0.03	-3.7	11.5	0.09
21N	8-10	9.0	0.51	0.32	-23.7	0.03	-1.1	12.4	0.08
21N	15-18	16.5	0.51	0.26	-23.7	0.02	-0.3	11.3	0.09
21N	18-21	19.5	0.48	0.25	-23.5	0.02	-0.8	11.5	0.09
21N	21-26	23.5	0.45	0.23	-23.6	0.02	-0.8	11.0	0.09
21N	26-31	28.5	0.46	0.21	-23.5	0.02	-1.1	10.9	0.09
21N	31-36	33.5	0.45	0.20	-23.4	0.02	-1.8	10.4	0.10
21N	36-41	38.5	0.45	0.22	-23.7	0.02	-0.2	11.9	0.08
20S	0-1	0.5	0.76	0.51	-22.3	0.06	7.2	8.8	0.11
20S	10-12	11.0	0.69	0.46	-22.9	0.05	6.2	8.8	0.10

20S	1-2	1.5	0.75	0.56	-22.3	0.06	7.2	8.6	0.12			
20S	12-15	13.5	0.67	0.47	-22.8	0.05	6.4	9.1	0.11			
20S	2-3	2.5	0.73	0.44	-22.6	0.05	6.1	8.4	0.12			
20S	3-4	3.5	0.70	0.52	-22.7	0.06	7.1	9.3	0.11			
20S	41-46	43.5	0.72	0.19	-24.2	0.02	3.6	8.3	0.12			
20S	4-5	4.5	0.60	0.50	-22.6	0.06	6.9	9.0	0.11			
20S	5-6	5.5	0.62	0.35	-22.7	0.04	5.3	7.9	0.13			
20S	6-8	7.0	0.67	0.47	-22.6	0.05	6.2	9.0	0.11			
20S	8-10	9.0	0.68	0.54	-22.6	0.06	6.6	9.4	0.11			
20S	15-18	16.5	0.70									
20S	18-21	19.5	0.70	0.35	-22.6	0.04	8.1	7.3	0.11			
20S	21-26	23.5	0.70	0.30	-23.1	0.03	5.8	9.1	0.11			
20S	26-31	28.5	0.73	0.25	-23.2	0.03	4.8	8.8	0.11			
20S	31-36	33.5	0.73	0.27	-24.5	0.03	6.1	9.6	0.10			
20S	36-41	38.5	0.72	0.27	-24.6	0.03	4.8	9.5	0.11			
20N	0-1	0.5	0.86	1.17	-22.1	0.12	3.5	9.6	0.10	406	-21.9	0.2
20N	10-12	11.0	0.80	1.11	-22.3	0.11	3.4	10.2	0.10			
20N	1-2	1.5	0.84	1.16	-22.1	0.12	4.2	9.6	0.10	703	-21.5	0.6
20N	12-15	13.5	0.78	1.19	-22.4	0.12	3.8	10.2	0.10	697	-21.0	1.4
20N	2-3	2.5	0.85	1.29	-21.9	0.13	3.3	10.0	0.10	954	-21.9	0.1
20N	3-4	3.5	0.81	1.21	-22.3	0.12	3.6	10.0	0.10	639	-21.2	1.2
20N	4-5	4.5	0.81	1.24	-22.3	0.12	3.7	10.0	0.10	665	-22.0	0.3
20N	5-6	5.5	0.81	1.08	-22.4	0.11	4.1	10.0	0.10	717	-22.2	0.3
20N	6-8	7.0	0.80	1.07	-22.5	0.10	3.5	10.5	0.10	527	-22.0	0.4
20N	8-10	9.0	0.80	1.08	-22.6	0.10	2.8	10.5	0.10	1299	-21.1	1.5
20N	15-18	16.5	0.80	1.01	-22.5	0.10	3.7	10.2	0.10			
20N	18-21	19.5	0.80	1.15	-22.2	0.11	3.9	10.1	0.10	580	-22.7	-0.5
20N	21-26	23.5	0.80	0.81	-22.5	0.08	3.1	10.2	0.10			
20N	26-31	28.5	0.80	0.71	-22.7	0.07	3.2	10.3	0.10	440	-23.0	-0.2
20N	31-36	33.5	0.79	0.86	-23.9	0.07	2.5	11.4	0.09	524	-23.8	0.1
20N	36-41	38.5	0.76	0.97	-24.8	0.08	2.9	12.0	0.08	524	-23.8	1.0
23	0-1	0.5	0.89	1.33	-23.9	0.12	4.0	10.9	0.09	226	-23.4	0.6
23	10-12	11.0	0.79	1.24	-24.2	0.11	1.6	11.8	0.08			
23	1-2	1.5	0.87	1.33	-23.8	0.12	1.7	11.5	0.09	234	-23.0	0.7
23	12-15	13.5	0.79	1.19	-24.6	0.10	1.4	12.4	0.08	525	-23.0	1.6
23	2-3	2.5	0.86	1.32	-23.7	0.12	1.5	11.2	0.09			

23	3-4	3.5	0.84	1.30	-23.8	0.11	1.8	11.3	0.09	299	-22.7	1.1
23	4-5	4.5	0.84	1.27	-24.1	0.11	2.3	11.9	0.08	397	-22.8	1.3
23	5-6	5.5	0.82	1.31	-23.8	0.12	2.4	11.1	0.09	452	-23.1	0.6
23	6-8	7.0	0.80	1.17	-23.9	0.10	1.0	11.3	0.09	477	-23.1	0.8
23	8-10	9.0	0.78	1.27	-24.1	0.11	1.9	11.7	0.09	461	-23.3	0.7
23	15-18	16.5	0.76	1.21	-24.5	0.10	1.6	12.4	0.08			
23	18-21	19.5	0.77	1.16	-24.8	0.09	2.8	12.3	0.08	511	-23.9	0.9
23	21-26	23.5	0.78	1.16	-24.4	0.09	-0.9	12.7	0.08	585	-24.7	-0.3
23	26-31	28.5	0.77	1.04	-24.3	0.08	1.3	12.6	0.08	621	-24.2	0.1
23	31-36	33.5	0.78	0.99	-24.8	0.08	2.4	12.7	0.08			
23	36-41	38.5	0.77	0.97	-24.8	0.08	2.9	12.0	0.08			
22	0-1	0.5	0.89	0.98	-23.4	0.11	6.0	9.2	0.11			
22	10-12	11.0	0.77	1.09	-23.8	0.10	6.2	11.2	0.09			
22	1-2	1.5	0.86	1.00	-22.6	0.11	5.4	9.2	0.11			
22	12-15	13.5	0.75	1.01	-23.8	0.09	7.9	11.4	0.09			
22	2-3	2.5	0.84	1.20	-22.8	0.12	5.1	10.3	0.10			
22	3-4	3.5	0.85	0.95	-23.1	0.10	5.9	9.4	0.11			
22	4-5	4.5	0.79	1.28	-23.6	0.12	7.3	10.8	0.09			
22	5-6	5.5	0.79	0.95	-23.8	0.10	5.5	9.9	0.10			
22	6-8	7.0	0.78	1.10	-21.8	0.11	4.7	10.3	0.10			
22	8-10	9.0	0.77	0.89	-24.0	0.09	4.5	10.0	0.10			
22	15-18	16.5	0.74	0.97	-23.6	0.09	5.6	11.2	0.09			
22	18-21	19.5	0.76	0.86	-23.5	0.08	5.5	10.4	0.10			
22	21-26	23.5	0.75	0.73	-23.6	0.08	3.1	9.6	0.10			
22	26-31	28.5	0.75	0.89	-23.4	0.09	7.2	10.2	0.10			
22	31-36	33.5	0.75	0.82	-22.9	0.08	2.6	9.8	0.10			
21.5	0-1	0.5	0.80	1.11	-23.6	0.10	5.0	11.0	0.09			
21.5	10-12	11.0	0.70	0.96	-23.9	0.08	4.5	12.2	0.08			
21.5	1-2	1.5	0.80	1.05	-23.7	0.09	4.6	11.4	0.09			
21.5	12-15	13.5	0.69	0.83	-23.8	0.07	4.1	12.7	0.08			
21.5	2-3	2.5	0.73									
21.5	3-4	3.5	0.72	1.01	-23.8	0.09	4.6	11.7	0.09			
21.5	4-5	4.5	0.74	0.98	-23.7	0.08	5.0	11.7	0.09			
21.5	5-6	5.5	0.72	0.97	-23.8	0.08	4.6	11.8	0.08			
21.5	6-8	7.0	0.72	0.98	-23.9	0.08	4.2	11.9	0.08			
21.5	8-10	9.0	0.63	0.94	-23.8	0.08	4.6	12.4	0.08			

21.5	15-18	16.5	0.58	0.63	-23.6	0.05	3.8	12.2	0.08			
21.5	18-21	19.5	0.64	0.66	-23.4	0.06	3.9	11.9	0.08			
21.5	21-26	23.5	0.57									
21.5	26-31	28.5	0.57	0.66	-23.3	0.05	3.1	13.4	0.07			
21.5	31-36	33.5	0.56	0.47	-23.6	0.03	3.1	13.8	0.07			
21.5	36-41	38.5	0.57	0.71	-23.5	0.05	0.9	15.0	0.07			
21	0-1	0.5	0.88	1.33	-23.2	0.14	5.7	9.7	0.10			
21	10-12	11.0	0.79	1.10	-23.4	0.11	5.9	10.3	0.10			
21	1-2	1.5	0.87	1.28	-23.2	0.13	6.0	9.6	0.10			
21	12-15	13.5	0.76	1.14	-23.5	0.11	5.7	10.2	0.10			
21	2-3	2.5	0.86	1.27	-23.2	0.13	6.0	9.8	0.10			
21	3-4	3.5	0.84	1.26	-23.3	0.13	5.7	9.8	0.10			
21	4-5	4.5	0.84	1.24	-23.4	0.12	5.5	10.0	0.10			
21	5-6	5.5	0.75	1.20	-23.3	0.12	5.9	10.1	0.10			
21	6-8	7.0	0.78	1.16	-23.4	0.11	5.8	10.2	0.10			
21	8-10	9.0	0.77	1.21	-23.5	0.11	5.5	10.6	0.09			
21	15-18	16.5	0.77	1.09	-23.5	0.11	5.3	10.3	0.10			
21	18-21	19.5	0.77	1.07	-23.2	0.11	5.4	10.1	0.10			
20	0-1	0.5	0.88	*0.95*	*-23.1*	*0.15*	*5.0*	*6.5*	0.16	223	-22.4	0.7
20	10-12	11.0	0.81	*0.61*	*-24.2*	*0.05*	*2.2*	*11.3*	0.09			
20	1-2	1.5	0.87	*0.51*	*-23.8*	*0.06*	*5.0*	*8.1*	0.12	262	-22.5	1.3
20	12-15	13.5	0.80	*0.49*	*-23.7*	*0.05*	*2.4*	*10.8*	0.09	1029	-21.7	2.0
20	2-3	2.5	0.86	*0.73*	*-22.8*	*0.07*	*4.2*	*10.5*	0.10	390	-22.9	-0.1
20	3-4	3.5	0.85	*0.92*	*-23.6*	*0.14*	*4.7*	*6.6*	0.15	408	-22.4	1.2
20	4-5	4.5	0.84	*0.65*	*-23.7*	*0.07*	*4.9*	*9.4*	0.11	599	-22.6	1.0
20	5-6	5.5	0.83	*0.50*	*-23.8*	*0.05*	*4.4*	*9.5*	0.11	599	-22.0	1.8
20	6-8	7.0	0.83	*0.64*	*-23.1*	*0.06*	*3.7*	*10.9*	0.09			
20	8-10	9.0	0.82	*0.58*	*-23.6*	*0.06*	*3.5*	*10.2*	0.10	687	-22.6	1.0
20	15-18	16.5	0.80	*0.35*	*-24.8*	*0.04*	*2.5*	*9.6*	0.10			
20	18-21	19.5	0.82	*0.34*	*-25.9*	*0.03*	*3.4*	*10.9*	0.09	872	-22.8	3.2
20	21-26	23.5	0.80	*0.81*	*-22.5*	*0.08*	*3.1*	*10.2*	0.10			
20	26-31	28.5	0.81	*0.71*	*-22.7*	*0.07*	*3.2*	*10.3*	0.10	633	-22.3	0.4
20	31-36	33.5	0.81	*0.86*	*-23.9*	*0.07*	*2.5*	*11.4*	0.09			
20	36-41	38.5	0.80	*0.97*	*-24.8*	*0.08*	*2.9*	*12.0*	0.08			

Notes

[a] Italicized values are questionable due to poor nitrogen data and omitted from the

asssessment

[b] Difference in $\delta^{13}C$ of pwDOC from SOC

Table A5-2. Water column Organic carbon data

Stn	Depth (m)	Year	[DOC] (µmolC/L)	$\delta^{13}C_{DOC}$ (‰)	[POC] (µmolC/L)	µmolC/mg SPM	mgSPM/L	$\delta^{13}C_{POC}$ (‰)	N/C	Temp	Salinity	Density	O2
K	2	2007	126	-23.9	22.9	0.69	33.15	-25.4	0.10	2.7	27.0	21.5	305
K	25	2007	118	-23.8	16.2	0.52	31.10	-25.3	0.11	1.3	29.8	23.9	294
K	90	2007	70	-22.1	12.8	0.47	27.18	-25.3	0.10	1.3	32.7	26.2	232
I	2	2007	178	-27.7	15.7	0.68	23.06	-29.1	0.07	4.4	21.0	16.7	309
I	25	2007	114	-23.0	24.2	0.56	42.76	-26.6	0.10	1.8	27.8	22.2	305
I	140	2007	91	-21.5	24.2	0.36	66.79	-27.8	0.08	0.6	30.9	24.8	293
G	20	2006	182							7.3	20.6	16.0	0
F1am	3	2006	182	-27.0						7.9	19.1	14.8	
F1pm	3	2006	173	-26.0						8.1	18.7	14.5	
F1	2	2007	172	-25.2	62.0	0.93	66.73	-25.1	0.09	7.0	12.3	9.6	315
F1	15	2007	194	-27.6	133.0	1.17	113.76	-27.5	0.09	4.5	20.0	15.9	306
F1	40	2007	118	-24.5	379.3	1.13	336.64	-24.9	0.09	2.2	26.6	21.3	293
EF	3	2006	194	-26.4						12.0	9.7	7.0	
EF	10	2006	257	-27.5						11.4	10.9	8.0	
DE	2	2007	342	-26.5	81.6	1.88	43.44	-25.8		9.5	4.9	3.6	322
DE	15	2007	296	-27.0						9.4	5.1	3.7	322
A	40	2006	425	-26.8						17.2	0.1		
23S	2	2007	166	-24.5	3.6	1.07	3.31	-25.3	0.14	5.1	24.0	19.0	320
23S	40	2007			3.0	0.82	3.70	-23.8	0.14	0.1	31.9	25.6	356
23S	65	2007			1.8	0.12	14.54	-27.8	0.13	-0.7	32.3	25.9	336
23S	150	2007			2.2	0.09	24.57	-28.5	0.15	3.0	33.6	26.8	154
23S	250	2007			1373.2	0.49		-25.5	0.11	5.1	34.5	27.3	66
23S	310	2007			90.2	0.51	177.47	-25.1	0.12	5.2	34.6	27.3	59
23N	2	2007	154	-25.9	3.9	1.26	3.09	-25.9	0.11	3.7	26.8	21.3	316
23N	35	2007			3.1	1.85	1.70	-23.9	0.14	-0.3	32.0	25.7	354
23N	100	2007			1.8	0.12	14.89	-25.6	0.12	0.8	32.9	26.3	264
23N	200	2007			14.7	0.06	254.74			4.5	34.2	27.1	85
23N	240	2007			20.1	0.51	39.27	-25.5	0.10	4.9	34.4	27.2	72
23N	250	2007			6.3	0.32	19.42	-24.8		4.9	34.4	27.2	69
22N	2	2007	132	-23.0	17.7	3.53	5.01	-24.3	0.18	5.5	24.6	19.4	350
22N	50	2007			44.6	1.19	37.64	-26.7	0.16	-0.6	32.2	25.9	337
22N	295	2007			18.7	0.64	29.11	-26.1	0.11	5.1	34.5	27.3	63

21N	2	2007	184	-23.7	11.2	5.57	2.01	-20.6	0.19	5.4	25.5	20.1	407
21N	2	2007	184	-23.7	13.0	5.49	2.36	-20.4	0.19	5.4	25.5	20.1	407
21N	50	2007			28.1	0.75	37.37	-22.3	0.14	0.1	32.3	25.9	318
21N	250	2007			148.0	0.59	252.30	-21.7	0.12	5.2	34.5	27.3	97
21N	305	2007			32.2	0.56	57.88	-21.6	0.11	5.4	34.6	27.3	98
215N	2	2007	120	-21.6	433.8	13.79	31.47	-20.3	0.12	6.3	25.2	19.8	412
215N	50	2007			23.1	1.39	16.67	-21.8	0.17	-0.7	32.4	26.0	335
215N	125	2007			242.4	0.64	378.18	-25.7	0.12	2.4	33.4	26.6	184
215N	165	2007			257.4	0.94	274.94	-22.3	0.11	3.9	33.9	26.9	116
20S	2	2007	126	-21.4	3.1	2.80	1.11	-21.7	0.16	4.0	31.2	24.8	379
20S	41	2007			2.6	3.26	0.79	-20.3	0.15	-0.3	32.3	26.0	334
20S	125	2007			11.5	0.10	113.86	-26.2	0.14	3.3	33.7	26.8	157
20S	200	2007			10.7	0.07	154.12			4.9	34.3	27.1	96
20S	235	2007			76.7	0.83	92.76	-21.5	0.13	5.3	34.6	27.3	90
20S	300	2007			61.6	0.61	101.39	-21.4	0.14	5.4	34.7	27.4	90
20N	2	2007	143	-21.4	20.4	2.41	8.44	-20.5	0.15	4.2	31.5	25.0	366
20N	28	2007			8.8	3.12	2.83	-19.9	0.16	-0.4	32.2	25.9	375
20N	75	2007			7.8	1.16	6.70	-21.4	0.13	3.0	33.6	26.7	168
20N	150	2007			10.9	0.61	17.76	-22.4	0.12	5.0	34.3	27.2	95
20N	210	2007			107.7	0.55	195.52	-21.5	0.12	5.4	34.6	27.3	86
20N	280	2007			211.2	0.76	278.64	-24.0	0.11	5.4	34.7	27.4	103
23	0.5	2006	143	-25.6						8.8	25.7	19.9	
23	5	2007		-24.4	247.5	1.43	173.70	-25.3		5.1	23.9	18.9	327
23	10	2006	136	-25.4						8.8	26.8	19.9	
23	20	2006	136	-24.9						8.5	27.1	19.9	
23	25	2007	78	-22.3	8.8					0.4	30.8	24.7	296
23	30	2006	129	-24.6						5.6	28.0	19.9	
23	40	2006	91	-24.0						4.6	29.6	19.9	
23	50	2007			6.7	1.73	3.86	-23.9		-0.6	32.2	25.9	348
23	50	2006	91	-23.7						2.7	30.4	19.9	
23	70	2006	79	-22.7						1.0	31.9	19.9	
23	75	2007	69	-22.4	2.8	0.07	40.87			-0.4	32.5	26.1	321
23	100	2006	66							1.0	32.5	19.9	
23	150	2006	68	-22.0						3.3	33.7	19.9	
23	150	2007	58	-22.0	10.0	0.05	194.90			2.8	33.5	26.7	163
23	200	2007			11.5	0.08	146.54	-28.1	0.16	4.3	34.1	27.1	90

23	200	2006	61	-21.7						4.4	34.2	19.9	
23	250	2007	56	-21.7	65.7	0.60	109.30	-24.3		5.1	34.5	27.3	66
23	250	2006	57	-21.5						4.8	34.4	19.9	
23	300	2007			59.2	0.10	599.32	-28.9	0.14	5.2	34.6	27.3	60
23	300	2006	60	-21.7						5.1	34.5	19.9	
23	330	2007	65	-21.6	239.3	10.35	23.13	-28.2		5.2	34.6	27.3	60
23	330	2006	61	-21.6						5.2	34.5	19.9	
22	2	2007	155	-22.2	41.2	4.52	9.11	-19.8	0.17	6.4	22.7	17.8	408
22	50	2007			1.9	1.21	1.54	-21.4	0.15	-0.6	32.2	25.8	343
22	240	2007			2.4	0.47	5.06	-22.6	0.13	4.7	34.3	27.2	76
22	305	2007			50.8	0.49	102.93	-22.8	0.14	5.1	34.5	27.3	61
21	2	2007	163	-25.3	5.3	4.05	1.31	-19.4	0.20	5.5	25.3	20.0	395
21	19	2007			2.1	1.31	1.58	-22.5	0.15	1.7	28.9	23.1	322
21	60	2007			2.2	0.46	4.76	-24.1	0.14	-0.7	32.2	25.9	349
21	150	2007			1.5	0.39	3.93	-25.1	0.14	0.3	32.7	26.2	284
21	250	2007			2.0	0.37	5.39	-23.7	0.14	5.1	34.4	27.2	89
21	300	2007			38.6	0.43	89.55	-24.3	0.14	5.4	34.7	27.4	101
20	2	2007	109	-22.8	17.1	1.96	8.72	-21.2	0.13	3.7	31.8	25.3	406
20	25	2007	123	-23.4	4.2					1.4	32.1	25.7	407
20	75	2007			1.9	0.14	12.94	-22.2	0.14	2.6	33.4	26.7	196
20	224	2007			4.3	0.64	6.70	-23.0	0.13	5.4	34.6	27.3	84
20	250	2007			39.2	0.07	597.29	-26.0	0.16	5.5	34.7	27.4	97